

Sheffield Hallam University

Developing energy-loss test techniques for large buildings.

CLOSS, Stephen.

Available from the Sheffield Hallam University Research Archive (SHURA) at:

<http://shura.shu.ac.uk/19483/>

A Sheffield Hallam University thesis

This thesis is protected by copyright which belongs to the author.

The content must not be changed in any way or sold commercially in any format or medium without the formal permission of the author.

When referring to this work, full bibliographic details including the author, title, awarding institution and date of the thesis must be given.

Please visit <http://shura.shu.ac.uk/19483/> and <http://shura.shu.ac.uk/information.html> for further details about copyright and re-use permissions.

SHEFFIELD HALLAM UNIVERSITY
LEARNING CENTRE
CITY CAMPUS, POND STREET,
SHEFFIELD S1 1WB.



Fines are charged at 50p per hour

REFERENCE

ProQuest Number: 10694364

All rights reserved

INFORMATION TO ALL USERS

The quality of this reproduction is dependent upon the quality of the copy submitted.

In the unlikely event that the author did not send a complete manuscript and there are missing pages, these will be noted. Also, if material had to be removed, a note will indicate the deletion.



ProQuest 10694364

Published by ProQuest LLC (2017). Copyright of the Dissertation is held by the Author.

All rights reserved.

This work is protected against unauthorized copying under Title 17, United States Code
Microform Edition © ProQuest LLC.

ProQuest LLC.
789 East Eisenhower Parkway
P.O. Box 1346
Ann Arbor, MI 48106 – 1346

Developing Energy-loss Test Techniques for large buildings

Stephen Closs

A thesis submitted in partial requirement of the requirements of
Sheffield Hallam University
for the degree of Master of Philosophy



October 2004

Collaborating Organisation: HRS Services Ltd

CONTENTS PAGE

ABSTRACT	5
CHAPTER 1 INTRODUCTION	6
1.1 Overview	6
1.2 CO ₂ emissions and climate change	7
1.3 Government measures to reduce carbon dioxide emissions	8
1.4 The impact of air leakage in buildings on energy consumption	11
1.5 Assessment of building infiltration rates	12
1.6 Airtightness testing methods	14
1.6.1 Steady state (DC) pressurisation techniques	14
1.6.2 Unsteady (AC) pressurisation techniques	15
1.7 Testing of large buildings	15
1.8 Computer modelling of air infiltration and energy use in buildings	17
1.9 Aims and structure of the study	18
CHAPTER 2 LITERATURE REVIEW	21
2.1 Historical airtightness of buildings	21
2.2 Building heat loss and envelope degradation associated with air leakage	22
2.3 Airtightness testing in the UK and internationally	22
2.4 Testing very large buildings	28
2.5 Summary	31
CHAPTER 3 THEORY	32
3.1 Steady state pressure measurements	32
3.2 Least square power law	32
3.3 Air leakage index vs. air permeability calculation methods	33
3.4 Effective leakage area	35
3.5 Calculation of infiltration heat loss	36
3.6 Repeatability of airtightness tests	38
3.7 Summary	39
CHAPTER 4 METHODOLOGY	40
4.1 Design and construction of large test rig	40
4.2 Calibration of large air test rig	45
4.3 Calibration procedure	48
4.4 Testing of very large buildings	54
4.5 Remedial sealing measures	56
4.6 Summary	62
CHAPTER 5 FIELD TESTING	63
5.1 Field testing of large buildings	63

5.2	<i>Testing of a large warehouse (Building A) to determine building envelope airtightness using the Megafan rig</i>	63
5.3	<i>Testing of a very large retail store (Building B) to determine building envelope airtightness using the Megafan rig</i>	65
5.4	<i>Testing of a very large warehouse building (Building C) to determine airtightness using multiple rigs</i>	71
5.5	<i>Summary</i>	75
CHAPTER 6 RESULTS		76
6.1	<i>Testing of a large warehouse (Building A) to determine building envelope airtightness using the Megafan rig</i>	76
6.1.1	<i>Log-log data plot for building pressurisation test</i>	78
6.1.2	<i>Linear data plot for building pressurisation test</i>	79
6.1.3	<i>Environmental and measured data</i>	80
6.1.4	<i>Building envelope data</i>	81
6.1.5	<i>Measured fan and building envelope data</i>	82
6.2	<i>Testing of a very large retail store (Building B) to determine building envelope airtightness using the Megafan</i>	83
6.2.1	<i>Log-log data plot for building pressurisation test</i>	84
6.2.2	<i>Linear data plot for building pressurisation test</i>	85
6.2.3	<i>Environmental and measured data</i>	86
6.2.4	<i>Building envelope data</i>	87
6.2.5	<i>Measured fan and building envelope data</i>	88
6.3	<i>Testing of a very large warehouse (Building C) to determine airtightness using multiple rigs</i>	89
6.3.1	<i>Log-log data plot for building pressurisation test</i>	90
6.3.2	<i>Linear data plot for building pressurisation test</i>	91
6.3.3	<i>Environmental and measured data</i>	92
6.3.4	<i>Building envelope data</i>	93
6.3.5	<i>Measured data</i>	94
6.4	<i>Discussion</i>	95
6.5	<i>Summary</i>	96
CHAPTER 7 COMPUTER SIMULATION		97
7.1	<i>Modelling of a very large warehouse in Bedford</i>	97
7.2	<i>Computational fluid dynamics modelling of Building C</i>	99
7.2.2	<i>Boundary Conditions</i>	101
7.2.3	<i>Grid and Grid independence</i>	102
7.2.4	<i>Solution control and Convergence</i>	102
7.2.5	<i>Jet Plume Calibration</i>	103
7.2.6	<i>Air-leakage test infiltration rate (0.07 ach⁻¹)</i>	103
7.3	<i>Results of dynamic thermal modelling of Building C using original design specification and airtightness level determined from airtightness test to produce energy consumption model</i>	104
7.4	<i>Results of computational fluid dynamics modelling of Building C</i>	105
CHAPTER 8 CONCLUSIONS AND FURTHER WORK		107
8.1	<i>Feasibility of testing large buildings in the UK</i>	107
8.2	<i>Airtightness of large warehouse buildings in the UK</i>	108
8.3	<i>Energy savings in Building C associated with improved envelope airtightness</i>	108
8.3.1	<i>Dynamic thermal modelling (DTM) simulation</i>	108

8.3.2	<i>Computational fluid dynamics (CFD) simulation</i>	109
8.4	<i>Further work on the impact of energy savings with improved envelope airtightness</i>	110
8.4.1	<i>Further work with dynamic thermal modelling</i>	110
8.4.2	<i>Further work with Computational Fluid Dynamics Simulation (CFD)</i>	111
9.0	ACKNOWLEDGEMENTS	112
10.0	REFERENCES	113
11.0	RELEVANT LITERATURE	121
	APPENDIX A.1 FORMULAE USED IN THIS STUDY	138
A.1	<i>Altas main equations</i>	139
	APPENDIX A.2	142
A.2	<i>Pressure testing a very large building: theory and practice</i>	142
	APPENDIX A.3	149
A.3	<i>Sample of Building C Dynamic Thermal Modelling output data</i>	149
	APPENDIX A.4	155
A.4	<i>2000 mm fan calibration data</i>	155
	APPENDIX A.5	167
A.5	<i>1250 mm fan calibration data</i>	167

Abstract

Studies have noted that the concentration of carbon dioxide in the atmosphere has risen by more than a third since the Industrial Revolution and is now rising faster than ever before. During the 20th Century there was an observed global mean temperature rise of around 0.6 °C. Analysis of these two coinciding events has resulted in the now widely accepted theory of “the greenhouse effect”. In 1997 the UK Government signed up to the Kyoto Treaty. This stipulated that all ratified states would enter an agreement to either curb, or reduce their total CO₂ emissions, depending on the country’s current output. Building energy use currently accounts for 46% of total UK energy consumption, resulting in the annual release of 66 million tonnes of carbon into the atmosphere.

As one step in addressing this issue the Government introduced the Approved Document Part L2 of the Building Regulations – *Conservation of Fuel and Power* on the 1st April 2002. A requirement of the document was that a fan pressurisation airtightness performance assessment be made of the completed building envelope. For all non-domestic buildings with a gross floor area of greater than 1000m² an air leakage test would be required in accordance with CIBSE TM 23:2000 to prove that the construction was reasonably airtight. The improvements made in the thermal performance of building materials have raised the importance of designing and constructing less air leaky building envelopes. It has been reported that heat loss associated with air leakage could account for 30% of heat loss through the building envelope.

It has been noted that previously available fan pressurisation rigs in the UK could not produce the flow rates to attain a satisfactory pressure difference across the envelope for large buildings. 'Large' building tests were previously classed as those carried out on structures with a floor area of up to only 5000m². However, a modern UK warehouses can have a floor area of 60,000m² or greater.

The thesis provides an account of the origins of airtesting and the evolving airtightness rules and regulations in the UK and other European Union member states. The methodologies for the practical application of airtightness testing and the calculation and interpretation of results are provided. The design, construction and calibration of the largest air testing rig in the UK (and possibly the world) are discussed. Three examples of very large buildings tested using this rig are presented; the largest of which has a floor area of nearly 60,000 m². Analysis of the airtightness test results and practical considerations for testing such large structures are presented. Examples of remedial sealing measures to improve building envelope airtightness performance are presented.

The largest building tested was then used as a case study for an investigation into the space heating energy saving benefits of improved building envelope airtightness. Dynamic Thermal Modelling (DTM) and Computational Fluid Dynamics (CFD) simulations were utilised to provide a space heating assessment of the building through a one month period. The study concludes that testing of very large warehouse buildings is practically feasible and that there are considerable energy saving benefits to be had from sealing building envelopes to best practice levels.

Chapter 1 Introduction

1.1 Overview

The continual increase of the world's population and improving standards of living have resulted in an ever growing requirement for energy to facilitate demand. Whilst the search for new sources of energy and types of fuel has previously been the priority, there has now been a shift towards finding methods of reducing demand. This has been partially realised through improved efficiency of production machinery and transport vehicles. Analysis of the breakdown of energy use by sector reveals that the processes providing space heating within buildings are a significant contributor to the overall figure. Heat loss from buildings can occur by conductive, convective and radiant losses through or from the structure or by infiltration losses from external air entering and leaving the building. The gradual improvement in the effectiveness of insulation in the walls, floors and roofs of buildings has focused attention on the airtightness of the building structure. A building envelope with greater airtightness properties will reduce the amount of unwanted external air entering the building, known as infiltration, and warm internal air leaving the building, known as exfiltration. There are a number of methods available to estimate building envelope airtightness and the associated air change rate within a building. One method which has become increasingly prevalent, due to its inclusion as a requirement in the latest revision of the Building Regulations, is a fan pressurisation test. This entails subjecting the building envelope to a differential pressure using a fan, usually mounted in an external doorway. The results of an airtightness test can be used as a basis for calculating an indicative air change rate for the building in question.

1.2 CO₂ emissions and climate change

Since the appearance of the human race on this planet, mankind has strived for progress to improve standards of living and remove subservience to the harsh environment. Throughout recorded history there has been a gradual progression towards what is now described as modern civilisation. The latter half of the eighteenth century in Britain saw a very rapid change from work carried out in the home with simple machines to industries in factories with power driven machinery. This was the beginning of the industrial revolution, a phenomenon that would eventually propagate over most of the modern world.

The search for energy to power machinery led to the requirement for mining and burning of fossil fuels. One of the main products of combustion of fossil fuels is carbon dioxide. Studies of trace gases in the atmosphere have noted that the concentration of carbon dioxide has risen by more than a third since the industrial revolution and is now rising faster than ever before. During the twentieth century there has been an observed global mean temperature rise of around 0.6 °C (White Paper 2003). Analysis of these two coinciding events has resulted in the now widely accepted theory of “the greenhouse effect”. The principles of the greenhouse effect are that trace gases in the atmosphere absorb infrared radiation emitted by the Earth’s surface, causing a warming of the atmosphere. This has traditionally been vital for maintaining temperatures for life to flourish. However, the burning of fossil fuels has upset the balance and a gradual increase in global temperatures has ensued. Carbon dioxide is thought to account for half of the warming effect associated with greenhouse-gas emissions (Shorrocks and Henderson 1990).

The IPCC report (2001) highlights projections that globally averaged surface temperatures are set to increase by 1.4 to 5.8 °C by 2100. Computer modelling (Graves and Phillipson 2000) has been used to predict that mean annual temperatures will increase by up to 2.4 °C by 2050 and up to 3.3 °C by 2080 in London. Climate change is already having a noticeable impact in the UK. Vidal and Brown (2003) summarised that *“drought stress in crops has increased sharply in the past 20 years, with farmers now saving irrigation water for higher value vegetables and salad crops. Climate change is already affecting foundations of buildings as the soil dries out, according to the Building Research Establishment. The government is also considering new regulations, particularly for tall buildings, so they can withstand higher wind speeds. A decade of sudden downpours, ferocious storms, flash floods and prolonged cloudbursts all consistent with global warming have provoked the government to increase spending on defending towns from river flooding by hundreds of millions of pounds. It has also raised the standard height of sea defences”*.

1.3 Government measures to reduce carbon dioxide emissions

UK carbon dioxide emissions currently account for about 2% of the global total (White Paper 2003). In 1997 the UK Government signed up to the Kyoto treaty. This stipulated that all ratified states would enter an agreement to either curb, or reduce their total CO₂ emissions, depending on the country's current output. The UK target was set at a 12.5% reduction of 1990 greenhouse gas emissions by the year 2008 – 2012. This covers a basket of six greenhouse gases (carbon dioxide, methane, nitrous oxide, hydro fluorocarbons, per fluorocarbons and sulphur hexafluoride), weighted for their global warming impact (Pout *et al.* 2002). In addition to this, the UK government imposed a

more stringent domestic target of reducing carbon dioxide emissions to 20% below 1990 levels by 2010.

A long term strategy was revealed in February 2003, when the Government released the White Paper entitled “Our energy future – creating a low carbon economy”. The target set by the Government is to reduce emissions of carbon dioxide by 60% by 2050. The target is based on a report by the Royal Commission for Environmental Pollution (2000), which estimates that reductions in the region of 60% relative to current day emissions would be required by 2050 to prevent CO₂ concentrations exceeding safe limits. It is hoped that this will be achieved by an increased reliance on renewable energy for production of electricity and a speeding up of changes to building regulations and setting tougher standards for energy efficiency in new homes, refurbishments and electrical products. Building energy use currently accounts for 46% of total UK energy consumption, resulting in the release of 66 million tonnes of carbon into the atmosphere (Pout *et al.* 2002).

To address the issues of energy use in buildings, the Approved Document Part L2 of the Building Regulations – Conservation of Fuel and Power was introduced on the 1st April 2002. For the first time a framework was proposed that would produce an assessment of the total energy performance of new buildings. Three different approaches; Elemental, Whole Building or Carbon Emissions Calculation Method could prove compliance in ascending order of complexity. The route chosen would satisfy Building Regulations at design stage. Upon completion of construction two performance measures were stipulated to assess the build quality of the finished product.

1.2 CO₂ emissions and climate change

Since the appearance of the human race on this planet, mankind has strived for progress to improve standards of living and remove subservience to the harsh environment. Throughout recorded history there has been a gradual progression towards what is now described as modern civilisation. The latter half of the eighteenth century in Britain saw a very rapid change from work carried out in the home with simple machines to industries in factories with power driven machinery. This was the beginning of the industrial revolution, a phenomenon that would eventually propagate over most of the modern world.

The search for energy to power machinery led to the requirement for mining and burning of fossil fuels. One of the main products of combustion of fossil fuels is carbon dioxide. Studies of trace gases in the atmosphere have noted that the concentration of carbon dioxide has risen by more than a third since the industrial revolution and is now rising faster than ever before. During the twentieth century there has been an observed global mean temperature rise of around 0.6 °C (White Paper 2003). Analysis of these two coinciding events has resulted in the now widely accepted theory of “the greenhouse effect”. The principles of the greenhouse effect are that trace gases in the atmosphere absorb infrared radiation emitted by the Earth’s surface, causing a warming of the atmosphere. This has traditionally been vital for maintaining temperatures for life to flourish. However, the burning of fossil fuels has upset the balance and a gradual increase in global temperatures has ensued. Carbon dioxide is thought to account for half of the warming effect associated with greenhouse-gas emissions (Shorrocks and Henderson 1990).

The first requirement was that insulation should be reasonably continuous and that excessive thermal bridging should be avoided. Submitting a certificate from a suitably qualified person that appropriate design details and building techniques have been used could satisfy this. Alternatively, an infrared thermographic inspection could be used to show that the insulation is reasonably continuous over the envelope.

The second requirement was that an airtightness performance assessment be made of the completed building envelope. For all non-domestic buildings with a gross floor area of greater than 1000m² an air leakage test would be required in accordance with CIBSE TM 23:2000 to prove that the construction was reasonably airtight. Prior to the Part L2 Regulations 2002, no requirement had been stipulated for the airtightness performance of the building envelope. Increased enthusiasm from the UK government to meet carbon dioxide emission reduction targets has deemed it necessary to bring forward the next revision of Part L of the Building Regulations to 2005. This will see tighter targets for building energy performance and airtightness of the building envelope (Office of the Deputy Prime Minister 2003) across a broader spectrum of the UK building stock.

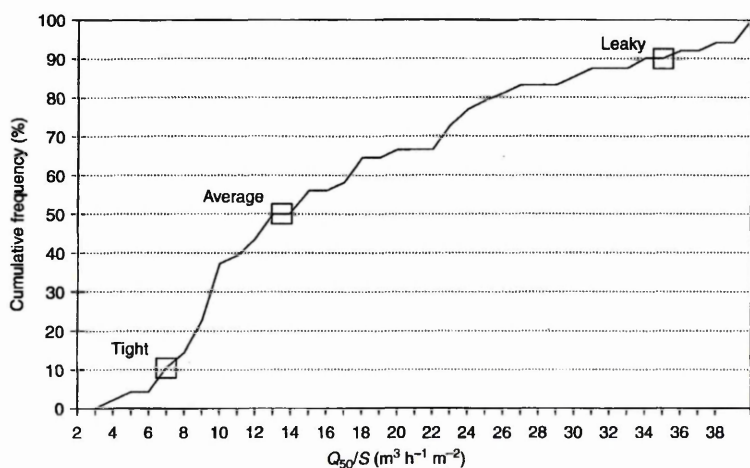


Figure 11 Sample size: $n = 384$.
 Mean value: $11.49 \text{ m}^3 \text{ h}^{-1} \text{ m}^{-2}$. Median
 value: $11.27 \text{ m}^3 \text{ h}^{-1} \text{ m}^{-2}$.

Figure 1. Airtightness of UK buildings
 Source: CIBSE TM23:2000

Growing concerns amongst the European Union of the energy use in buildings has resulted in the design and implementation of the EU Energy Performance of Buildings Directive (Council of the European Union 2002). The EU Directive notes that “the residential and tertiary sector, the majority of which are buildings, accounts for more than 40% of final energy consumption in the community and is expanding, a trend which is bound to increase its energy consumption and hence also its carbon dioxide emissions”. In response to this the Directive lays down the general framework for a methodology of calculation of the integrated energy performance of buildings, which may include airtightness standards for the building envelope. This culminates in a requirement for the application of minimum performance standards for the energy consumption of new buildings. The stipulation is also placed upon large existing buildings that are subject to renovation. All buildings subject to the EU Directive will be labelled with a transparent energy performance indicator, such as is currently seen on white electrical household goods.

1.4 The impact of air leakage in buildings on energy consumption

The improvements made in the thermal performance of building materials have raised the importance of designing and constructing less air leaky building envelopes. Air leakage in buildings is described as the unwanted infiltration and exfiltration of air. This can enter a building through a number of infiltration paths, usually located at junctions between elements in the building envelope. Perera *et al.* (1994) noted that heat loss associated with air leakage could account for 30% of heat loss through the building envelope. A recent study by the UK’s Air Infiltration and Ventilation Centre (Orme 2001) puts forward estimates of annual air change rates of commercial and residential buildings in 13 industrial countries, with the potential for reducing air change related

losses. Unnecessary ventilation was noted to account for two-thirds of the energy wastage through the loss of conditioned air.

The original design specification and the attention to detail during construction will determine the airtightness of a building envelope. The airtightness of a building will dictate the level of unintentional infiltration and exfiltration of air. The movement of colder external air into the interior of the building will create a thermal load. This thermal load is a function of the rate at which the air enters the building and the difference between the indoor and outdoor temperature (Jackman 1973). The figures for best practice airtightness levels in new UK buildings by Potter (2001) show that there is great scope for improvement of the construction of building envelopes. With the rapid rise in demand for air conditioning in offices and retail premises over the past 20 years (Scrace 2001), the need for airtight buildings is paramount.

1.5 Assessment of building infiltration rates

Air that enters a space comes from a combination of infiltrating and intentional sources. While the measurement of air flow rate through identifiable openings is possible by direct measurement, it is not practical to measure air flow through the many unknown gaps and cracks that may appear in the construction of the building, or to measure air flow rate through more than one or two purpose provided openings at a time (Liddament 1996). Amongst the field of air infiltration measurement techniques within buildings a number of methods are available. However the two that are most commonly used are the tracer gas and fan pressurisation assessment methods.

Tracer gas assessment involves the inserting of a seeded inert gas into a building and measuring the decay of concentration as mixing occurs with unseeded infiltrating air over time. Examples of the adaptation of tracer gas techniques to larger and more complex multi-cellular buildings can be found in Walker and Perera (1990) and Walker and White (1995). However, the use of tracer gas techniques can be a long and laborious task, with the estimation of building infiltration rates taking days or even weeks.



*Figure 2. Tracer gas equipment – gas bottle, sampler unit and bags.
Source: Walker and Perera 1990*

The fan pressurisation method entails the use of a fan to create a pressure differential across the envelope. The input of a constant flow rate to produce a steady state (DC) pressure differential is the currently accepted method (CIBSE TM23:2000). After fan set-up and building preparation, an airtightness test may take only ten minutes. Results for the airtightness of the building envelope are reported as an air leakage rate per

square metre of building envelope per hour at a reference differential pressure of 50 Pascal. From this airtightness result estimation can be made of the indicative infiltration rate, based on comparisons with data obtained from tracer gas techniques. Sherman and Grimsrud (1980) demonstrated the use of the fan pressurisation test to estimate building airtightness. This technique was used to determine the total leakage area of the structure. From this the infiltration rates were calculated for a variety of conditions. The steady state technique is the most commonly used method; however, other pressurisation assessment processes are available.

1.6 Airtightness testing methods

1.6.1 Steady state (DC) pressurisation techniques

Steady state (DC) assessment of building airtightness performance involves establishing a pressure difference Δp across the envelope. This can be achieved utilising portable fans temporarily installed in a doorway, or other suitable opening. HVAC plant is switched off and all external doors closed. Measurements taken of the flow rate Q across the fans and Δp across the envelope allow a relationship to be established between the two. In accordance with the current building regulations adherence to CIBSE TM23, this is defined in terms of the power law equation of the form:

$$Q = C (\Delta p)^n \quad (1.1)$$

where C and n are constants that are assumed to relate to the geometry of a single opening in the building envelope. The building envelope is subjected to differential pressures ranging from 20 up to 100 Pascal. If a pressure differential of at least 25 Pascal cannot be obtained, then the test is deemed to be invalid. Values for C and n are

calculated using least square regression analysis. The flow rate required to obtain a differential pressure is a function of the building envelope area. Very large buildings will therefore require a fan with a large volume flow rate.

1.6.2 Unsteady (AC) pressurisation techniques

Unsteady techniques (AC and pulse techniques) have been suggested as alternatives to the conventional steady state technique (Modera 1985, Nishioka 2000, Carey and Etheridge 2001). The theoretical advantage is that large expensive rigs would not be required and disruption to operations during building testing would be minimised. However, uncertainties introduced by the inertia of the flow through imperfections in the building envelope add increased complexity to the calculations and the technique is currently impractical for widespread commercial use. The DC technique is therefore preferable if an acceptable differential pressure is achievable across the building envelope.

1.7 Testing of large buildings

Available data for the airtightness of UK buildings is limited. Stephen (1998) noted that only two large scale databases of air leakage rates in UK dwellings are known: one held by British Gas plc and covering some 200 dwellings (Etheridge 1987); and the other held by BRE covering some 471 dwelling and 87 large panel system flats. No databases are currently available for larger non-domestic buildings.

Carey and Etheridge (2001) noted that previously available fan pressurisation rigs in the UK provided by BRE and BSRIA could not produce the flow rate to attain a satisfactory pressure difference across the envelope for larger buildings. The accuracy of the results would be affected as a result of pressure forces generated by buoyancy and wind.

“Large building” tests were previously classed as those carried out on structures with a floor area of up to only 5000m². Modern UK warehouses can have a floor area of 60,000m² or greater. Calls from CIBSE, BRE and BSRIA (Brundrett and Jackman (1997)) to produce a joint initiative aimed at improving building airtightness resulted in the introduction of mandatory testing in the UK. However, no progress was made with the testing of large buildings, such as the Bedford warehouse shown in figure 3, which has a floor area of nearly 60,000 m² and a volume of nearly 800,000 m³. This building will be one of the case studies analysed in Chapter 5.



Figure 3. Very large warehouse building, Bedford UK.

Computer simulations may be used to assess the effects of external conditions on the internal building environment. Boundary conditions can be established using the known variables of building thermal properties and external environmental conditions. Modern computer thermal analysis software allows for all conceivable component properties to be accounted for in the determination of thermal load upon a building. The level of thermal load determining the size of heating plant that must be installed. Software packages such as TAS (Kitson 2003) have been used to calculate the heating demands and specify plant for prestigious projects such as the Swiss Re building in London (Building Services Journal, June 2003).



For a given set of wind conditions (illustrated by pathlines) FLUENT predicts surface pressures (illustrated by contours) on the building exterior and external aerodynamic air flow characteristics ventilation

*Figure 4. Dynamic Thermal Computer Modelling used to assist in the specification of M and E plant at the Swiss Re building, London.
Source: Kitson 2003*

Infiltration is a variable that will be instrumental in the calculation of building heating demands. However, due to limited data on building airtightness, values are assumed as a rule of thumb (Boushear 2001). This may lead to inaccuracies and under or over-sizing of heating plant. Over sizing may be a problem, particularly in new buildings that have been constructed to a demanding airtightness specification. Stuart Borland, director of Building Sciences Ltd, claimed that in one case the M and E plant was halved in size because the designers knew the building would be pressure tested (Stephen 2002). Using currently available technology it is possible to compile building envelope performance data obtained from building airtightness tests and comprehensive building component data available in O and M manuals. The parameters may be used to assess the effect of the external environment on internal building conditions. The data sets obtained may be inputted in computer thermal modelling software and a simulation run with a weather data file to calculate the heating load placed on the building during a heating season. From this simulation it may be possible to more accurately assess heating requirements for plant sizing.

1.9 Aims and structure of the study

In Chapter 2 of the study a review will be made of the historical airtightness of buildings in the UK and abroad. This will be followed by a summary of the heat loss from a building and envelope degradation associated with air leakage. The literature review will also include a chronological account of airtightness testing regulations and recommendations in the UK and internationally.

Chapter 3 will highlight the theory used to support airtightness testing of buildings; beginning with an overview of steady state and dynamic pressure measurement

techniques. Methods for calculation and interpretation of results will be presented along with an assessment of infiltration heat loss and the equivalent leakage area calculation. Finally, previous research into the repeatability of airtightness tests will be highlighted.

Chapter 4 will give an insight into the methodology required for the creation and calibration of a large test rig. A review of the design and construction process for the large test rig, along with lessons learned from mistakes will be provided. Required equipment and methodology for the calibration of the rig will also be presented. The practical requirements for airtightness testing will also be noted, with particular reference to the testing of large and very large buildings. Finally, a summary will be made of some remedial sealing measures that are currently in use on new and refurbished buildings.

Chapter 5 will report on the field testing of one large and two very large UK buildings. In chapter 6 the output graphs and tables from the field data will be presented. A brief interpretation of the results will be given.

Chapter 7 will summarise the computer modelling work carried out in conjunction with Hilson Moran consulting engineers. Airtightness data obtained from the testing of a very large warehouse will be input into a currently available computer thermal-modelling program along with available building envelope thermal data. Simulations will be run to assess the thermal loads imposed on the building during the heating season. One simulation will be run with the building airtightness specification utilised at the design stage (Current Building Regulations standard). The second simulation will be run with a building airtightness specification actually achieved during the building test.

Chapter 8 will firstly discuss the viability of testing very large buildings in the UK. The current information available on the airtightness of large warehouses in the UK will be summarised. Following this, analysis of the energy saving associated with the improved envelope airtightness observed at the very large warehouse will be given. Finally, an investigation into the further work that can be carried out into the impact of energy savings with improved envelope airtightness will be presented.

Chapter 2 Literature review

2.1 *Historical airtightness of buildings*

Early measurements of airtightness in dwellings entailed small fans mounted in doorways, known as “blower door fans”. Blower door technology was first used in Sweden as a window mounted fan to test the tightness of building envelopes (Blomsterberg 1977). Sherman and Grimsrud (1980) noted the disadvantages of tracer gas methods and devised a technique using fan pressurisation results and weather data to calculate infiltration.

Potter *et al.* (1995) carried out airtightness on twelve large UK office buildings with volumes ranging from 1,951 m³ to 44,335 m³. The average normalised leakage of the structures was found to be 21.8 m³h⁻¹m⁻². Naturally ventilated buildings were found to be tighter (17.40 m³h⁻¹m⁻²) than air-conditioned buildings (23.98 m³h⁻¹m⁻²). Pre 1990 buildings (17.81 m³h⁻¹m⁻²) were found to be tighter than post 1990 buildings (24.62 m³h⁻¹m⁻²). They summarised that a UK office could have an air leakage performance anywhere between 10 and 40 m³h⁻¹m⁻². Potter (1992) also found the average air leakage of a UK factory/warehouse building to be 35.68 m³h⁻¹m⁻².

Stephen (1998) noted that UK dwellings built since about 1980 do appear to be more airtight (on average) than those built since the 1930's. He attributed this to fewer chimneys and adoption of energy efficiency measures. The same trend comparing post 1980 houses with pre 1980 was also noted in the USA (Sherman 1990), no reasons for this were specified. Further work was carried out in the USA (Sherman and Dickerhoff 1998) on much larger datasets that represented much more comprehensive cross-

sections of homes in particular locations than had not previously been studied. They discovered that USA dwellings were leakier than previously estimated. Furthermore the datasets studied showed that less than 10% of dwellings in the U.S. would meet ASHRAE's airtightness standard (1988).

2.2 Building heat loss and envelope degradation associated with air leakage

Warm conditioned air exfiltrating through the building envelope causes more problems than just greater heating requirements. Studies on rural hospitals in the province of Alberta, Canada (Ogle and Connor 1995) have shown that a lack of airtightness may result in serious building envelope problems. This is particularly true for non-domestic types of buildings, which can be humidified and pressurised by a mechanical HVAC system. Potter and Jones (1992) analysed the effects of environmental conditions on energy usage on a sample of factories and warehouses using the "CRKFLO" computer program. This software calculates the flow rates between components, taking into account inside/outside temperature differences and wind effects on the building.

2.3 Airtightness testing in the UK and internationally

In an AIVC review (Colthorpe 1990) assessed the building airtightness and ventilation standards in various European countries. All countries analysed stipulated minimum air change for ventilation requirements, with most countries producing a methodology for calculation of energy use. Legislation for airtightness of building fabric varied from non-existent to extremely stringent. A summary for the airtightness requirements for each country was: -

Sweden

The average air leakage coefficient, for that part of the enclosed surface that forms part of the enclosing surface which forms the boundary with outdoor air or an unheated area may not exceed $3 \text{ m}^3\text{h}^{-1}\text{m}^{-2}$ for dwellings and $6 \text{ m}^3\text{h}^{-1}\text{m}^{-2}$ for other premises at a pressure difference of 50 Pa. The air test results were taken as averages of the pressurisation tests at 50 Pa (Q_{50}). Alongside airtightness requirements, stipulation was also enforced for minimum air exchanges to maintain air quality.

Denmark

The Danish Building Regulations 1982 give construction standards for all new buildings, to a high level of energy efficiency. These standards were also being applied to existing building stock under the 1981 Act on reduction of energy consumption in buildings, issued by the Danish government. No requirement was in place to test whole buildings, though component testing was specified.

Finland

Whilst air sealing of fabric and windows was considered, there were no numerical values for acceptable building airtightness in the building codes. However, thermal insulation regulations require that the airtightness had to be good enough to comply with the thermal indoor climate guidelines. Classification of window airtightness was voluntary, but widely used amongst manufacturers and builders.

Belgium

National standards were in place for the public building sector, which comprised 30% of the building stock. There were no overall airtightness requirements for whole buildings. Windows were classed in groups according to their air leakage performance

and degree of exposure i.e. height of building in which the window is situated.

Maximum air permeability rates for joints were set at each exposure level.

Canada

Standards were in place to determine the airtightness of buildings by the fan depressurisation method. There was no legal requirement to test whole buildings. However, testing of windows and doors was mandatory with maximum air leakage rates set for different component ratings.

Germany

No regulations in place for airtightness testing of buildings. However standards in place classified windows by exposure level and gave acceptable air permeability values for each group under pressure. Standards were also available making recommendations for sealing joints and installing vapour barriers, with further standards for wind resistance tests etc.

Italy

Testing was in place for building components. Recommendations were also made for the airtightness testing of whole buildings.

Table 1. Requirements and recommendations for airtightness and ventilation rates in some countries.

Source: AIVC 1990

	Scandinavia				Europe					America	Far East			
	Den.	Fin.	Nor.	Swe.	Belg.	Fra.	Ita.	Neth.	Swi.	UK.	FRG.	Can.	USA.	N.Z.
Airtightness:														
Components	W	R	R	N	W	-	W	W	W	W	W	W+D	W+D	W
Whole Buildings	N	R	R	R	N	-	R	N ¹	R	N	N	N ¹	N ¹	N
Minimum Ventilation Rates:														
Dwellings	R	R	R	R	R ³	R	R	R	N ²	R	R	R	R	N ²
Other (Industrial/Commercial)	R	R	R	R	-	-	R	R	R ⁵	R	R	R	R	N ⁴
<p>Key: R = Recommendation exists N = No recommendation exists W = Recommendation for windows only W+D = Recommendation for doors and windows only</p> <p>1 Draft standard in preparation 2 Recommendations exist for internal kitchens, bathrooms, toilets. 3 A voluntary standard that may soon be replaced. 4 Government legislation exists for bathrooms, toilets and laundries. 5 Only for some types of rooms.</p>														

Country Abbreviations:

Den:Denmark; Fin:Finland; Nor:Norway; Swe:Sweden; Belg:Belgium; Fra:France; Ita:Italy; Neth:Netherlands; Switz:Switzerland; UK:United Kingdom; FRG:West Germany; Can:Canada; USA:United States of America; NZ:New Zealand.

Table 2. Overview of Airtightness Levels in Standards and Regulations in 1994.

Source: AIVC 1994

Country	Whole Building	Components	
		Windows	Doors
Belgium	< 3ach for dwellings fitted with bal.mech.at 50 Pa. <1 ach when heat rec.is fitted at 50 Pa.	2 - 6 m ³ /h per metre length of crack at 100Pa	20-40 m ³ /h per door at 10 or 50 Pa.
Canada	Maximum 1.5 ach at 50 Pa (For HUDAC constructed dwelling)	Extreme 0.25 - 8.35 m ³ /h.m at 75 Pa Normal 0.55 - 2.79 m ³ /h.m at 75 Pa	2.54 l/s .m ² of door area at 75 Pa
Denmark		0.5 dm ³ /s.m length of joint at 30 Pa 0.4 - 0.7 ach for dwellings	0.50 dm ³ /s.m length of crack at 50 Pa
Finland		<0.5 - >2.5 m ³ /h. m ² at 50 Pa	
France	Max. 0.2 ach for non residential buildings	<7.0 - 60 m ³ /h. m ² at 100 Pa	<7 - 60 m ³ /h. m ² at 100 Pa
Germany		1 - 20 m ³ /h. m length of joint depending upon exposure level over the pressure range 10 -1000 Pa	
Italy	1 m ² of envelope should not exceed 10 m ³ /h at 98 Pa 1.5 - 5.0 ach for schools	1.4 - 8.0 m ³ /h. m (Crack) at 50 Pa 4.8 - 31 m ³ /h. m ² (Area) at 50 Pa	
Netherlands	Class 1 Max. 100 - 200 dm ³ /s at 10 Pa (1.4 - 2.24 ACH at 10 Pa) Class 1 Min. 30 - 50 dm ³ /s (0.4 - 0.72 ACH at 10 Pa) Class 2 Max. upto 80 dm ³ /s (0.72 - 1.15 ACH at 10 Pa)	2.5 dm ³ /s per m length of crack at 75 Pa 0.5 dm ³ /s per 100 mm of frame section	
New Zealand		0.6 - 4.0 dm ³ /s. m of joint at 150 Pa 2.0 - 17.0 dm ³ /s .m ² window area at 150 Pa	
Norway	1.5 - 4.0 ach at 50 Pa		
Sweden	3 - 6 m ³ /h m ² at 50 Pa		
Switzerland	Lower limit 2 - 2.5 ach at 50 Pa Upper limit 3 - 4.5 ach at 50 Pa. NOTE Upper limit for Buildings with balanced mech. is 1 ACH at 50 Pa	0.2 m ³ /h.m at 1 Pa (When n=0.66) (a)5.65 m ³ /h.m at 150 Pa (b)8.95 m ³ /h.m at 300 Pa (c)14.25 m ³ /h.m at 600 Pa	
United Kingdom		1.22 - 6.2 at 50 Pa m ³ /h m of open joint	
United States of America	Normalised leakage range taken from measurements at 4 Pa ELA for whole of USA. From <0.1 - 1.60 (from ASHRAE 119-1988, APP.B ACH=Ln. Therefore <0.1 to 1.6 ach) NOTE: Standard requires no part of US to be tighter than 0.28 (only small part of upper midwest) Mostly the tightness requirement is 0.4.	0.77 dm ³ /s per m of sash at 75 Pa	2.5 - 6.35 dm ³ /per m ² area at 75 Pa 17.0 dm ³ /s per m length of crack at 75 Pa

In the UK (England and Wales), an air permeability target of $10\text{m}^3\text{h}^{-1}\text{m}^{-2}$ was introduced on April 1st 2002 for all new non-domestic buildings with a floor area greater than 1000m^2 in the Approved Document Part L2. A period of leniency was granted up to the 30th September 2003 in which a building with an originally unsatisfactory test would have to undergo appropriate remedial work and a retest to show that: -

- (i) an improvement of 75% of the difference between the initial test result and the target standard of $10\text{m}^3\text{h}^{-1}\text{m}^{-2}$ at 50 Pa; or, if less demanding
- (ii) a performance no worse than $11.5\text{m}^3\text{h}^{-1}\text{m}^{-2}$ at 50 Pa.

The Building Regulations Part J were introduced in Scotland during the same period. Methods were identified for the conservation of fuel and power, although there was no mandatory requirement to airtight buildings. Some enlightened clients, such as IKEA have chosen to airtight their Scottish based stores, despite there being no legal requirement.

Stephens (2002) noted that before its introduction into the building regulations it was estimated that fewer than 5% of buildings were pressure tested. Implementation and enforcement of the new airtightness testing regulations in England and Wales has been slow and largely uncoordinated. In a survey of new buildings identified by the Glennigans database, HRS Services Ltd estimated that only 30% of projects were subject to an airtight test upon completion of the envelope. This has not been helped by factors such as Billington (2001) in his manual to the building regulations, in which he states "Construction, offers insulation continuity thermography and air pressure testing as options to show compliance but it is expected that designers and contractors will

prefer to use the new robust details”. In response to the increasing confusion surrounding the requirements for airtightness testing of buildings, King (2003) of the Building Regulations Division at the Office of the Deputy Prime Minister wrote a letter of clarification, for circulation amongst the industry. In this he states that, *“The current introduction to AD L2 says there is no obligation to adopt any particular solution contained in an Approved Document if you prefer to meet the relevant requirements in some other way. However, the underlying objective remains the achievement of a fabric performance that – if put to a pressure test – would achieve the performance standard. In relation to larger buildings, the AD offers no alternative to pressure testing as a way of showing compliance with the airtightness aspect of Part L2”*.

2.4 Testing very large buildings

The ease of testing dwellings with blower door fans has meant that some data are available for the airtightness of residences. The commercial realities of testing large buildings have meant that there is very little data available for industrial buildings. British Gas carried out pressurisation tests on seven “large” buildings, with volumes ranging from 660 to 12,600m³ (Lilly 1987). Measurements were made with four Watson House leakage testers used in parallel. Each unit was capable of producing a maximum flow rate of 1.25m³s⁻¹ at 50 Pa. The study noted that measurements of the buildings under test required pressurisation equipment sufficient to generate flow rates in excess of 65,000m³h⁻¹. The conclusion was that it was impractical to pressurise most industrial buildings larger than 5000 to 10,000m³ in volume to a pressure of 50 Pa. However, the author illustrated the fact that a purpose built leakage tester for large buildings was now in operation to generate 50 Pa pressure differences at flow rates of up to 150,000m³h⁻¹.

Potter and Jones (1992) documented the improvements that could be made to buildings using basic sealing techniques. Perera *et al.* (1994) highlighted the following areas as the main sources of air leakage.

1. **At junctions between main structural elements;** wall to roof junctions, wall to floor junctions, wall to foundation junctions, junctions between parapets and roofs.
2. **At joints between walling components;** sealant or gasketed joints between heavyweight or curtain walling panels, overlapping joints between lightweight sheet metal wall panels and at boundaries of different cladding/walling systems.
3. **Around windows, doors and rooflights;** between window or doorframes and walls or floors, between doors and windows and their frames, between frames and sills.
4. **Through gaps in membranes, linings and finishes;** in wall membranes and dry linings, in ceiling linings and boundaries with wall linings, gaps in floor finishes and around skirtings
5. **At service penetrations;** electrical sockets and conduits, gas and electricity entry points, ventilation pipes for sanitary waste, overflow pipes and flues.
6. **Around access and emergency openings;** to roof space, to roof, to floors, to services and delivery points.

Through permeable materials; some materials, such as brickwork cladding, are not impermeable to air, and may be very permeable if construction quality is low.

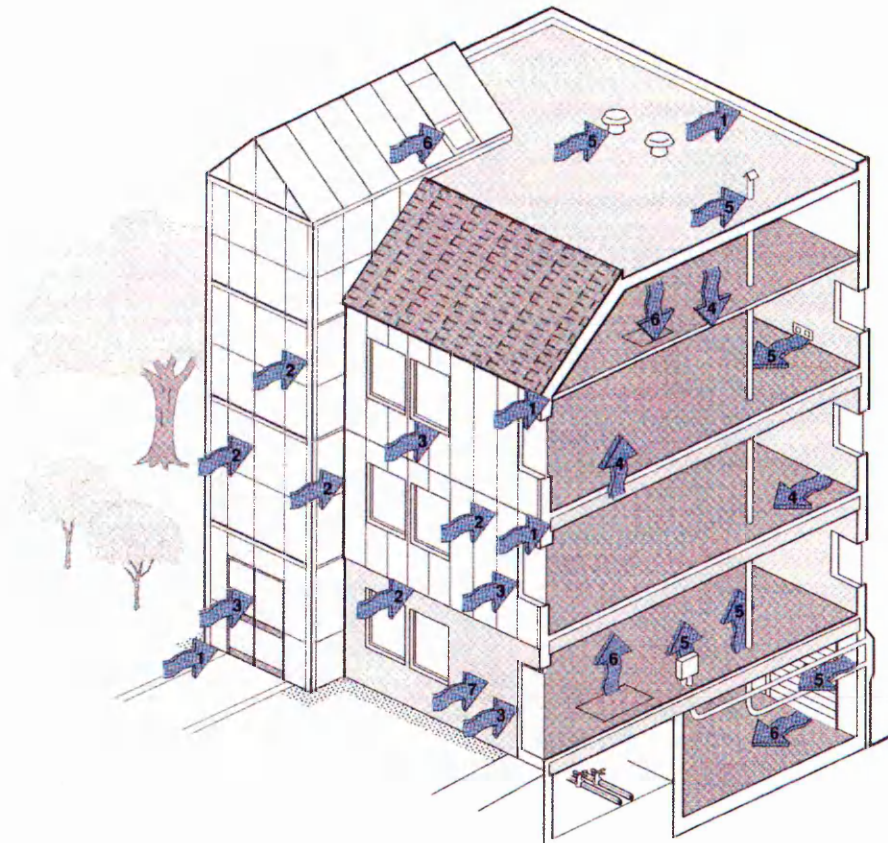


Figure 5. Potential air leakage pathways in generic office building

Source: Perera et al. 1994

2.5 *Summary*

This chapter has outlined the origins of building airtightness testing and has given an overview of the historical airtightness of buildings in the UK and abroad. An account has been made of the regulations and recommendations in force for the testing of buildings in the aforementioned countries. An introduction has also been provided into the major sources of building air leakage. The following chapter will summarise the theory used to support the airtightness testing of buildings. Methods for calculation and interpretation of results will be presented, along with an assessment of infiltration heat loss and the equivalent leakage area.

Chapter 3 Theory

3.1 *Steady state pressure measurements*

Steady state (DC) assessment of building airtightness performance involves establishing a pressure difference Δp across the envelope. This can be achieved utilising portable fans temporarily installed in a doorway, or other suitable opening. HVAC plant is switched off and all external doors closed. Measurements taken of the flow rate Q across the fans and Δp across the envelope allow a relationship to be established between the two. This can be defined in terms of the power law equation given in Chapter 1:

$$Q = C (\Delta p)^n \quad (1.1)$$

where C and n are constants that are assumed to relate to the geometry of a single opening in the building envelope. The building envelope is subjected to differential pressures ranging from 20 up to 100 Pascal. If a pressure differential of at least 25 Pascal cannot be obtained then the test is deemed to be invalid. Values for C and n are calculated using least square regression analysis. The flow rate required to obtain a differential pressure is a function of the building envelope area. Very large buildings will therefore require a fan with a large volume flow rate.

3.2 *Least square power law*

The results from a steady state building test will give a dataset comprising of building differential pressures (ΔP_{env}) and corresponding fan flow rates (Q). There are a number of curve fitting approximations available to produce a best fit line between these points.

The most straightforward of these is the least squares approximation. For this, the straight line

$$y = mx + b \quad (3.1)$$

should be fitted through the given points $(x_1, y_1), \dots, (x_n, y_n)$ so that the sum of the squares of the distances of those points from the straight line is minimum, where the distance is measured in the vertical direction (the y-direction).

The calculation of the factors m and b for a given pressurisation test are as follows:-

$$dSumXY = \sum(\ln \Delta P_{env} * \ln Q_c) \quad (3.2)$$

$$dSumXX = \sum(\ln \Delta P_{env} * \ln \Delta P_{env}) \quad (3.3)$$

$$dSumX = \sum(\ln \Delta P_{env}) \quad (3.4)$$

$$dSumY = \sum(\ln Q_c) \quad (3.5)$$

$$m = (dSumX * dSumY - Numpnts * dSumXY) / (dSumX * dSumX - dSumXX * Numpnts) \quad (3.6)$$

$$b = (dSumX * dSumXY - dSumXX * dSumY) / (dSumX * dSumX - dSumXX * Numpnts) \quad (3.7)$$

3.3 *Air leakage index vs. air permeability calculation methods*

Building pressure tests using the steady state (DC) method are usually reported at a reference internal to external building pressure of 50 Pascal. The flow rate through the fan(s) required to maintain this pressure is known as Q_{50} . When the fan(s) used are only capable of producing a low flow rate (Orme 1995) then the reference pressure for calculations may be set at 25 Pascal, with a fan flow rate recorded at Q_{25} . Tests to large buildings have traditionally required a minimum building pressure of 25 Pascal with the recorded data extrapolated to 50 Pascal to give a result at fan flow rate Q_{50} (CIBSE TM23:2000).

There are two criteria that may be used to report an airtightness test using steady state techniques. These are the air leakage index and air permeability index of a building. Both methods of calculation entail the determination of fan flow rate $Q \text{ m}^3\text{s}^{-1}$ into the building at a reference pressure of 50 Pascal. Q is then multiplied by 3600 to give the flow rate $Q \text{ m}^3\text{h}^{-1}$. This figure is then divided by the externally exposed envelope area of the building under test to give a result of $X \text{ m}^3\text{h}^{-1}\text{m}^{-2}$. It is the definition of envelope area that determines the criteria. The air leakage index entails the summation of the surface area of the walls and roof exposed to the external environment to calculate the envelope area. The air permeability of the building is devised by summation of the surface area of the solid ground floor, walls and roof. The calculations are as follows: -

Calculation of Air Leakage Index, ALI

$$Q_{50} = C * (50)^n \quad (3.8)$$

$$\text{Air Leakage Index} = 3600 * Q_{50} / S \quad (3.9)$$

Calculation of Air Leakage Permeability Index, API

$$Q_{50} = C * (\Delta P)^n \quad (3.10)$$

$$\text{Air Permeability Index} = 3600 * Q_{API} / S + F \quad (3.11)$$

Where S = exposed surface area of walls + roof

F = area of solid ground floor

In the UK, measurements have traditionally been reported using the air leakage index criteria (Potter and Jones 1992, Potter 1998). The vast majority of new buildings include a virtually impermeable concrete floor, therefore making the air leakage index a more stringent standard. As a rough approximation an air permeability result of $10 \text{ m}^3\text{h}^{-1}\text{m}^{-2}$ would equate to an air leakage index of $14 \text{ m}^3\text{h}^{-1}\text{m}^{-2}$. This relationship is wholly dependent on the design of the building.

The current Part L Building Regulations specify the air permeability calculation method as the criterion for testing of new buildings. This is in line with CIBSE TM23: 2000 and the CEN 13829 standard upon which it is based. Potter (2000) argues that the air permeability criterion is not a fair method upon which to judge the envelope airtightness performance of new buildings. He states that “If one compares office buildings of single storey, five storey and ten storey with the same net floor area with an air permeability of $10 \text{ m}^3\text{h}^{-1}\text{m}^{-2}$, then the single storey building would have to be considerably less airtight than multi-storey buildings. Equally large footprint buildings need to be less airtight than smaller ones”. Testing by HRS Service Ltd has shown that large warehouses and retail buildings can easily pass current building regulations with little attention to airtightness during construction (see Section 5.2).

3.4 Effective leakage area

The total leakage area for a building can be represented as an effective leakage area, ELA, which represents a single opening having the same airflow leakage. This can be helpful on site to conceptualise the amount of further sealing required to attain a building airtightness specification. The effective leakage area is calculated from:-

$$ELA = Q * ((\rho/2\Delta p)^{0.5}/C_D) \quad (3.12)$$

Q = airflow rate (m³ s⁻¹)

ρ = air density (kg m⁻³)

ΔP = pressure difference across the opening (Pa)

0.5 = exponent for large openings

C_D = discharge coefficient (set to 1.0 or ≈ 0.6 depending on the shape of the orifice)

The reference pressure differential across the building envelope during an airtightness test is 50 Pa. Naturally occurring pressures from wind are generally much lower than this. For this reason it is normal to quote the effective leakage area at between 4 Pa and 10 Pa (ASHRAE Fundamentals Handbook 2001). The value of Q at these low pressure differences may be extrapolated down from those during the test using the flow equation (1). Transforming the power law equation using natural logarithms gives:-

$$\ln(Q) = \ln(C) + n.\ln(\Delta P) \quad (3.13)$$

3.5 Calculation of infiltration heat loss

The natural air change rate of a building may be roughly calculated from an air leakage test. For domestic buildings it has been found that the natural air change rate (infiltration) is approximately equal to 1/20 of the 50 Pa air leakage rate. With the air leakage rate equal to Q₅₀/V (Q₅₀ being the leakage airflow rate per hour at a pressure differential of 50 Pa across the building envelope and V being the internal volume of the building). The association will become stronger with an increasingly airtight building. On a very leaky building it is very difficult to estimate the air change rate.

This 1/20th calculation for domestic buildings has not been effective in modelling the air change rates of non-domestic buildings. The BRE have carried out research, using tracer gas techniques, into this area and have found that the relationship is improved by incorporating the surface to volume ratio of the building into the calculation. This gives the relationship of

$$I = 1/20 * S/V * Q^{50}/S \quad (3.14)$$

- I = infiltration rate in air changes per hour (h⁻¹)
- S = exposed surface area of walls and roof (m²)
- V = internal volume of the building envelope (m³)

Equation 3.13 was found by HRS to give some low values for air change rate on buildings tested in comparison to BSRIA rules of thumb (Boushear 2001). The simplified form for this equation was found to give a more reasonable estimation.

$$I = 1/60 * Q^{50}/S \quad (3.15)$$

Using the air infiltration rates calculated from the previous equation, an approximation of the thermal load can thus be calculated using the following equation

$$E = \sum_{I=1}^{\text{total no of hours}} 3600\rho c_p Q_i (T_{\text{int}(I)} - T_{\text{ext}(I)}) \quad (J) \quad (3.16)$$

E	= thermal load	(J)
ρ	= air density	(kg/m ³)
C _p	= specific heat capacity of air	(J/kg. K)
Q _I	= combined air infiltration and ventilation rate at hour	(m ³ /s)
T _{int(I)}	= indoor air temperature at hour, I,	(K)
T _{ext(I)}	= outdoor air temperature at hour, I,	(K)

This may be approximated, assuming a constant air change rate and representing temperature variation by degree-days.

$$E = Q \cdot DD \cdot 24 \cdot 3600 \rho C_p \quad (J) \quad (3.17)$$

where DD = number of degree days

The degree-day measurement is a method of tracking and evaluating the difference between the internal and external temperatures. It is calculated by averaging the number of degrees temperature difference over a day, that the external temperature is below a set base internal temperature (usually assumed to be 15.5 °C). Degree-day data may be obtained from the Internet at the Vilnis Vesma web site (www.vesma.com).

3.6 *Repeatability of airtightness tests*

Air leakage measurements carried out at intervals in a heated but unoccupied test house at the BRE Garston site over a period of eighteen months clearly indicated an increase in air leakage rate of some 25% during the winter compared with the summer (Warren & Webb 1980). Persily (1982) also found a seasonal variation of the order of 25%.

This was attributed to changes in the moisture content of the building materials caused by yearly variations in the moisture content of outside air. However, Dickinson and Feustel (1985) found no significant correlation between the moisture content of wood components on the exterior and interior of the building and the seasonal swing in airtightness.

3.7 *Summary*

This chapter has highlighted the theory used to support the airtightness testing of buildings. Methods for the calculation and interpretation of results have been presented along with an assessment of infiltration heat loss and the equivalent leakage area calculation. A brief outline of the repeatability of results has also been presented. The following chapter will give an insight into the methodology required for the creation and calibration of a large test rig. A review of the design and construction process for the large test rig, along with lessons learned from mistakes will be provided. The practical requirements for airtightness testing will also be noted, with particular reference to the testing of large and very large buildings. A summary will then be presented of some remedial sealing measures that are currently in use on new and refurbished buildings.

4.1 Design and construction of large test rig

The size of building that can be airtightness tested using a steady state (DC) pressurisation technique is partly a function of the maximum flow rate Q that can be produced by the test rig. Previous trailer mounted rigs designed and constructed by the BRE and BSRIA had a maximum flow rate of $30 \text{ m}^3\text{s}^{-1}$. This imposed a limit on the size of building that could be tested with just one rig.

The author underwent a two year placement with HRS Services Limited as part of a Teaching Company Scheme. The aforementioned is a specialist construction company, with a decade of experience of sealing buildings to best practice levels of airtightness. Their main focus has been on the supermarket retail industry, who recognise the benefits for both energy consumption and thermal comfort. With knowledge of airtightness requirements and air test procedures, HRS Services limited decided to produce their own rigs. Through the support of the author these rigs were designed and calibrated to recognised British Standards. It was noted by the author that there was a current upper size limit for buildings in the UK that could be tested using the currently available equipment. It was therefore decided to design, construct and calibrate a rig that would be considerably larger than those used by existing airtightness testing companies.

When designing the very large test rig it was necessary to take into account many practical considerations. The rig and all equipment required to power it would need to

be contained on a 7.5 tonne lorry. This would allow personnel to transport the rig using a standard UK driving licence. The maximum diameter of the rig would be limited by the height of a standard building double doorway (2000 mm) and would require a means of connection from ground level to the height of the rear of the lorry. Transport would also be required on the rig for up to five personnel. A team of this size would be needed to seal the large array of mechanical ventilation on the roofs of some very large buildings. Storage room was also required for temporary sealing materials, door screens and smoke testing machines.

The 2000 mm fan required for the rig was purchased from Elta fans Ltd. Power demand and volume flow output data supplied by the manufacturer highlighted the requirement for a power source with an output of 90 kW to produce a volume flow rate of $90 \text{ m}^3 \text{ s}^{-1}$ (Figure 6). To achieve this level of output it was deemed necessary to employ a 5-litre diesel “donkey” engine, separate from the main vehicles power supply. A hydraulic system would then be incorporated to transfer power from the diesel engine to the 2000-mm fan at the rear of the vehicle.

Figure 6. Absorbed power (kW) vs. volume flow output rate ($\text{m}^3 \text{ s}^{-1}$) for various fan blade angles

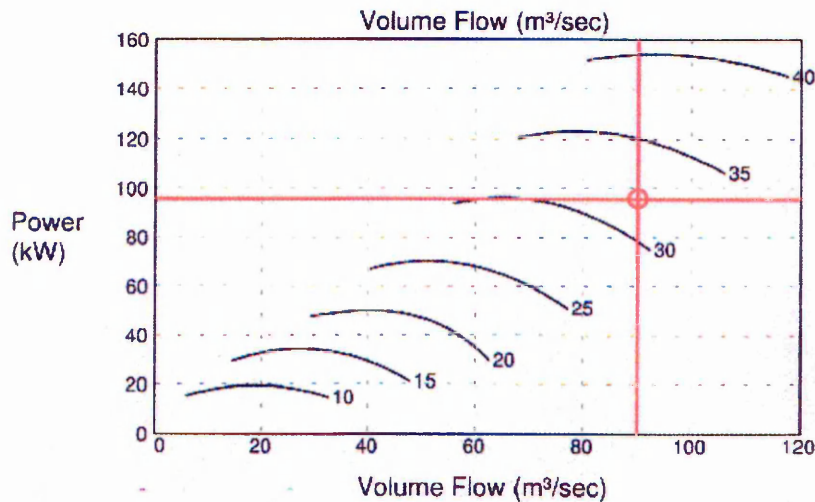


Figure 7. Volume flow rates achieved with different fan sizes through the manufacturer's range

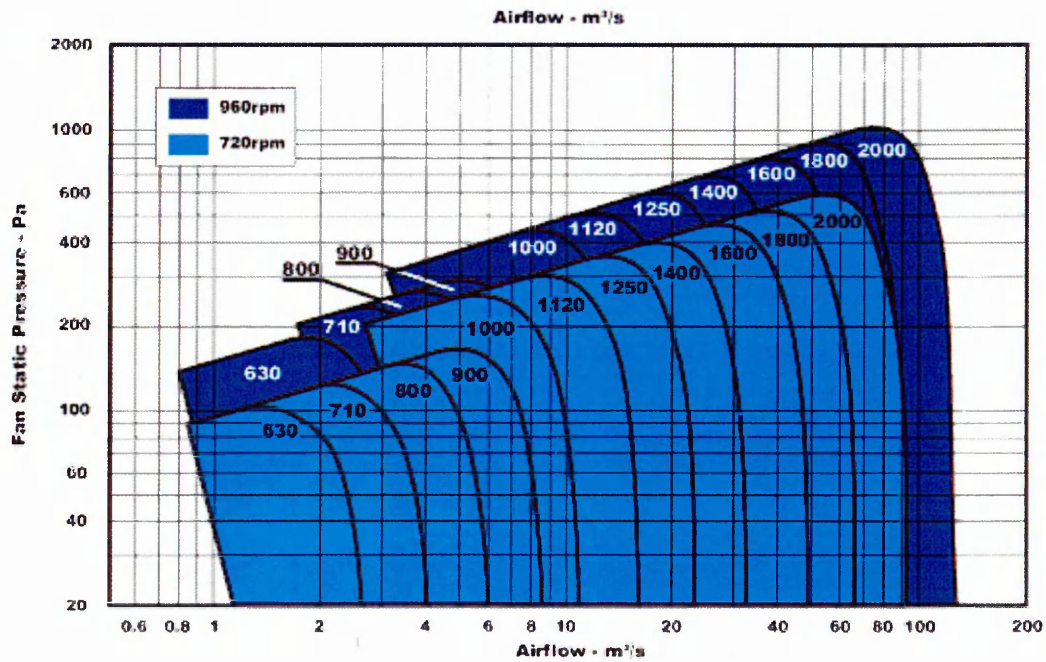


Figure 8 shows a side elevation of the lorry on which the plant was to be mounted. In addition to the driver's cab at the front of the vehicle, a sleeper cab was added. This increased the space available for transport from two to five personnel. The diesel donkey engine was to be mounted centrally between the front and rear wheels, at the point where the spare is indicated in Figure 8. The hydraulic pump, oil reservoir and air intake fan and grills would also be situated at this location. The diesel engine and hydraulic system would be housed in a boxed unit. This housing would also be large enough to contain all sundries required for carrying out the air tests.

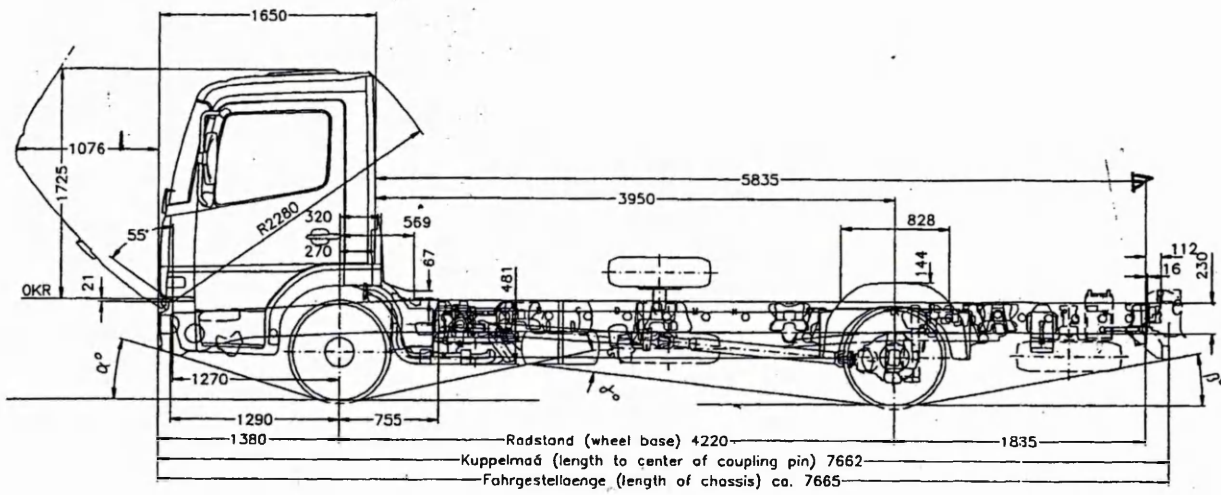


Figure 8. Transport lorry side elevation dimensions

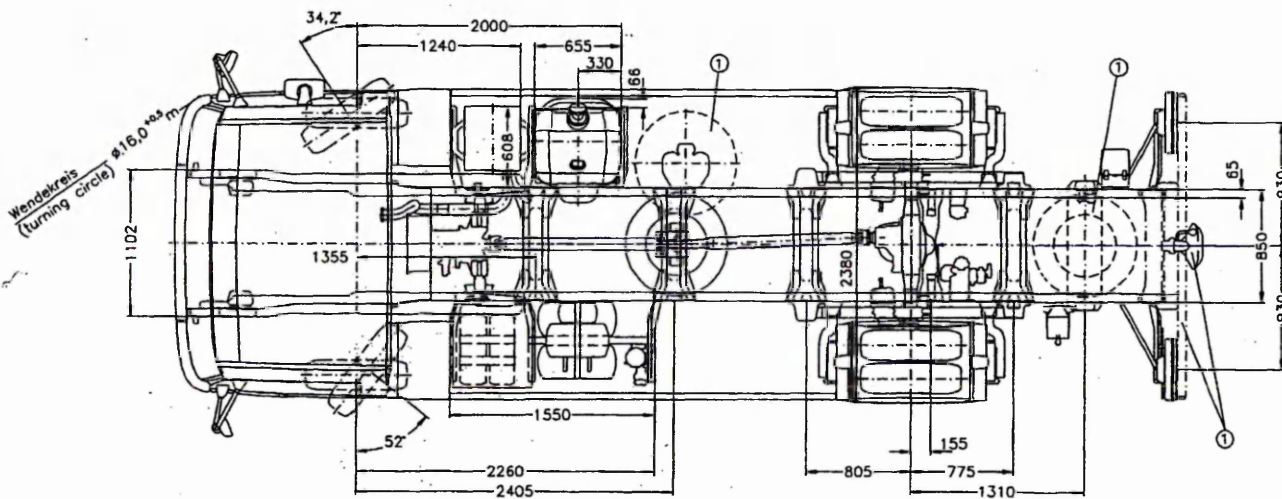


Figure 9. Transport lorry plan dimensions

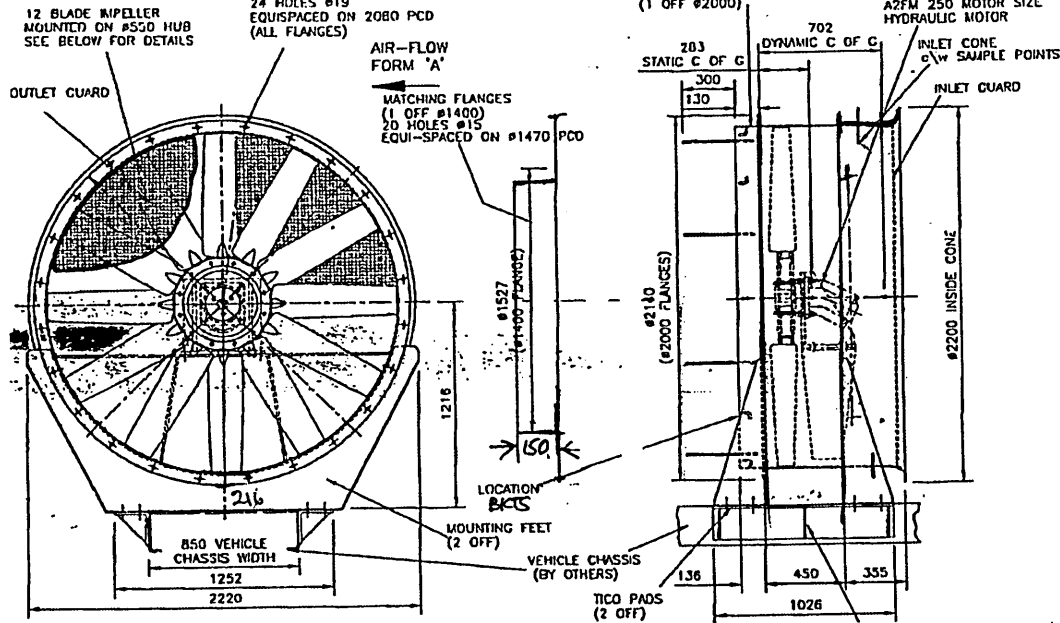


Figure 10. 2000 mm fan details.

The 2000-mm fan (figure 10) would be mounted at the rear of the vehicle on the tail plate. Hydraulic hoses would transport oil at up to 200-bar pressure from the reservoir to the fan system. For connection of the fan system to the door screens, it was decided that a flexible duct arrangement was most suitable. Two x 3 metre and one x 2 metre lengths were constructed, giving a cumulative length of eight metres. This would allow the rig to be parked at a reasonable distance from the building under test to avoid bollards and other items restricting access. The angle of the duct between the height of the fan off the ground (1.2 m) and floor level at the door entrance would also be minimised, to avoid restricting airflow at the fan outlet. The ducting would be stored in the donkey engine housing along with the other air testing sundries.

On completion of the test rig, it was noted that the front of the vehicle was sitting lower than the rear of the vehicle. Measurements of the vehicle weights on front and rear axles confirmed fears that too much load was being placed at the front of the vehicle. This meant that the vehicle and rig were not road legal. It was decided by the author that

the remedy would be to move the position of the donkey engine and housing towards the rear of the vehicle. Unfortunately, moving the boxed housing too close to the rear of the vehicle would restrict airflow into the fan. Consultations with the fan manufacturers and Halifax fan consulting engineers confirmed that no obstruction should be within 1.25 m of the fan to avoid airflow restriction into the fan. Contact with the lorry manufacturer lead to pinpoint analysis of the various items on the lorry to calculate the loads imposed on the front and rear axles. A compromise was reached, whereby the power source would be moved 0.5 m towards the rear and the front suspension would be up rated to keep the vehicle within the legal requirements of the DVLA. The large test rig was given the name of the “Megafan” for marketing purposes and was now suitable for transport around the country. To make accurate assessments of building air leakage rates the fan would now need to be accurately calibrated.

4.2 *Calibration of large air test rig*

There are a number of methods available for rig calibration. The author decided that for the most accurate calibration of the rig, the method entailing the use of a calibration duct would be best. The duct is used to create an environment where it is possible to measure the relationship between the pressures observed at the fan and the true flow volume measured at the outlet of the calibration duct. Tap-ins located around the inlet venturi of the fans were connected together with tubing to give a pressure reading for a given flow rate through the fan. Measurements of the velocity pressures at the outlet end of the duct, coupled with information about the air density, are used to calculate the true air flow volume resulting from the fan. Collecting data for various fan pressures and true airflow volumes at the duct outlet allowed a formula to be calculated for the relationship between observed and actual volume flow rates through the fan.

For the calibration of the Megafan the test was carried out in accordance with BS 1042: Section 2.1:1983 *Measurement of fluid flow in closed conduits*. This highlights the location and number of sampling points required close to the outlet end of the calibration duct. Section 10.2.1. of this document refers to the “Log-Tchebycheff” method in circular cross sections. Three full diameter traverses of the duct are required using a pitot static tube at a given position along the calibration duct (Figure 9. Megafan calibration duct). Eight measurements are made at each diameter traverse, giving a total of 24 velocity pressure readings for each fan pressure level. The calibration duct was designed and built in accordance with BS 848 Part 1 1980 type B – *ducted flow*, incorporating straighteners to remove swirl.

The two inlet venturies for the Megafan were manufactured according to clause 21 of BS 848 Part 1. One 2000-mm venturi was constructed for the highest flow rates. A 1400-mm venturi was constructed for lower flow ranges. On each venturi four tap-ins were created at 90-degree intervals. These were connected using rubber tubing and T-piece attachments to produce one outlet tube for pressure measurements.



Figure 11. Calibration duct for “Megafan” test rig

During the actual calibration procedure the airflow through the duct was measured and calculated from the pitot static traverse, utilising an NPL design pitot static tube. The static pressure drop at the fan venturi was measured using a digital micromanometer. The measured flow was then compared to the indicated flow from the inlet of the venturi subject to calibration. The procedure was carried out at ten approximately equally spaced values over the full operating range of the inlet venturi and the results plotted to give a straight line relationship between the measured and actual flows. This enabled a flow correction factor to be calculated for each venturi. This is in the form of a mathematical equation, such that: -

$$\text{Air flow } \text{m}^3.\text{s}^{-1} = f(\Delta P) \quad (4.1)$$

where ΔP is the measured pressure drop at the inlet venturi



Figure 12. Author connecting “Megafan” test rig to calibration duct

4.3 Calibration procedure

1. Ensure the lorry handbrake was on. Secure the fan to the calibration duct using the bolts provided
2. The barrier around the Megafan lorry was positioned to keep people a minimum of 10m away.
3. The fan rev counter was connected up to the digital readout in the cab.
4. The fan engine was turned on and the speed increased to a maximum of 2300rpm. At the same time slowly increase the fan speed to a maximum of 880rpm. These two actions should be done simultaneously.

5. The fan speed was reduced by decreasing the engine speed. Two way radio communication was maintained between the fan speed operator and the engine speed operator.
6. The doors of the storage box on the back of the lorry did not impede the airflow into the fan. Nothing was within 1.25 metres of the inlet cone of the fan.



Figure 13. Megafan rig ready for calibration

7. The procedure consisted of measuring observed volumes at the fan venturi and actual volumes at the other end of a calibration duct. These were compared to establish a relationship between the two. Comparative tests were carried out at ten equidistant points through the full working range of flow rates for the fan venturi in question. These data were inputted into the HRS spread sheet to

- calculate flow volumes from observed pressures. Values were plotted into a graph and a line equation calculated for the relationship.
8. The open area of the venturi and discharge duct was calculated from πr^2
 9. Atmospheric pressure was measured using a UKAS calibrated absolute pressure meter. Temperature was measured using a UKAS calibrated ETI Therma 1 Thermometer, with an uncertainty of calibration of ± 0.5 °C. These values were inputted into the spreadsheet, which then calculated a value for air density.
 10. Measurements of velocity pressures were made with the pitot static tube along four radius traverse points of each of three traverse diameters. Location of traverse points were indicated in BS 1042: Section 2.1:1983, item 10.2.1 Circular cross sections.
 11. For calibration of each venturi the fan flow rate was raised to the maximum for normal working conditions. For the Megafan with 2000mm venturi the pressure reading at the venturi was around 1100 Pascal. For the Megafan with 1400mm venturi this was around 500 Pascal.
 12. The flow rate was then reduced to the lower limit of calibration in ten equal stages. At each stage measurements from the pitot static traverse were taken on each of the three traverse diameters. The lower limit for venturi pressure readings with the 2000mm venturi was 220 Pascal.
 13. Velocity pressure readings for the three traverse diameters were then entered into the HRS Excel spreadsheet. From this square roots of velocity pressures were calculated and thus an average of the square roots obtained was then squared to give an average measured reading. This measured reading was then compared with the average reading obtained at the venturi.
 14. The pitot volume alpha is set at the known value of 0.997, calculated from BS848-1. Air density is calculated using the following equation: -

$$\text{Air density } (\rho) = P_{\text{atmos}} / 287 * (T_{\text{atmos}} + 273.15) \quad (4.2)$$

P_{atmos} = atmospheric pressure (Pa)

T_{atmos} = atmospheric temperature ($^{\circ}\text{C}$)

These values were substituted into the equation below to provide values for mass flow in the spreadsheet using the following equation: -

$$\text{Mass flow} = \alpha \cdot \pi r^2 \cdot (2\rho \cdot \Delta P)^{0.5} \quad (4.3)$$

α = pitot volume

ρ = air density ($\text{kg} \cdot \text{m}^{-3}$)

ΔP = average pitot reading (Pa)

15. With known values for mass flow and air density the flow volume was calculated by dividing mass flow by air density to give a value in $\text{m}^3 \cdot \text{s}^{-1}$. This gives a value for the average measured volume from the pitot static traverse.
16. The value for the venturi reading was used to calculate a value for the venturi velocity and thus venturi volume using the following equations: -

$$\text{Venturi velocity } (\text{m} \cdot \text{s}^{-1}) = (2\Delta P / \rho)^{0.5} \quad (4.4)$$

ΔP = average venturi reading (Pa)

ρ = air density ($\text{kg} \cdot \text{m}^{-3}$)

$$\text{Venturi volume} = \text{venturi velocity } (\text{m} \cdot \text{s}^{-1}) * \text{venturi area } (\pi r^2)$$

Inserting the values into a spreadsheet allowed a comparison to be made between observed volume at the venturi and actual measured volume at the pitot static traverse. With all ten readings for observed against actual volume input into an Excel graph, a line equation was calculated. Adherence to the British Standards using this method save an accuracy of $\pm 2\%$ for the venturi volume and $\pm 2\%$ for the measured pitot volume. Summation of these two values save an overall uncertainty of $\pm 4\%$ for true volume.

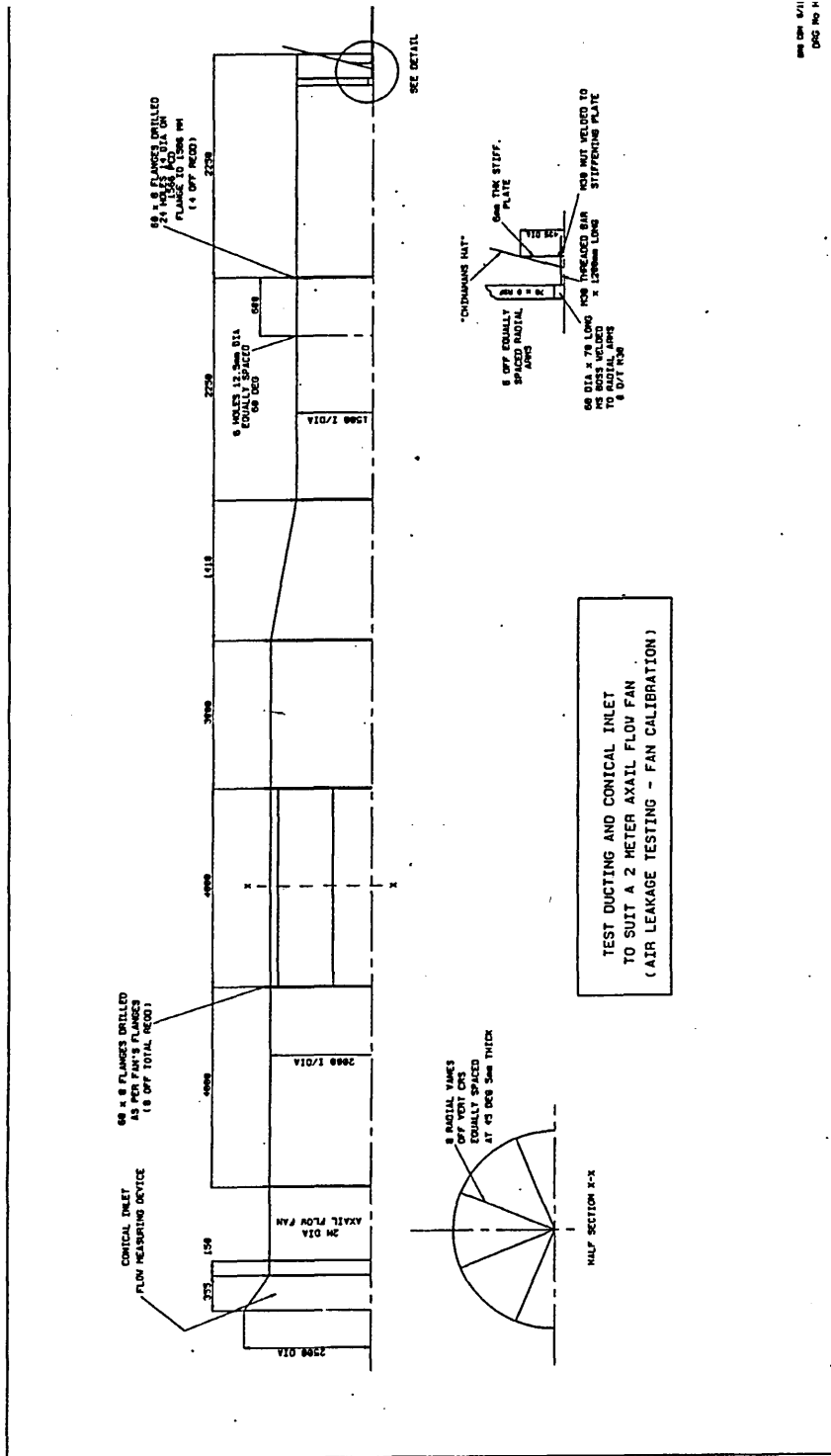


Figure 14. Megafan calibration duct.

4.4 *Testing of very large buildings*

It was hypothesised by the author that the procedure for testing a very large single cell warehouse building using the steady state technique would be similar to that for a smaller building. The principles of introducing a flow rate Q into a building to create a pressure Δp across the building envelope remains the same. With a very large rig, such as the Megafan, it may be quite possible to pressurise the whole building using only one rig. However, it should be borne in mind that there will be a large number of mechanical ventilation plant units that will need to be turned off and temporarily sealed. It may also be necessary to take measurements of pressure differentials across the building envelope at a number of locations simultaneously to obtain a representative result. The standard procedure in the run up to an air test of a building is as follows: -

The following must be in place:

1. Smoke vent and fan actuators should be operational
2. Envelope areas should be calculated and verified
3. All builders work should be complete to air seal envelope including windows, doors, hatches, cills, services etc.
4. Air inlets should be sealed
5. Extracts should be sealed
6. The Client must inform all contractors and personnel that access into and out of the building will be restricted for a period of at least 2 hours and ensure that this is observed.

7. H and V shall be shut off and all H and V equipment closed down and any other equipment that form openings or penetrations in the envelope shall be temporarily sealed
8. An adequate number of suspended ceiling tiles, if installed, shall be removed around the perimeter of the building, to allow inspection of the floor/wall junction at all points.
9. Attendance by a client representative on site during the air test
10. Full access to be provided to all roofs and elevations
11. All internal doors, plenums, suspended ceilings and raised floor systems are effectively fixed opened to enable unrestricted air flow into all parts of the building envelope.

In addition the following must be checked to ensure that accurate testing of the building envelope is taking place:

12. Temporary seals must not be made to the external doors and frames
13. Temporary seals must not be made to external door thresholds
14. Temporary seals must not be made to loading bay doors
15. Additional seals must not be applied to air handling plant
16. Temporary seals must not be applied to the boiler room
17. Temporary seals must not be applied to lift shaft vents and doors
18. Temporary seals must not be applied to windows and cills
19. Temporary seals must not be applied to the tank room
20. Temporary seals must not be applied to drains, plugs and overflows
21. Temporary seals must not be applied to smoke exhaust fans and vents
22. Temporary seals must not be applied to any electrical switch rooms

Building projects that have not incorporated envelope airtightness practices from design to completion may not attain the required performance specification. If the building fails the airtightness test then it may be necessary to carry out reductive sealing. This technique can be used to identify areas of permeable components or leakage paths. After the initial building test has been carried out individual or component multiple components such as trickle ventilators or building eaves can be sealed with polythene and tape. Further tests can be carried out to identify the contribution of each isolated area to the overall building leakage rate.

Figure 15 to Figure 19 indicate sealing measures that may be applied in a remedial manner to refurbished buildings. These techniques may be also be applied to a newly constructed building after completion, if the required airtightness specification has not already been achieved.



HRS SERVICES LTD.
The Maltings
81 Burton Road
Sheffield
S3 8BX

Tel: +44 114 272 3004
Fax: +44 114 272 3003

E Mail opman@highrise.co.uk

Block Work Wall Below Roof Sheet

Air Seal To Eaves Detail

Material Performance and Specifications

1. Celotex double-R GA2000 is a low density rigid foam board with tri-laminate foil facings on both sides. It provides a vapour barrier at the insulation surface as well as a high thermal resistance. It has a Class 1 surface spread of flame to BS476 pt 7. Product performance can be relied upon for 25-50 years.
2. Webbseal 56 LM is a low modulus, neutral cure silicone intended for use in movement joints. It conforms to ISO 11600 for construction use.
3. Vapour check plaster board is foil faced on one side. It has a Class 1 surface spread of flame to BS476 pt 7.

Typical Detail

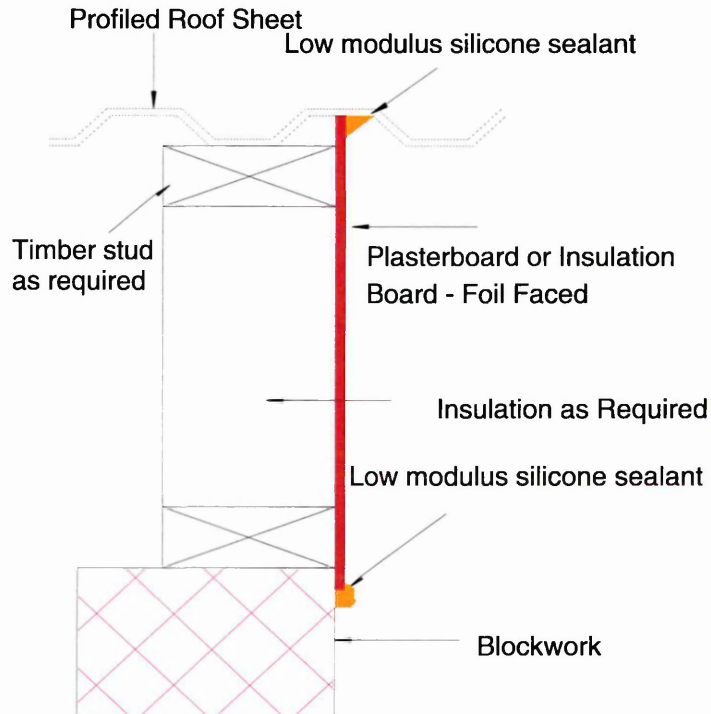


Figure 15. Airseal detail at blockwork wall to roof sheet eaves detail.



HRS SERVICES LTD.
The Maltings
81 Burton Road
Sheffield
S3 8BX

Tel: +44 114 272 3004
Fax: +44 114 272 3003
E Mail opman@highrise.co.uk

Block Work Wall Less Than 50 mm Below Roof Sheet

Air Seal To Top Of Internal Wall (Not Fire)

Material Performance and Specification

1. Closed cell foam fillers are produced from PEL. Bedded correctly, they are fully air tight and have a life expectancy of 30 years.
2. Webbseal 56 LM is a low modulus, neutral cure silicone intended for use in movement joints. It conforms to ISO 11600 for construction use.

Typical Detail

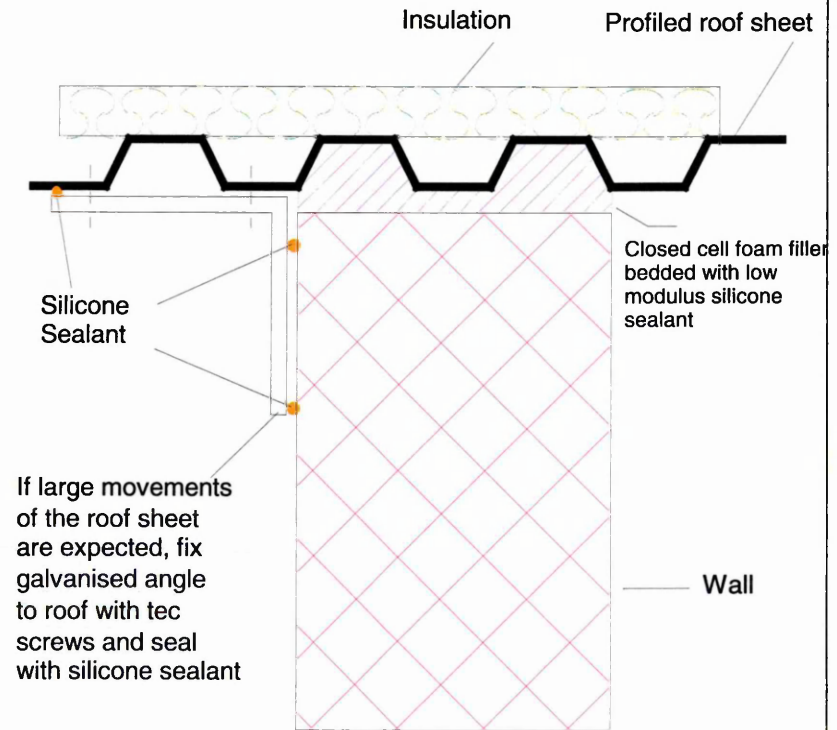


Figure 16. Airseal detail at blockwork wall adjacent to roof sheet eaves detail.



HRS SERVICES LTD.
The Maltings
81 Burton Road
Sheffield
S3 8BX

Tel: +44 114 272 3004
Fax: +44 114 272 3003
E Mail opman@highrise.co.uk

Mansard Roof Spanning Area Between Block Work Wall And Roof Sheet

Air Seal To Eaves Detail

Material Performance and Specifications

1. Celotex double-R GA2000 is a low density rigid foam board with tri-laminate foil facings on both sides. It provides a vapour barrier at the insulation surface as well as a high thermal resistance. It has a Class 1 surface spread of flame to BS476 pt 7. Product performance can be relied upon for 25-50 years.
2. Webbseal 56 LM is a low modulus, neutral cure silicone intended for use in movement joints. It conforms to ISO 11600 for construction use.
3. Vapour check plaster board is foil faced on one side. It has a Class 1 surface spread of flame to BS476 pt 7.
4. **Closed cell foam fillers are produced from PEL. Bedded correctly, they are fully air tight and have a life expectancy of 30 years.**

Typical Detail

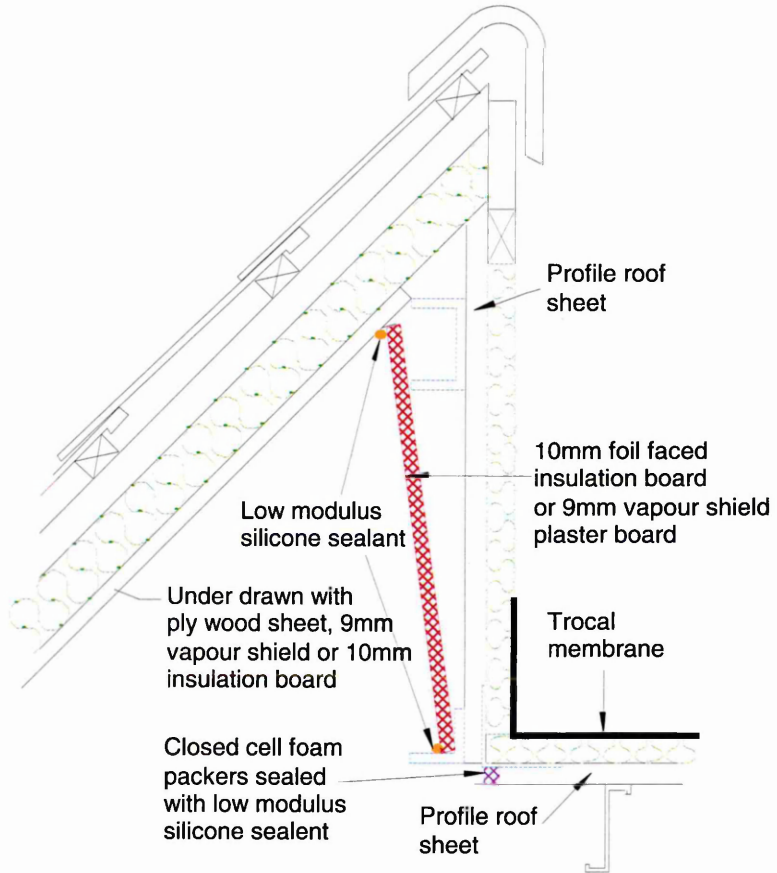


Figure 17. Airseal detail at blockwork wall adjacent to roof sheet eaves detail.



HRS SERVICES LTD.
The Maltings
81 Burton Road
Sheffield
S3 8BX

Tel: +44 114 272 3004
Fax: +44 114 272 3003
E Mail opman@highrise.co.uk

Penetration of External Wall by Steelwork or Services

Air Seal Detail

Material Performance and Specifications

1. Webbseal 56 LM is a low modulus, neutral cure silicone intended for use in movement joints. It conforms to ISO 11600 for construction use.
2. Vapour check plaster board is foil faced on one side. It has a Class 1 surface spread of flame to BS476 pt 7.
3. Celotex double-R GA2000 is a low density rigid foam board with tri-laminate foil facings on both sides. It provides a vapour barrier at the insulation surface as well as a high thermal resistance. It has a Class 1 surface spread of flame to BS476 pt 7. Product performance can be relied upon for 25-50 years.

Typical Detail Wall

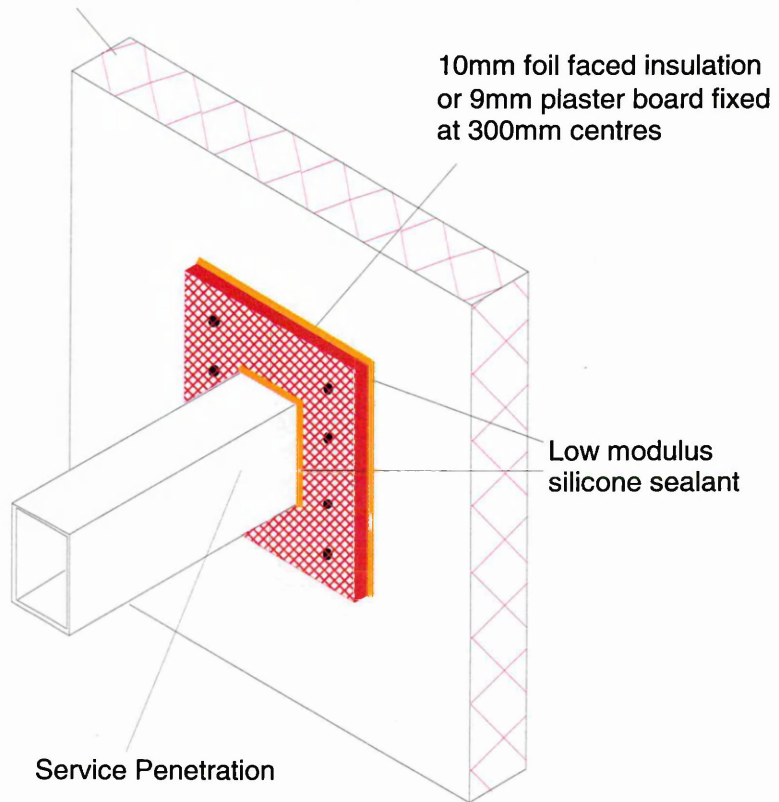


Figure 18. Airseal detail at external wall penetration.



HRS SERVICES LTD.
The Maltings
81 Burton Road
Sheffield
S3 8BX

Tel: +44 114 272 3004
Fax: +44 114 272 3003
E Mail opman@highrise.co.uk

Penetration of Roof Sheet by Steelwork or Services

Air Seal Detail

Material Performance and Specifications

1. Celotex double-R GA2000 is a low density rigid foam board with tri-laminate foil facings on both sides. It provides a vapour barrier at the insulation surface as well as a high thermal resistance. It has a Class 1 surface spread of flame to BS476 pt 7. Product performance can be relied upon for 25-50 years.
2. Webbseal 56 LM is a low modulus, neutral cure silicone intended for use in movement joints. It conforms to ISO 11600 for construction use.
3. Vapour check plaster board is foil faced on one side. It has a Class 1 surface spread of flame to BS476 pt 7.

Closed cell foam fillers are produced from PEL. Bedded correctly, they are fully air tight and have a life expectancy of 30 years.

Typical Detail

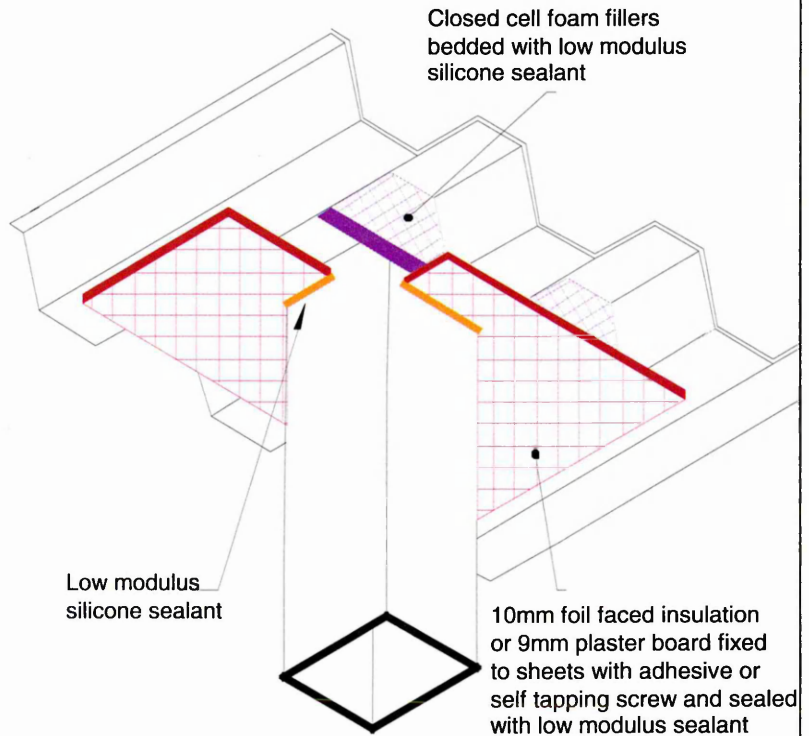


Figure 19. Airseal detail at external wall penetration.

4.6 *Summary*

This chapter have provided an insight into the methodology required for the creation and calibration of a large test rig. A review of the design and construction process for the large test rig, along with lessons learned from mistakes, has been provided. Information relating to the equipment and methodology required for the calibration of the rig has been provided. The practical requirements for testing large buildings have been noted. A summary of some remedial measures currently used on buildings have also been presented. The following chapter will report the field testing of one large and two very large UK buildings. The practical implications of testing very large buildings and some of the problems encountered on site will be discussed.

5.1 Field testing of large buildings

The implementation of Part L2 of the Building Regulations on 1st April 2002 brought into force the requirement for buildings with a gross floor area greater than 1000 m² to reach a reasonable level of envelope airtightness. For most buildings this could be assessed with an airtightness test. The following are three examples of buildings that were subject to an airtightness test in 2002. The results of these tests are presented in Chapter 6.

5.2 Testing of a large warehouse (Building A) to determine building envelope airtightness using the Megafan rig

Building A was a large steel framed, composite clad building, located in Bury. The building had an air permeability index envelope area of 35,544 m² and a total volume of 196,150 m³. The cladding contractor was responsible for the airtightness compliance of the building and had employed sealing techniques to gain approval. This included the correct closure of gasket joints and silicone sealing at composite panel junctions.

Prior to the test, the author met with the cladding contractor to ensure that all building work was complete to the air seal envelope including windows, doors, hatches, cills and services. H and V subcontractors shut down the H and V plant on the roof of the building and temporarily sealed them. For the purpose of the test, a large wooden screen was installed in the main entrance to the building. This contained a 1400-mm cut-out, into which the Megafan would be installed. On arrival to site, a building check was carried out by the author to ensure that all required areas were completed and

temporarily sealed where required. Inspection was also carried out to ensure that areas such as smoke exhaust vents and external doors were not sealed.

When the building was ready to be tested the Megafan was connected to the wooden screen using one three-metre flexible duct section. Temperature measurement probes were placed 20 m inside and outside away from the building and connected to digital thermometers in the Megafan lorry. 5-mm bore plastic tubing was placed 20 m inside and outside away from the building. This tubing was then connected to digital micromanometers inside the Megafan lorry. The pressure drop across the fans was measured using high quality digital manometers designed for measuring pressure differentials to an accuracy of $\pm 1\%$ of a reading. Temperature measurements were made before, during and after the test using Thermo 1 Thermometer Digital thermometers. These were calibrated by UKAS to an accuracy of ± 0.5 °C. A UKAS calibrated absolute pressure meter was used to establish the atmospheric pressure. Radio contact was maintained between personnel at the testing rig and personnel inside the building to ensure that all doors and windows remained shut and that no one left the building. The Megafan rig was used to impose a positive pressure of 62 Pa across the building envelope. Pressure differential was established across the fan. Fan speed was then lowered to give 10 building envelope differential pressure readings with corresponding fan pressure drop readings. The lowest building differential pressure recorded was 20 Pa. Results of the test can be found in Section 6.1.

5.3 *Testing of a very large retail store (Building B) to determine building envelope airtightness using the Megafan rig*

Building B was a very large retail store located in Glasgow. Although no mandatory requirement for testing was in force in Scotland, the client had decided to test the type of construction that would be used on other projects in the UK. The building has an air permeability index surface area of 42072 m² and a volume of 180760 m³. The construction was brick/block/cladding with a trocal membrane for the roof sheet.



Figure 20. Building B front entrance

Prior to the airtest, a site visit was carried out by HRS personnel to audit the building and make recommendations for improvements to the current sealing practices employed. Inspection revealed that some sealing practices had been employed around the building. However, omissions were noted at the roof sheet eaves (Figure 21) and at

service penetrations to the roof sheet. The client had been informed by the roofing contractor that air needed to pass from the building through the roof sandwich for it to “breathe”.



Figure 21. Lack of sealing at roof sheet detail

On the day of the airstest, sealing of H and V plant on the roof was left to HRS personnel. There were a large number of mechanical ventilation units (Figure 22) spread over a roof area of approximately 18000 m². Plant was sealed with Celotex board, polythene sheet and tape. The process of sealing all the roof plant took four hours with four personnel working consistently. Also present on the roof were a large number of smoke vents (Figure 23), which were closed but not sealed.



Figure 22. Large number of mechanical ventilation units



Figure 23. Large number of smoke vents

During the process of mechanical vent sealing in the roof, the author and two further HRS personnel were installing the Megafan into the entrance to the building at ground level. Concrete bollards present in front of the doorway were removed prior to the test. Unfortunately the entrance was only just greater than 2 m high. The wooden screen, pre-made for fixing the flexible duct into the doorway had to be cut to size. To support the flexible duct between the fan and wooden screen a scaffolding ramp was erected (Figure 24).



Figure 24. Megafan flexible duct sealed into wooden screen at entrance to retail store

A 40-m length of 5-mm bore plastic tubing was placed into the centre of the sales floor. The other end of the tubing was connected to the positive terminal on the digital micromanometer in the lorry cab. A further 20-m length of tubing was placed adjacent to the building with one end connected to the negative terminal of the digital

micromanometer. Temperature probes were placed in the centre of the sales floor and outside the building. Average wind speed was taken during the test using a digital anemometer. Atmospheric pressure was determined using an absolute pressure meter. The pressure drop across the fans was measured using high quality digital manometers designed for measuring pressure differentials to an accuracy of $\pm 1\%$ of a reading. Temperature measurements were made before, during and after the test using Thermo 1 Thermometer Digital thermometers. Before the test commenced a bunted barrier was erected to provide a 10 m by 10 m no go area around the fan, inside and outside the building. All moveable objects were removed from the airflow path of the fan inside the building. Control of the fan and reading data assimilation was carried out by an operator in the lorry cab (Figure 25)



Figure 25. Megafan ready to test with the author in the lorry cab to record results.

Radio contact was maintained between the fan operator, personnel within the building and personnel who were on the roof to check that none of the temporary sealing blew off during the test. With the donkey engine running the Megafan was taken up to maximum speed. The first results indicated a very low building pressure. Radio contact with personnel on the roof revealed that a roof hatch had been left open. With the hatch closed the test could proceed. The building was taken up to a differential pressure of 57 Pa. 10 building pressure readings were recorded, down to a differential pressure of 16Pa. The results are recorded in section 6.2.

5.4 *Testing of a very large warehouse building (Building C) to determine airtightness using multiple rigs*

In December 2002 the opportunity arose to air test the largest building to be subject to such a test in the UK (and probably the world). With an air permeability index envelope area of 128400 m² and a total volume of 746720 m³ the very large distribution centre would push the current air testing equipment and technology to its limits. The building was of a steel framed, composite clad construction. Careful attention had been taken during construction to ensure that all gaskets and joints were sealed. However, on a building this size there were tens of thousands of metres of linear joints. Even a 1-mm gap along the length of the joints would result in a massive open area for air leakage. To assess the possibility of joint leakage a sample of spot check were carried out around the building prior to the air test by the author (Figure 26). Indications from these samples were good, suggesting that the building would easily meet the current Building Regulations targets.



Figure 26. Joint leakage assessment by the author using a component tester

The pressure testing of such an enormous building provided the perfect opportunity to demonstrate the capabilities of the Megafan and answer questions about the impossibilities of testing large buildings. A two-day publicity event was organised by the author and HRS Services Ltd to highlight the available testing rigs, ease of large building testing and the energy saving benefits that can be accrued from good envelope airtightness in large buildings. The event was attended by government officials from the ODPM, clients, main contractors, cladding contractors, academics, building control and approved inspectors.

For the purpose of this test, the author decided that three variable speed fans would be used to generate the pressure differential Δp across the building envelope; the Megafan, 2000mm in diameter and two medium sized fans, 1250mm in diameter. The 1250mm fans were driven using the power take off from 3.5 tonne Mercedes vans with a similar design to the 2000mm-fan rig. The pressure drop across the fans was measured using high quality digital manometers designed for measuring pressure differentials to an accuracy of $\pm 1\%$ of a reading. Temperature measurements were made before, during and after the test using Thermo 1 Thermometer Digital thermometers.

The three fans were positioned at equal intervals along one side of the building envelope. Prior work had been carried out by the author with Nelson Chilengwe at Sheffield Hallam University using Computational Fluid Dynamics (CFD) modelling to investigate any interactions between the fan plumes. The study had constructed a model of the building under test and assigned properties to the building boundaries to try and accurately represent conditions on site. The three fans were introduced into the model as fixed flows. Full details of this work can be found in Appendix A.2.

The large fan was connected with a flexible duct to a wooden screen situated within one of the dock levellers, as illustrated in Figure 27. The two medium sized fans were positioned within dock leveller entrances and sealed in with a wooden frame and Celotex board.



Figure 27. Megafan sealed into dock leveller entrance

For the purpose of the test, all external doors and windows were closed, with internal doors to the offices left open. Mechanical ventilation openings on the building roof were to be sealed with polythene sheet and adhesive tape by the cladding contractor. On arrival at site, it was noted that this had not been carried out. HRS personnel spent three hours sealing mechanical ventilation plant on the roof. Personnel who had been requested to monitor the temporarily sealing on the roof during the test were also not available.

Large openings containing permanently open louvers had been noted on previous visits to site and a requirement to have them sealed had been communicated to the project team. On the date of the scheduled air test, the louvers, constituting an area of around 40m^2 , were still unsealed. To carry out a test under these conditions would have been pointless. The louvers were therefore covered with polythene sheet and tape, under the premise that they would be properly sealed at a latter date and remain sealed during operational conditions. Three 1m^2 openings in the building envelope remained unsealed to fulfil the requirement of ventilation to the gas boilers. On a visit to the site six months latter the author observed that permanent sealing to these louvers was being installed, coincidentally on the day of the visit.

Three parties of two personnel were required to operate the fans and record the observed pressure differentials. Further personnel were positioned around the building and on the roof, to ensure that vents remained sealed and doors remained closed. Communication was maintained by radio contact. To establish the pressure differential across the building envelope that would satisfy Building Regulation requirements, a 60m length of 5mm internal diameter plastic tube was connected from the digital manometer located at the large fan and placed inside the building at a 45° angle to the fan at ground level. A 20m length of tube was connected to the manometer and placed outside the building at a 45° angle to the fan. The pressure differential across the building envelope was raised to 81 Pascal and then lowered in ten stages to 23 Pascal. Pressure differentials across the three fans were maintained with a difference of not greater than 20% at each respective test level. Results for the test can be found in Section 6.3.

5.5 *Summary*

This chapter has reported on the field testing of one large and two very large UK buildings. The practical implications of testing very large buildings has been discussed and some of the problems highlighted on site have been discussed. The current knowledge gap in the UK construction industry relating to building airtightness has also been noted. The following chapter will report the output graphs and tables from the field data. A brief interpretation of the results will be given.

6.1 Testing of a large warehouse (Building A) to determine building envelope airtightness using the Megafan rig

The following reports detail the results from the airtightness test carried out at Building A, on the 20th of May 2004. The test was performed using the Megafan rig with 2000-mm venturi attached. The data shown are output graphs and tables from the Altas program. The Altas program was produced by the author in conjunction with Sheffield Hallam University for HRS Services to carry out and report the results of airtightness tests. Altas takes as input measured parameters of the air-leakage test i.e. pressure differentials across the fans and building envelope, temperatures and wind speed prevailing during the test period. Altas then derives the airflow rates through the fans from the measured pressures across the fans. The measured air flow rates through the fans and building envelope are corrected for deviations in density from standard temperature and barometric pressure (20°C and 101325 Pa). Correcting the air leakage parameter to standard conditions enables tests carried out under different conditions to be properly compared. In addition Altas determines the Airtightness Performance and Air Leakage Characteristic of a building based upon the input. The later involves regression analysis to determine the flow exponent and coefficient in the power law equation, which relates the airflow rate across the building envelope to the pressure differential across it. Output from Altas is in the form of presentable printouts ready for issue to clients for inclusion in reports or for general record keeping.

Figure 28 shows a log-log plot using a power law regression fit of the measured fan flow rate Q , against the building differential pressure ΔP . A value for the measured

flow rate at a building differential pressure of 50 Pa, Q_{50} , is quoted as $53.94 \text{ m}^3\text{s}^{-1}$. This is calculated by interpolating the measured results using a least square law approximation. The calculated value for air permeability was $5.46 \text{ m}^3\text{h}^{-1}\text{m}^{-2}$, which easily satisfies the current Building Regulations target of $10 \text{ m}^3\text{h}^{-1}\text{m}^{-2}$. The reported value for air leakage index is $9.08 \text{ m}^3\text{h}^{-1}\text{m}^{-2}$. The value for the correlation coefficient of the power law regression fit is 0.9956. Figure 29 shows a linear plot using a power law regression fit of the measured fan flow rate Q , against the building differential pressure ΔP . Figure 30 highlights the environmental and fan output data during the test. Average wind speed was noted to be 2.2 ms^{-1} at the beginning, falling to 2.0 ms^{-1} at the end of the test. Figure 31 summarises the building details. Figure 32 reports the fan and building pressures recorded during the test.

6.1.1 Log-log data plot for building pressurisation test

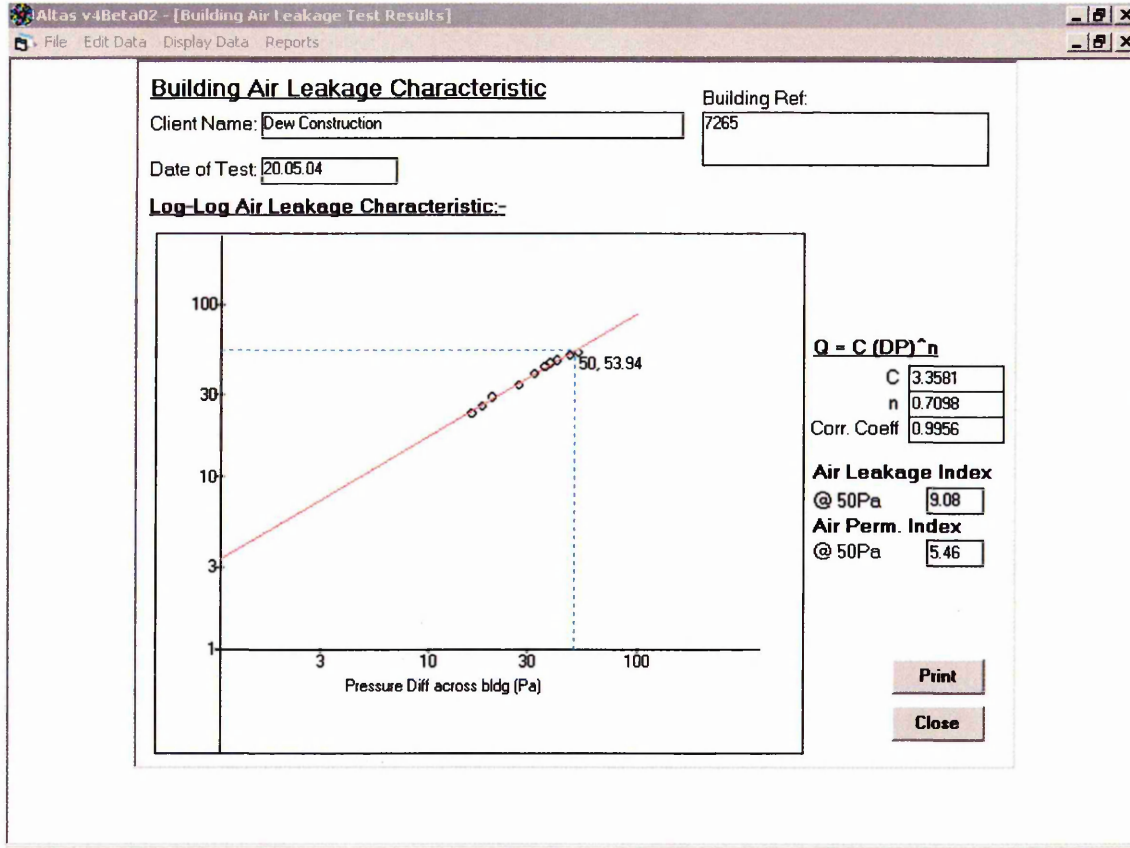


Figure 28. $Q(m^3 s^{-1})$ v. $\Delta p(Pa)$ log-log data points for the building pressurisation test.
With a power law regression fit.
Source Altas v3.36.

6.1.2 Linear data plot for building pressurisation test

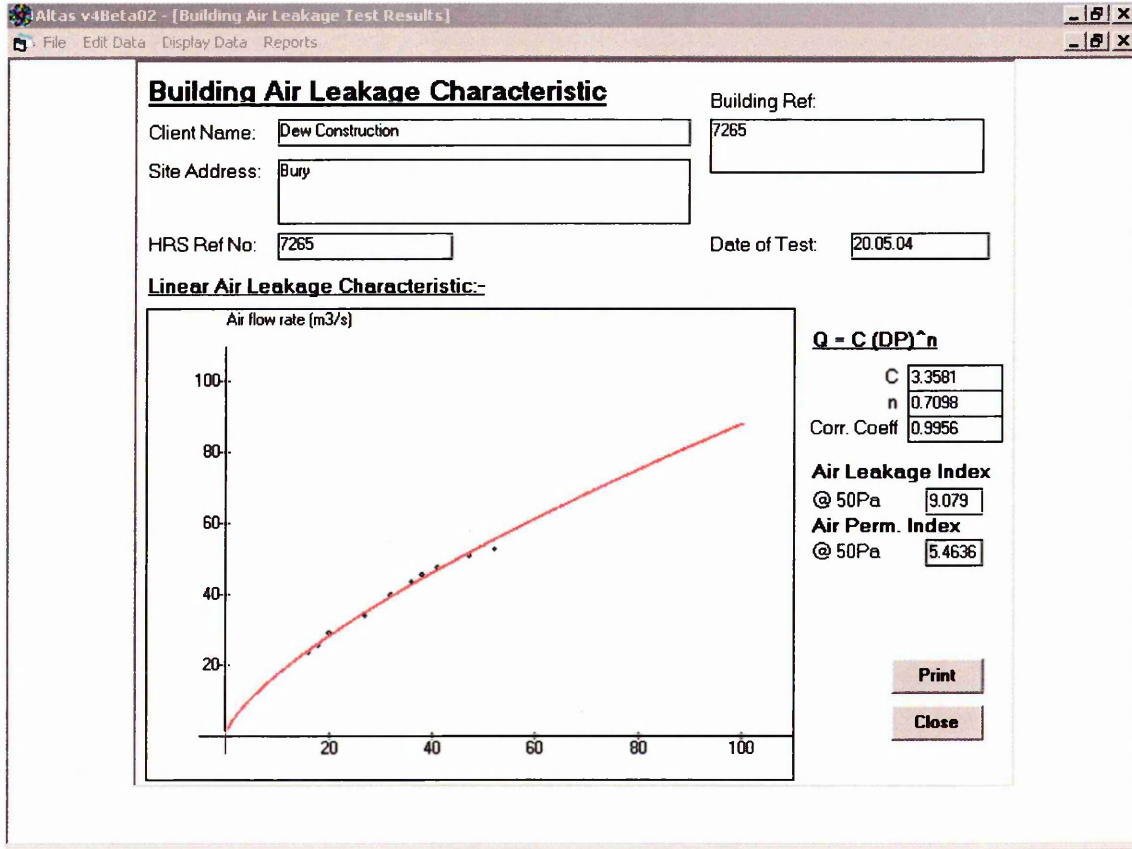


Figure 29. $Q(m^3 s^{-1})$ v. $\Delta p(Pa)$ linear data points for the building pressurisation test.
 With a power law regression fit.
 Source Altas v3.36.

6.1.3 Environmental and measured data

Altas v4Beta02 - [Air Leakage Test Data Sheet]

File Edit Data Display Data Reports

Building Air Leakage Test Data Sheet

Client Name: Dew Construction Date of Test: 20.05.04

Site Address: Bury Building Ref: 7265 Test Start Time: 12.30

Test Finish Time: 1.00

Test database No: 7265 Pressurisation: X

Depressurisation:

General Weather Conditions: Clear, light winds

Wind Speed at Start of Test: 2.2 m/s

Wind Speed at End of Test: 2 m/s

Barometric Press. at Start of Test: 101000 Pa

Barometric Press. at End of Test: 101000 Pa

External Temp at Start of Test: 16.5 deg C

External Temp at End of Test: 16.8 deg C

Fan off, press. diff. at Start of Test: 0 Pa

Fan off, press. diff. at End of Test: 0 Pa

Internal Temp Sensor Location	Internal Temp (deg C)	
	Start	End
centre of building	12.8	13.5

Fan Speed	634	608	564	540	506	465	405	338	306	272
Press. Diff (Pa)	52	47	41	38	36	32	27	20	18	16
Air Flow (m3/s)	53.41	51.60	48.11	46.24	44.17	40.27	34.45	29.39	25.86	23.73

Engineer: S.Closs Date: 20.05.04 Checked by: Date:

Figure 30. Environmental and measured data
Source Altas v3.36.

6.1.4 Building envelope data

Building Air Tightness Performance

Client Name: Dew Construction Date of Test: 20.05.04
HRS Ref No: 7265 Building Ref: 7265
Site Address: Bury

Building Physical Parameters

Building Vol: 196150 m3 Floor Area: 14154 m2
Walls Area: 7236 m2 Roof Area: 14154 m2

Building Air Tightness Results:

ALI Envlp Area = 21390 m2 Air Leakage Index (ALI) = 9.08 m3/h per m2 at 50 Pa
ALP Envlp Area = 35544 m2 Air Permeability (API) = 5.46 m3/h per m2 at 50 Pa
Indic. Infil Rate = 0.15 ACH

General Comments:

Print
Close

Engineer: S.Closs Date: 20.05.04 Checked by: Date:

Figure 31. Building envelope data
Source Altas v3.36.

6.1.5 Measured fan and building envelope data

Measured Data

Fan	Fan 1		Envlp	
	2000mm		Meas.	Total
Speed	[Pa]	[m3/s]	[Pa]	[m3/s]
634	570	53.414	52	53.414
608	531	51.597	47	51.597
564	460	48.108	41	48.108
540	424	46.236	38	46.236
506	386	44.171	36	44.171
465	319	40.266	32	40.266
405	231	34.447	27	34.447
338	166	29.387	20	29.387
306	127	25.857	18	25.857
272	106	23.728	16	23.728

Fan ID: Fan Type:

Figure 32. Measured fan and building envelope data.
Source Altas v3.36.

6.2 *Testing of a very large retail store (Building B) to determine building envelope airtightness using the Megafan*

The following reports detail the results from the airtightness test carried out at Building B, on the 8th of September 2002. The test was performed using the Megafan rig with 2000-mm venturi attached. The data shown are output graphs and tables from the Altas program.

Figure 33 shows a log-log plot using a power law regression fit of the measured fan flow rate Q , against the building differential pressure ΔP . A value for the measured flow rate at a building differential pressure of 50 Pa, Q_{50} , is quoted as $69.36 \text{ m}^3\text{s}^{-1}$. This is calculated by interpolating the measured results using a least square law approximation. The calculated value for air permeability is $5.93 \text{ m}^3\text{h}^{-1}\text{m}^{-2}$, which satisfies the current Building Regulations target of $10 \text{ m}^3\text{h}^{-1}\text{m}^{-2}$. The reported value for air leakage index is $10.41 \text{ m}^3\text{h}^{-1}\text{m}^{-2}$. The value for the correlation coefficient of the power law regression fit is 0.9968. Figure 34 shows a linear plot using a power law regression fit of the measured fan flow rate Q , against the building differential pressure ΔP . Figure 35 highlights the environmental and fan output data during the test. Average wind speed was noted to be 1.0 ms^{-1} at the beginning, falling to 0.6 ms^{-1} at the end of the test. Figure 36 summarises the building details. Figure 37 reports the fan and building pressures recorded during the test.

6.2.1 Log-log data plot for building pressurisation test

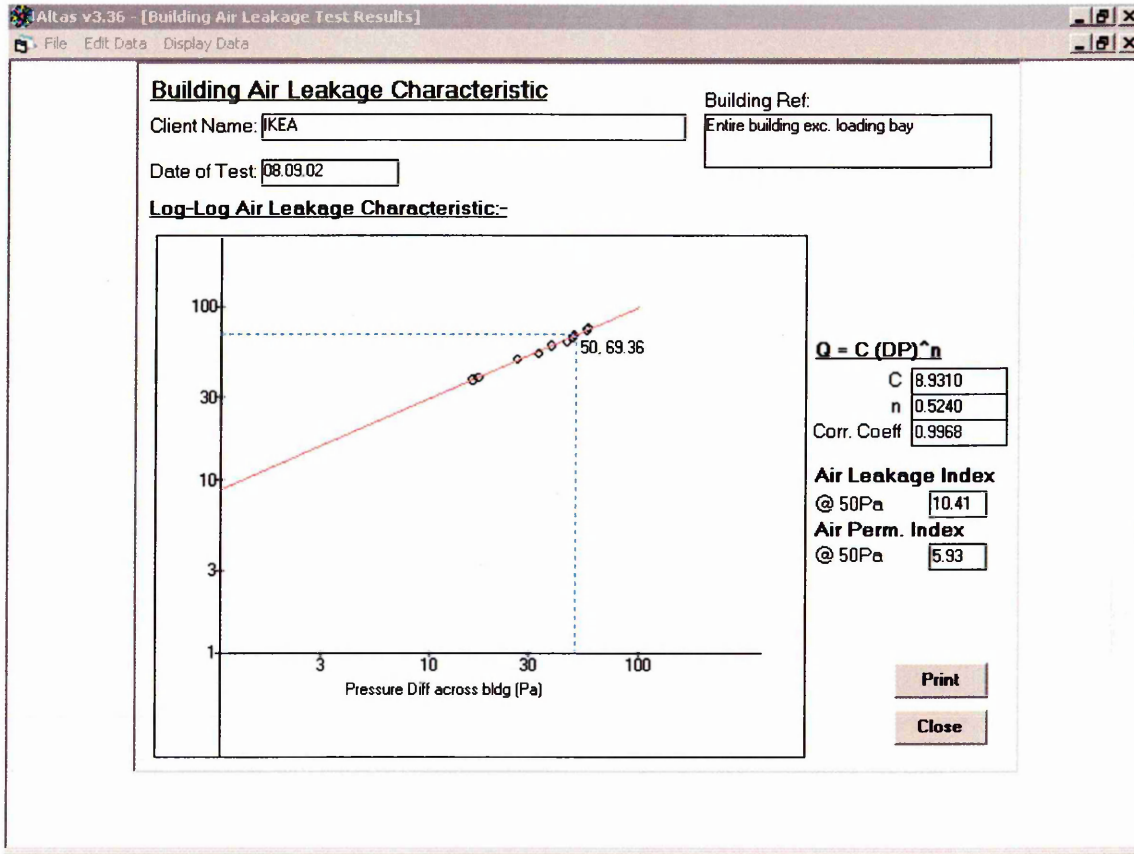


Figure 33. $Q(m^3 s^{-1})$ v. $\Delta p(Pa)$ log-log data points for the building pressurisation test. With a power law regression fit. Source Altas v3.36.

6.2.2 Linear data plot for building pressurisation test

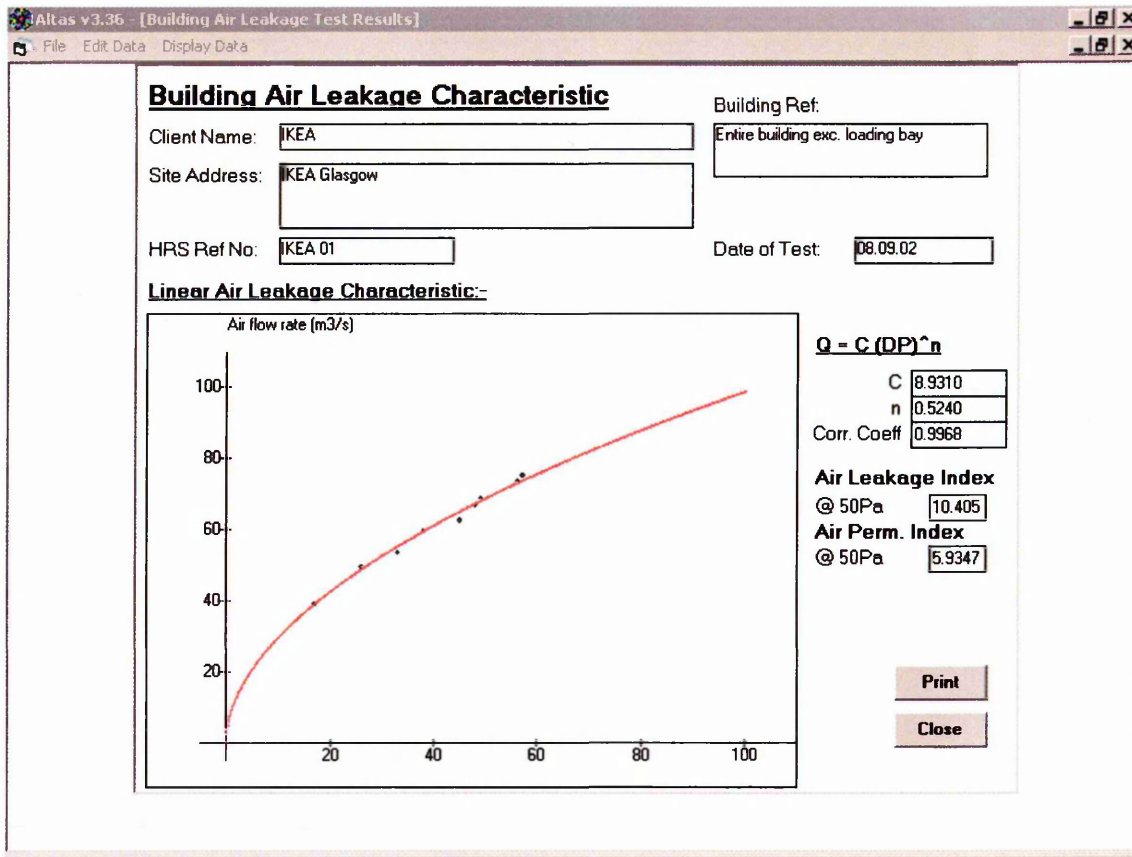


Figure 34. $Q(\text{m}^3 \text{s}^{-1})$ v. $\Delta p(\text{Pa})$ linear data points for the building pressurisation test.
With a power law regression fit.
Source Altas v3.36.

6.2.3 Environmental and measured data

Altas v3.36 - [Air Leakage Test Data Sheet]

File Edit Data Display Data

Building Air Leakage Test Data Sheet

Client Name: Date of Test:

Site Address: Building Ref: Test Start Time:

Test database No: Test Finish Time:

Pressurisation: Depressurisation:

General Weather Conditions:

Wind Speed at Start of Test: m/s

Wind Speed at End of Test: m/s

Barometric Press. at Start of Test: Pa

Barometric Press. at End of Test: Pa

External Temp at Start of Test: deg C

External Temp at End of Test: deg C

Fan off, press. diff. at Start of Test: Pa

Fan off, press. diff. at End of Test: Pa

Internal Temp Sensor Location	Internal Temp (deg C)	
	Start	End
Sales area	18.4	17.3

Fan Speed	880	845	805	775	725	682	597	560	445	415
Press. Diff (Pa)	57	56	49	48	45	38	33	26	17	16
Air Flow (m3/s)	74.50	72.88	68.12	66.34	62.03	59.06	53.04	49.27	38.81	37.54

Engineer: Date: Checked by: Date:

Figure 35. Environmental and measured data
Source Altas v3.36.

6.2.4 Building envelope data

Altas v3.36 - [Building Air Tightness Performance]

File Edit Data Display Data

Building Air Tightness Performance

Client Name: Date of Test:
HRS Ref No: Building Ref:
Site Address:

Building Physical Parameters

Building Vol: m3 Floor Area: m2
Walls Area: m2 Roof Area: m2

Building Air Tightness Results:

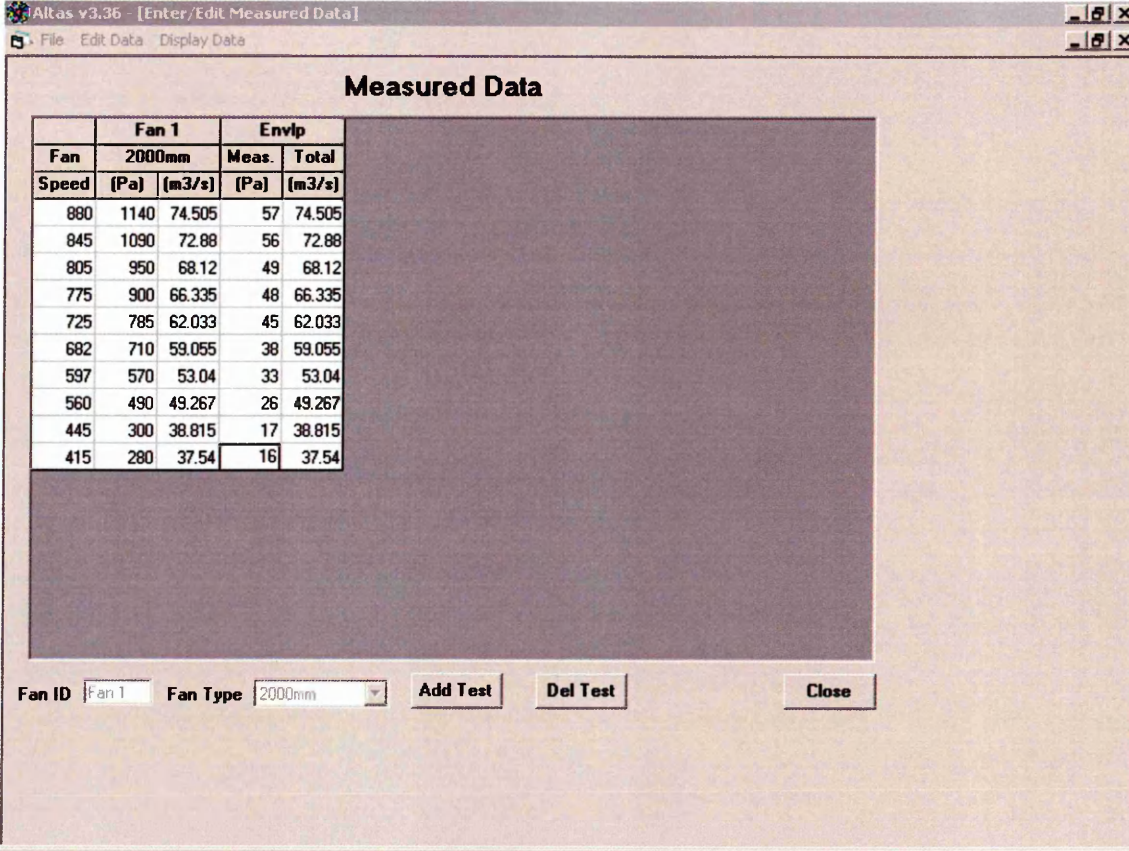
ALI Envlp Area = m2 Air Leakage Index (ALI) = m3/h per m2 at Pa
ALP Envlp Area = m2 Air Permeability (API) = m3/h per m2 at Pa
Indic. Infil Rate = ACH

General Comments:

Engineer: Date: Checked by: Date:

Figure 36. Building envelope data
Source Altas v3.36.

6.2.5 Measured fan and building envelope data



The screenshot shows a software window titled "Altas v3.36 - [Enter/Edit Measured Data]". The window contains a table titled "Measured Data" with the following data:

Fan	Fan 1		Envlp	
	2000mm	Meas.	Total	
Speed	[Pa]	[m3/s]	[Pa]	[m3/s]
880	1140	74.505	57	74.505
845	1090	72.88	56	72.88
805	950	68.12	49	68.12
775	900	66.335	48	66.335
725	785	62.033	45	62.033
682	710	59.055	38	59.055
597	570	53.04	33	53.04
560	490	49.267	26	49.267
445	300	38.815	17	38.815
415	280	37.54	16	37.54

Below the table, there are controls for "Fan ID" (set to "Fan 1"), "Fan Type" (set to "2000mm"), and buttons for "Add Test", "Del Test", and "Close".

Figure 37. Measured fan and building envelope data.
Source Altas v3.36.

6.3 *Testing of a very large warehouse (Building C) to determine airtightness using multiple rigs*

The following reports detail the results from the airtightness test carried out at Building C, on the 12th of December 2002. The test was performed using the Megafan rig with 2000-mm venturi attached and two medium sized fans, each with a 1250mm venturi attached. The data shown are output graphs and tables from the Altas program.

Figure 38 shows a log-log plot using a power law regression fit of the measured fan flow rate Q , against the building differential pressure ΔP . A value for the measured flow rate at a building differential pressure of 50 Pa, Q_{50} , is quoted as $80.14 \text{ m}^3\text{s}^{-1}$. This is calculated by interpolating the measured results using a least square law approximation. The calculated value for air permeability was $2.25 \text{ m}^3\text{h}^{-1}\text{m}^{-2}$, which easily satisfies the current Building Regulations target of $10 \text{ m}^3\text{h}^{-1}\text{m}^{-2}$. The reported value for air leakage index was $4.07 \text{ m}^3\text{h}^{-1}\text{m}^{-2}$. The value for the correlation coefficient of the power law regression fit is 0.9997. The exponent “n” has a value of 0.6182. Figure 39 shows a linear plot using a power law regression fit of the measured fan flow rate Q , against the building differential pressure ΔP . Figure 40 highlights the environmental and fan output data during the test. Average wind speed was noted to be 1.8 ms^{-1} at the beginning, rising to 2.3 ms^{-1} at the end of the test. Figure 41 summarises the building details. Figure 42 reports the fan and building pressures recorded during the test.

6.3.1 Log-log data plot for building pressurisation test

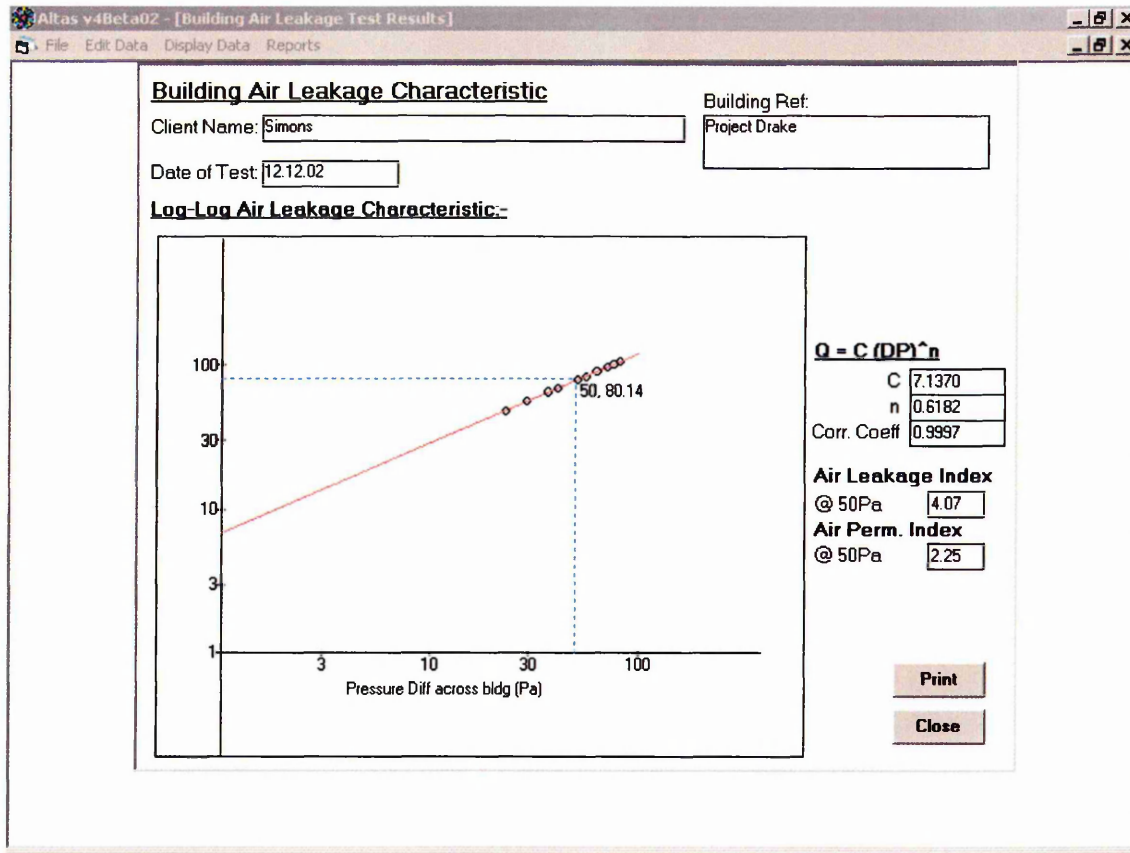


Figure 38. $Q(m^3 s^{-1})$ v. $\Delta p(Pa)$ log-log data points for the building pressurisation test. With a power law regression fit. Source Altas v3.36.

6.3.2 Linear data plot for building pressurisation test

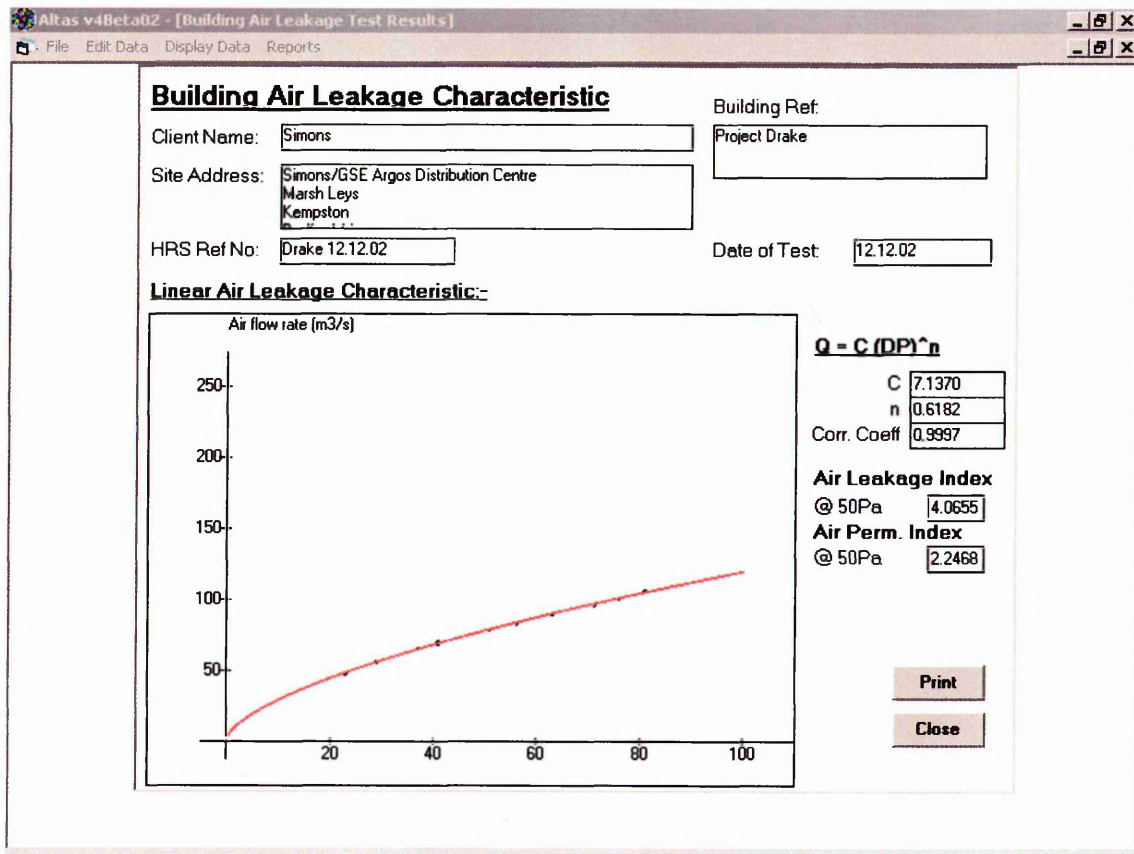


Figure 39. $Q(m^3 s^{-1})$ v. $\Delta p(Pa)$ linear data points for the building pressurisation test.
 With a power law regression fit.
 Source Altas v3.36.

6.3.3 Environmental and measured data

Altas v3beta02 - [Air Leakage Test Data Sheet]

File Edit Data Display Data Reports

Building Air Leakage Test Data Sheet

Client Name: Date of Test:

Site Address:

 Building Ref: Test Start Time:

Test Finish Time: Pressurisation:

Test database No: Depressurisation:

General Weather Conditions:

Wind Speed at Start of Test: m/s
 Wind Speed at End of Test: m/s

Barometric Press. at Start of Test: Pa
 Barometric Press. at End of Test: Pa

External Temp at Start of Test: deg C
 External Temp at End of Test: deg C

Fan off, press. diff. at Start of Test: Pa
 Fan off, press. diff. at End of Test: Pa

Internal Temp Sensor Location	Internal Temp (deg C)	
	Start	End
Centre of warehouse	<input type="text" value="14"/>	<input type="text" value="12.8"/>

Fan Speed	0	0	0	0	0	0	0	0	0	0
Press. Diff (Pa)	81	76	71	63	56	51	41	37	29	23
Air Flow (m3/s)	101.4	97.20	92.53	86.16	79.22	75.97	66.70	62.34	53.83	45.95

Engineer: Date: Checked by: Date:

Figure 40. Environmental and measured data
 Source Altas v3.36.

6.3.4 Building envelope data

Building Air Tightness Performance

Client Name: Date of Test:

HRS Ref No: Building Ref:

Site Address:

Building Physical Parameters

Building Vol: m3 Floor Area: m2

Walls Area: m2 Roof Area: m2

Building Air Tightness Results:

ALI Envlp Area = m2 Air Leakage Index (ALI) = m3/h per m2 at Pa

ALP Envlp Area = m2 Air Permeability (API) = m3/h per m2 at Pa

Indic. Infil Rate = ACH

General Comments:

Engineer: Date: Checked by: Date:

Figure 41. Building envelope data
Source Altas v3.36.

6.3.5 Measured data

Measured Data

Fan	Fan 1		Fan 2		Fan 3		Envlp	
	1250mm		2000mm		Meas.	Total		
Speed	[Pa]	[m3/s]	[Pa]	[m3/s]	[Pa]	[m3/s]	[Pa]	[m3/s]
0	536	27.693	528	27.481	470	46.278	81	101.451
0	470	25.893	440	25.034	470	46.278	76	97.205
0	386	23.41	368	22.843	470	46.278	71	92.53
0	391	23.565	370	22.907	360	39.685	63	86.156
0	390	23.534	371	22.938	260	32.744	56	79.215
0	330	21.6	309	20.882	270	33.492	51	75.973
0	196	16.509	192	16.333	275	33.861	41	66.703
0	148	14.267	147	14.217	275	33.861	37	62.344
0	77	10.123	68	9.477	280	34.227	29	53.827
0	80	10.33	68	9.477	180	26.146	23	45.953

Fan ID: Fan Type:

Figure 42. Measured fan and building envelope data.
Source Altas v3.36.

Table 3 C, n and air permeability values for very large buildings subject to test

Building type / ref	Volume (m ³)	Envelope Area (m ²)	C	n	Air permeability (m ³ /hr/m ²)
Building A	196,150	35,544	3.358	0.7098	5.46
Building B	180,760	42,072	8.931	0.524	5.93
Building C	746,720	128,400	7.137	0.6182	2.25

6.4 Discussion

The testing of these three buildings has demonstrated that technically and operationally it is possible to carry out airtightness pressure tests of such large structures. The results for Building A and Building B in Table 3 also show that the Part L air permeability target value of $10 \text{ m}^3\text{h}^{-1}\text{m}^{-2}$ is readily achievable on large warehouse buildings using standard construction techniques and paying little attention to detail at the airseal line. Table 3 also shows, admittedly for a small sample, that there is no obvious link between building size and C and n values. This is not unexpected, as each building in Table 3 was constructed differently. Great attention to the detailing and construction at the airseal line was made during the construction of building C. On buildings A and B there was very little attention to the design and quality of workmanship at the airseal line. Table 3 also indicates that the air permeability increases as the surface area of the building decreases. Based on further tests carried out by HRS one hypothesis is that as the overall surface area of warehouse increases, the relative contribution of the generally impermeable floor area to the overall surface area (i.e. floor, walls and roof) also increases. However, in this small sample the answer is probably related to the quality of workmanship and type of construction. Buildings A and B probably attained greater air leakage, due to limited attention to airseal details during construction.

6.5 *Summary*

This chapter has reported the output graphs and tables from the field data obtained from the airtightness testing of one large and two very large UK buildings. A summary and interpretation of the results has been provided. The following chapter will summarise the computer modelling work carried out in conjunction with Hilson Moran consulting engineers. Airtightness data obtained from the testing of the very large warehouse (Building C) will be input into a currently available computer thermal-modelling program along with available building envelope thermal data. Simulations will be run to assess the thermal loads imposed on the building during the heating season. One simulation will be run with the building airtightness specification utilised at the design stage (Current Building Regulations standard). The second simulation will be run with a building airtightness specification actually achieved during the building test.

Chapter 7 Computer simulation

7.1 Modelling of a very large warehouse in Bedford

The airtightness testing of building C set a new standard for the size of building that could be subject to such an investigation. Building C was a warehouse known as Project Drake at the design stage. This building is now occupied by Argos and utilised as a large storage and distribution centre with a total of 60,000 m² floor area. Thermal performance data for all the components used in the construction of the building were collated in the operation and maintenance manuals. This information was stored on DVD; search menus were available with filters to aid easy access to required information. The author decided that the abundance of building performance data available for this particular project was sufficient to fulfil the parameters of a computer simulation for dynamic thermal modelling. A number of software packages are commercially available for dynamic thermal modelling. These include the Virtual Environment, produced by IES, and TAS (Thermal Analysis System) produced by EDSL. TAS is a suite of software products which simulate the dynamic thermal performance of buildings and their systems. The main module is the TAS Building Designer, which performs dynamic building simulation with integrated natural and forced airflow. It has 3D graphics based geometry input that includes a CAD link. TAS Systems is a HVAC systems/control simulator, which may be directly coupled with the building simulator. It performs automatic airflow and plant sizing and total energy demand (EDSL website). TAS uses a Finite Element to convert geometry into an accurate resistor/capacitor representation, which is then accurately solved using a finite difference method (Harvard thermal website). For the purpose of modelling the

building, the author decided to liase Hilson Moran Consulting Engineers. They helped to carry out dynamic thermal modelling of building C using the TAS software.

At conception the building had been designed to operate within certain environmental parameters, with an envelope airtightness level set at current building regulations standards. Testing of the building had shown the envelope airtightness to exceed current regulations. Reducing building air leakage will theoretically reduce the space heating requirements during the heating season. To investigate this two computer models of the building were created; one with the design level of envelope airtightness and the other with the envelope airtightness observed during the airtightness test. Simulations were then run with a local weather file for January to assess the heating requirements to maintain design temperatures within the building.

Space heating in the warehouse is supplied by 5 gas burners (2 x 800kW and 3 x 600kW) providing a total output of 3400kW. 5 ducts encompassing 241 jet nozzles at ceiling level are designed to maintain an internal temperature of 16 °C. The original design specification for the level of infiltration was 0.25 ACH which, using the BRE $1/20^{\text{th}}$ rule adapted for large buildings, would be indicative from a building attaining current building regulations of airtightness of $10\text{m}^3\cdot\text{h}^{-1}\cdot\text{m}^{-2}$. HRS air tested the building and found the actual building envelope permeability to be $2.25\text{m}^3\cdot\text{h}^{-1}\cdot\text{m}^{-2}$. This would give an indicative infiltration rate of 0.07 ACH. The initial hypothesis was that a reduction in infiltration loading could facilitate a possible downsizing of plant at the design stage.

The author formulated the line of investigation for the dynamic thermal modelling.

This was as follows: -

From the design drawings a wireframe model of the project was constructed. Data for the thermal properties of all components used in the construction were collected from the O and M manuals and by contacting manufacturers. These thermal properties were assigned to the components in the computer model. Where manufacturer data was not available, worst case scenarios were used. A weather data file for Bedford was incorporated into the model and a simulation run to substantiate infiltration and fabric losses for the building in the worst case environmental temperature (-4°C external) on January 31st. Two models were run with natural air change rates of 0.25 and 0.07 respectively, to maintain the design internal conditions of 16°C . Building component surface temperatures were established from the model.

7.2 *Computational fluid dynamics modelling of Building C*

A theoretical negative side effect of plant downsizing in such a high building was that design lateral temperatures would not be maintained across the building and that stratification would occur resulting in uneven temperatures between the floor and ceiling. This was investigated using Computational Fluid Dynamics (CFD) modelling. FLOVENT - a commercial CFD programme was utilised to model in detail the airflow patterns and heat transfer which occurred within the Warehouse. Output from FLOVENT takes the form of temperature profiles and vector plots within the domain being investigated and, as such, allows the designer to investigate in detail the local thermal conditions, such as stratification, that are generated.

The simulation model was created within the FLOVENT software package and comprised a domain measuring 359 x 160 x 15.5 m high to represent the Warehouse. Racking was included as solid/cuboid shelves. The internal offices within the Warehouse area were also included in the model and allowance made for air to leak out

via the offices. External wind on the day the air-leakage test was carried out was relatively low and therefore this was not included in the CFD model.

Limitations in the version of FLOVENT used meant that expected fabric leakage rates could not be applied to whole surfaces of the building. Therefore, air-leakage paths were represented by resistances to flow applied to sections of the building fabric. These leakage paths in the building fabric had to be estimated in terms of their size and location. To simplify the model, and in order to avoid complications in solution convergence, a uniform width was assigned to the leakage paths, which were located along the perimeters of the building.

An approximate size of the total leakage path was obtained from the Effective Leakage Area calculated from Altas based up on equation 7.1 below. The minimum allowable width of a resistance in FLOVENT applied evenly over the length of the building symmetries resulted in a total leakage path area of 213.72m². To adjust this to the required effective leakage area a free area ratio of approximately 0.038 was applied to the resistances. The effective leakage area was then used to estimate the loss coefficient ("k" in equation 7.2) representing the resistance in the CFD model. For this model a value of 1.0 was assigned to the discharge coefficient as the geometry of the orifices were not known.

$$ELA = Q * ((\rho/2\Delta p)^{0.5}/C_D) \quad (7.1)$$

$$\Delta p = 0.5(k\rho v^2) \quad (7.2)$$

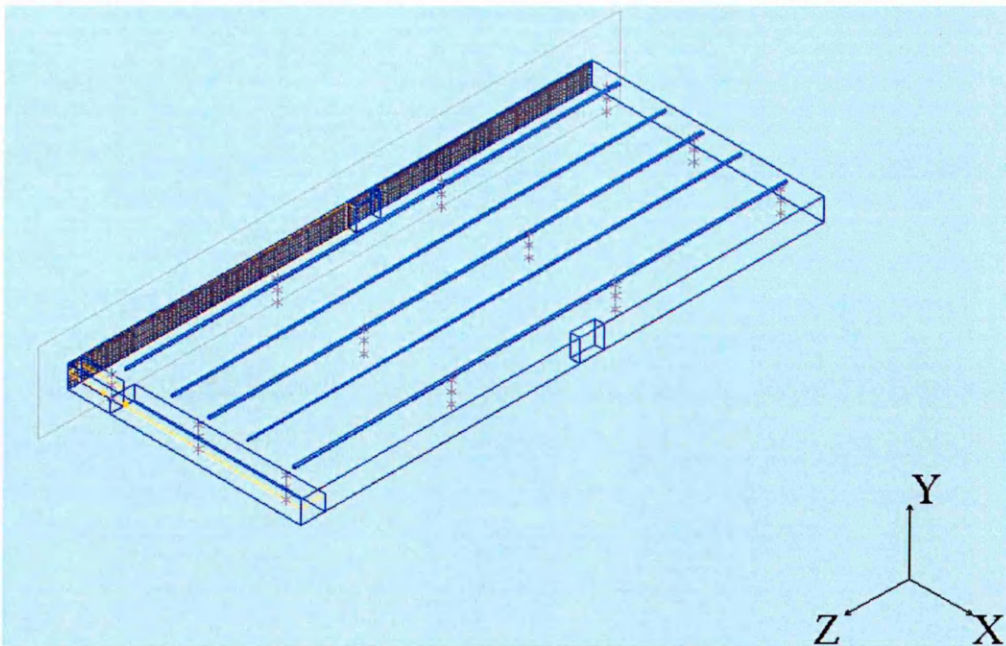


Figure 43: CFD model of warehouse

7.2.1 Turbulence model

The domain modelled was huge with significant open spaces. This, coupled with the fact that airflow discharge from the high-velocity nozzle diffusers is very chaotic and irregular, implied that the flow would be of a turbulent nature. Hence, turbulence was represented by the LEVEL $k-\varepsilon$ model in accordance with FLOVENT modelling advice.

7.2.2 Boundary Conditions

External walls, internal walls, roof and floor were modelled as constant temperature surfaces. Surface temperatures were obtained from TAS simulation results. Inflow into the domain was represented by constant volume flow rate nozzle diffusers each with the airflow rate and jet temperatures set to match the actual design/commissioned data. The location of nozzle diffusers was derived from "As-built" drawing layouts. Outflow from

the domain was via pressure loss leakage paths represented by planar resistances whose loss coefficient was derived as described above. Heat gains from occupants and other sources such as forklift trucks working within the building were ignored. Heat gain from internal lights was assigned a constant value of 15W/m^2 of floor area.

7.2.3 *Grid and Grid independence*

A grid *localised* at diffuser locations and totalling about 720 000 cells was used. The large number of cells used was mainly due to the need to capture the development of the plume at nozzle diffuser locations. This final grid was arrived at by performing a simple grid sensitivity assessment on a number of cases. This indicated that whilst maintaining the plume profile, by reducing the cell sizes by 30% the difference in results averaged less than 1% difference in temperatures predicted at various points within the computational domain. This level of accuracy was considered adequate taking into account the other uncertainties in problem definition such as representing the air leakage paths by planar resistances likely to be encountered in practice.

7.2.4 *Solution control and Convergence*

False-time-steps and individual variable residual termination levels automatically generated by FLOVENT were utilised in the solution. Convergence based on the residual errors reaching an acceptably low-level, automatically calculated by FLOVENT, was achieved within 10 000 iterations lasting over several days on a Toshiba P4 laptop with 512Mb of RAM.

7.2.5 Jet Plume Calibration

Manufacturer's bench-test technical data for the nozzle jet diffusers could not be obtained for this study, hence, calibration of the jet plume was not undertaken. However, the airflow pattern from the nozzles was set by resolving the resultant jet velocity into the three co-ordinate directions (x, y, z) and ensuring the vector perpendicular to the nozzle diffuser face was 20m/s with an angle of 45° in line with the design data. The resulting jet plume had the desired effect.

7.2.6 Air-leakage test infiltration rate (0.07 ach⁻¹)

Simulations were carried out using actual results from the air-leakage test i.e. an infiltration rate of 0.07 ach⁻¹, and commissioned data for the induction air heating system (50°C supply air temperature and 20m/s nozzle jet velocity). Temperatures of all surfaces included in the CFD model were assigned using results from TAS calculations, taking into account the reduced infiltration rate. The CFD model was run and solved using nozzle data obtained from the manufacturer and surface temperatures obtained from the results of the CFD modelling.

7.3 *Results of dynamic thermal modelling of Building C using original design specification and airtightness level determined from airtightness test to produce energy consumption model*

The dynamic thermal model for building C was constructed and run using an infiltration level of 0.25 ac/h and a worst case heating scenario month from January 1st to 31st. The same initial model was then run with an infiltration level of 0.07 and a worst case heating scenario month from January 1st to 31st.

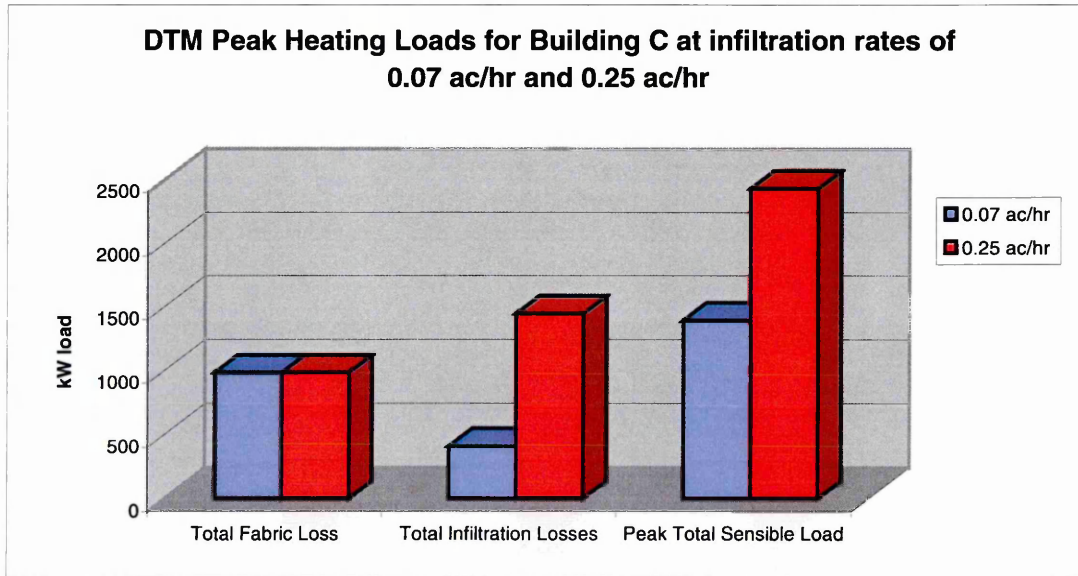


Figure 44: Results for peak heating loads for building C at 0.07 and 0.25 ac/hr during the month of January 2003

Figure 44 highlights the results for peak heating loads from the dynamic thermal modelling simulation. With the infiltration level set at 0.25 ac/hr the total fabric losses are 982 kW; the total infiltration losses are 1444 kW and the peak total sensible load is 2426 kW. With the infiltration level set at 0.07 ac/hr the total fabric losses are 982 kW; the total infiltration losses are 409 kW and the peak total sensible load is 1391 kW. The result of reducing the infiltration level from 0.25 ac/hr to 0.07 ac/hr are a 1035 kW reduction in infiltration load.

7.4 Results of computational fluid dynamics modelling of Building C

The results for the solved case for 0.07ach^{-1} indicate temperatures in the Warehouse ranging from about 14°C at floor level to 18°C at ceiling level (Figure 45). These were consistent with measurements made on site. It can be seen from figure 45, which shows a typical section along the height of the building, that the temperature is fairly uniform across the Warehouse. As such it can be said that most of the "occupied zone" within the Warehouse falls within the expected range of design parameters. It is clear from figure 45 that a "cold zone" occurs at the end of the building opposite where the offices are located. The reason for this cold zone not being reflected on the other side of the model is that the cold outdoor air entering the Warehouse via the offices is warmed up as the office areas were at a relatively higher temperature than the Warehouse.

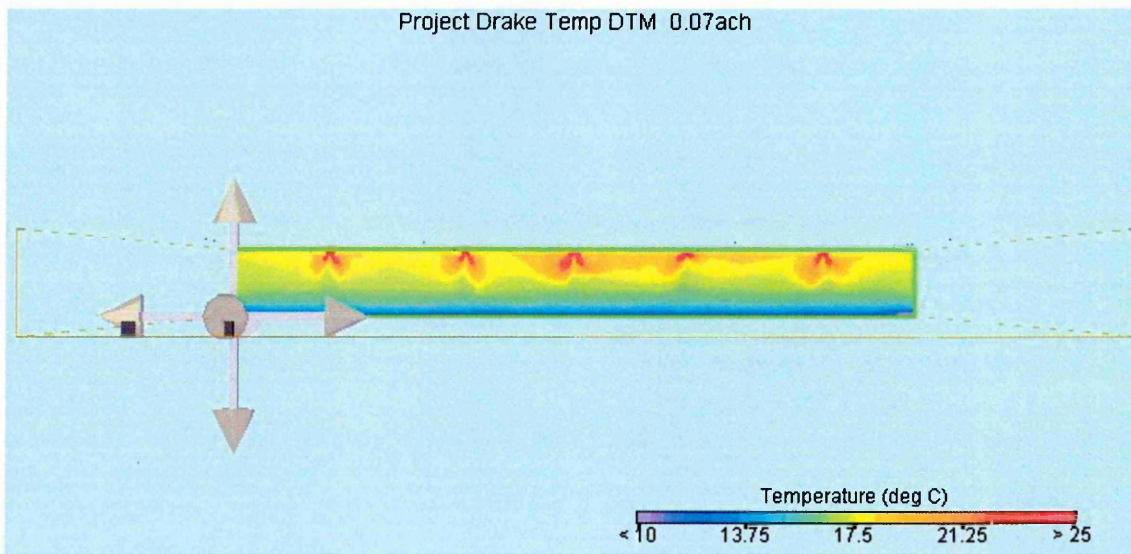


Figure 45: Typical section across building showing discharge from jet diffusers

7.4 Summary

This chapter has summarised the computer modelling work carried out in conjunction with Hilson Moran consulting engineers. Airtightness data obtained from the testing of the Building C was input into a currently available computer thermal-modelling program along with available building envelope thermal data. Dynamic thermal simulations were run to assess the thermal loads imposed on the building during the heating season. One simulation was run with the building airtightness specification utilised at the design stage (Current Building Regulations standard). The second simulation was run with a building airtightness specification actually achieved during the building test. The simulation results indicate a large reduction in the total peak heating load for Building C with a reduction in infiltration from 0.25 ac/hr to 0.07 ac/hr.

The following chapter will discuss the viability of airtightness testing very large buildings. There will then be a discussion on the energy savings achieved with improved envelope airtightness at Building C. Current information available on the airtightness of very large UK buildings will be summarised. Finally, an investigation into the further work that can be carried out into the impact of energy savings with improved airtightness will be presented.

8.1 Feasibility of testing large buildings in the UK

The theory and equipment to carry out airtightness testing using the steady state pressurisation technique has been readily available since the 1980's. The widespread uptake of this facility in the UK was negligible up until 2002. This was possibly due to resistance from the construction industry and a lack of information available for clients about the thermal benefits of airtight buildings. The implementation of the requirement to airtight buildings in the Approved Document Part L2 2002 has resulted in a relatively slow increase in the number of buildings tested and the availability of rigs to test these buildings. One possible excuse for this was the perceived technical problem of testing of buildings with floor areas over 5000 m². This study has demonstrated the design, construction and calibration of a rig capable of testing very large buildings using a steady state pressurisation technique.

The successful airtightness testing of Building C using a large rig and two medium sized rigs has set a precedent for the envelope performance analysis of very large buildings (see Appendix A.2). The preparation of the building, set-up of the rigs, airtightness test and analysis of results can all be achieved within one day. The actual cost to the main contractor, for the quality assurance spot checks of composite panel joints during construction and final airtightness test, was less than 0.1% of the total contract expenditure. The results from an air test provide the main contractor with information about the quality of the workmanship of the subcontractor who has constructed the airseal line. For Building C the cladding subcontractor was responsible for this detail. The results from an airtightness test can also be used as a performance indicator for the client.

8.2 *Airtightness of large warehouse buildings in the UK*

This study has highlighted the feasibility of air testing large warehouse buildings. A number of testing companies have the resources and technical expertise to carry out the testing of large buildings. These companies have formed the basis of the Airtightness Testing and Measurement Association (ATTMA). The Association, currently chaired by David Pickavance of BSRIA, has recently been awarded a DTI grant to carry out further research into the testing of large buildings.

Airtightness testing of large buildings in the UK using the steady state technique requires large, expensive test rigs. The provision of these rigs has not been commercially viable for non-governmental organisations until the introduction of the Building Regulation 2002 Part L2 Conservation of Fuel and Power. The slow uptake of the new regulations by the UK construction industry has meant that many large rigs currently remain idle for most of the year. Air testing companies are looking to the Office of the Deputy Prime Minister to enforce the regulations that it has put in place.

8.3 *Energy savings in Building C associated with improved envelope airtightness*

8.3.1 *Dynamic thermal modelling (DTM) simulation*

The DTM simulation highlighted the reduction in infiltration load that can be attained from improved building airtightness. The DTM model simulated Building C with air permeability levels of $10 \text{ m}^3 \cdot \text{h}^{-1} \cdot \text{m}^{-2}$ (current building regulations requirement) and $2.25 \text{ m}^3 \cdot \text{h}^{-1} \cdot \text{m}^{-2}$ (actual figure observed on site). From the DTM simulation it was noted that this improvement in building envelope airtightness resulted in a 40% reduction in peak total sensible load. The indicative infiltration rate of 0.07 was calculated from the

air test. During air test conditions all dock levellers and doors were closed and therefore the test does not truly represent operational conditions. However, it should be noted that the plant was specified for a project attaining current Building Regulation standards of airtightness (i.e. $10\text{m}^3\cdot\text{h}^{-1}\cdot\text{m}^{-2}$). Given this parameter the indicative infiltration rate would be at least 0.25 ac/hr under air test conditions. The boiler design margin for the plant currently installed is large (approximately 40%) to allow for increased infiltration rate due to open dock levellers etc. This design margin should also be applied when specifying boiler sizes for a project with improved building airtightness.

8.3.2 Computational fluid dynamics (CFD) simulation

The study successfully established a CFD model incorporating results from the building envelope airtightness test (analysed using Altas) and DTM simulations. This model can be employed in carrying out simulations with a view of assessing the impact on in-door parameters in relation to plant downsizing. The exercise re-enforced the fact that there is currently no guidance available on accurately assigning boundary conditions to represent air-leakage paths. This study has highlighted a possible way of deriving these boundary conditions. Thus the resulting model can be used as a basis of carrying out simulations to assess the impact of tighter buildings on plant sizes and the resulting in-door air quality and comfort parameters.

The solved case showed temperatures in the warehouse ranging from 14°C at floor level to 17.5°C at ceiling level. The majority of cells within the warehouse space were around 16°C , which is concurrent with design specification and readings actually recorded on site. It is therefore safe to assume that the boundary conditions for the CFD

Drake simulation are correct. Further investigation on the effects of plant downsizing on lateral temperatures and stratification can be carried out using this model.

8.4 Further work on the impact of energy savings with improved envelope airtightness

It has been established that there is a significant reduction (40%) in peak total sensible load associated with improving building envelope airtightness from current building regulation levels, to those measured at Building C. Further investigation is required to establish whether plant can be downsized at the design stage of a project, with knowledge of the expected level of completed building airtightness. This would allow an initial cost saving. An assessment of operation costs with the smaller heating and ventilation units would then be required. The effect of downsized plant on the internal building conditions would also need to be analysed.

8.4.1 Further work with dynamic thermal modelling

Prior to further investigation using DTM, information about downsized plant will be required. Information on the boiler efficiency curves from the manufacturer for currently installed plant and the next model down within the product range would need to be obtained. An energy simulation in DTM would be run for a full year at Building C to establish total load and requirements for heating throughout the year at 0.07 ac/hr. Investigation would be carried out to assess the heating load demands on the currently installed and downsized boilers and the level of required output with associated associated boiler efficiency. Further to this a lifetime cost analysis would be carried out for the currently installed plant and the theoretical reduced plant scenario.

8.4.2 Further work with Computational Fluid Dynamics Simulation (CFD)

Prior to further investigation with CFD manufacturers benchmark data would be obtained for jet plumes from the nozzles. It is anticipated that reducing the size of plant installed in the building would result in lower jet temperatures or possibly reduced jet velocities. A further CFD simulation would therefore be run with reduced nozzle jet velocity and/or temperature as required to assess stratification and lateral temperatures within Building C.

9.0 Acknowledgements

The author would like to thank the Teaching Company Scheme (Programme No. 3790) for their financial support of this research study. Special thanks go to Professor Steve Sharples for his encouragement, advice and dry humour. Thanks are also due to the staff at HRS Services Ltd, in particular the director Ed Westgate. His advice and support have been invaluable during the past two years.

10.0 References

ASHRAE Handbook 2001: Fundamentals. Chapter 26 Ventilation and Infiltration.

ASHRAE Standard 119 (1988) Air Leakage Performance for Detached Single Family Residential Buildings, American Society of Heating, Refrigerating and Air Conditioning Engineers, 1988.

Billington M. J. (2001) Manual to the Building Regulations Third Edition 2001. The Stationary Office.

Blomsterberg A. (1977) Air leakage in dwellings. Dept. Bldg. Constr. Report No.15, Swedish Royal Institute of Technology, 1977.

Boushear M. (2001) Rules of Thumb – Guidelines for assessing building services. Technical Note TN 15/2001. BSRIA, August 2001.

Brundrett G. and Jackman P. et al (1997) Ventilation – airtightness campaign. Building Services Journal September 1997, vol. 19, no. 9. Chartered Institute of Building Service Engineers.

BS 848-1:1997. Fans for general purposes. British Standard Institution.

BS EN 1042: Section 2.1:1983 Measurement of fluid flow in closed conduits. British Standards Institution.

BS EN 13829. Thermal performance of buildings – Determination of air permeability of buildings – Fan pressurization method. British Standards Institution.

Carey P.S. and Etheridge D.W. (2001) Leakage measurements using unsteady techniques with particular reference to large buildings. Building Serv. Eng. Res. Technol. 22,2 (2001) pp. 69-82.

CIBSE (2000) Technical Memoranda TM23:2000 Testing Buildings for Air Leakage. The Chartered Institution of Building Services Engineers. London, October 2000.

Colthorpe K. (1990) A review of building airtightness and ventilation standards. AIVC 1990, Technical Note 30.

Council of the European Union (2002) DIRECTIVE 2002/ /EC OF THE EUROPEAN PARLIAMENT AND OF THE COUNCIL of the energy performance of buildings. Brussels, 5 September 2002.

Dickinson J.B. and Feustel H.E. (1985) Seasonal variations in effective leakage area. (Thermal performance of the exterior envelopes of buildings III. Proc. of ASHRAE/DOE/BTECC Conference) Florida, 2-5 December 1985. ASHRAE SP 49. 144 – 160.

DTLR (2002) Approved Document Part L2. Conservation of Fuel and Power in Buildings other than Dwellings. The Stationary Office.

Etheridge D. W., Nervalva D.J. and Stanway R.J. (1987) Ventilation in traditional and modern housing. Research and Development Division, British Gas plc, 1987. (presented at the 53rd autumn meeting of the Institution of Gas Engineers, London, November 1987).

Graves H.M. and Phillipson M.C. (2000) Potential implications of climate change in the built environment. Foundation for the Built Environment. Building Research Establishment.

IPCC, WGI Climate Change 2001: The Scientific Basis, Summary for Policymakers: A report of working group I on the Intergovernmental Panel on Climate Change, 2001.

Jackman P.J. (1973) Heat loss in buildings as a result of infiltration – “Environmental temperature and the calculation of heat losses and gains”. I.H.V.E Symposium, June 1973.

King T. (2003) Building Regulations Part L2 – Pressure Testing. Personal communication. Building Regulations Division. Office of the Deputy Prime Minister. 24th January 2003.

Kitson M. (2003) Swiss Re Headquarters Inside and Out. FLUENT newsletter, Spring 2003.

Kitson M. (2003) Turning Green. Building Services Journal, June 2003.

Liddament M.W. (1996) A guide to Energy Efficient Ventilation. AIVC, March 1996.

Lilly J.P. (1987) Ventilation and leakage measurements in industrial buildings. (Ventilation Technology Research and Application) 8th AIVC Conference, Uberlingen, Federal Republic of Germany, 21 – 24 September 1987. Bracknell Poster P4, 18.1-18.12.

Limb M.J. (1994) Ventilation and Building Airtightness: an International Comparison of Standards, Codes of Practice and Regulations. AIVC Technical Note 43. AIVC February 1994.

Modera M.P. and Sherman M.H. (1985) AC pressurisation: a technique for measuring the air leakage area in residential buildings. ASHRAE Symposium on Air Leakage Analysis Techniques, Honolulu, Hawaii, June 23-26, 1985.

Nishioka T. (2000) A New Technique for Measuring Airtightness of the Building Envelope Using Pulse Pressurisation. Progress in modern ventilation. Proceedings of Ventilation 2000, 6th international symposium on ventilation for contaminant control, June 2000, Helsinki, Vol. 1, pp 80-83.

Office of the Deputy Prime Minister (2003) Possible Future Performance Standards for Part L: October 2003.

Ogle R. and O'Connor J. (1995) Failure of the building envelope: two case studies. (Thermal performance of the exterior envelopes of buildings VI. Conference proceedings), Florida, December 1995, ASHRAE 55 – 66.

Orme M. (1995) A Storm Building Up – Low Energy Housing in the Orkney Islands.

Air Infiltration Review, June 1995, vol. 16, no. 3, 1–4.

Orme M. (2001) Estimates of the energy impact of ventilation and associated financial expenditures. Energy and Buildings., 2001, vol.33, pp 199-205.

Perera M.D.A.E.S., Turner C.H.C. and Scivyer C.R. (1994) Minimising air infiltration in office buildings. BRE Report BR265 (Garston: Building Research Establishment), July 1994.

Persily A. (1982) Repeatability and Accuracy of Pressurization Testing. Thermal performance of the exterior envelopes of buildings II. Proc. of ASHRAE/DOE Conference. Las Vegas, 6-9 December 1982. ASHRAE SP 38, pp 380 –390.

Potter I.N. (1998) Airtightness Specifications. Specification 10/98. BSRIA, March 1998.

Potter I.N. (2000) Air Permeability vs. Air Leakage Index. Report 99931A/1. BSRIA, July 2000.

Potter I.N. (2001) Airtightness testing. TN 19/2001. BSRIA October 2001.

Potter I.N., Jones T.J. and Booth W.B. (1995) Air Leakage in Office Buildings. BSRIA Technical Note TN8/95, May 1995.

Potter I.N. and Jones T.J. (1992) Ventilation Heat Loss in Factories and Warehouses. BSRIA Technical Note 7/92, February 1992.

Pout C.H., MacKenzie F. and Bettle R. (2002) Carbon dioxide emissions for non-domestic buildings: 2000 and beyond. BRE Report 442. Building Research Establishment.

Royal Commission on Environmental Pollution, Energy – The Changing Climate, The Stationary Office, June 2000.

Scrase J.I. (2001) Curbing the growth in UK commercial energy consumption.. Building Research and Information, 2001.

Sherman M. H. (1990) Air change rate and airtightness in buildings. ASTM 1990.

Sherman M.H. and Dickerhoff D.J. (1998) Airtightness of U.S. dwellings. ASHRAE Trans. 1998, vol. 104, part 2, paper no. TO-98-25-1, 1359 – 1367.

Sherman M.H. and Grimsrud D.T. (1980) Measurement of infiltration using fan pressurization and weather data. Air Infiltration Conference “Instrumentation and Measuring Techniques”. Windsor, 6-8 October 1980.

Shorrock L.D. and Henderson G. (1990) Energy use in buildings and carbon dioxide emissions. BRE, 1990.

Stephen R.K. (1998) Airtightness in UK dwellings: BRE's test results and their significance. Building Research Establishment.

Stephens M. (2002) Airtight regulations. *Electrical Times*, November 2002, pp24-26.

Vidal J. and Brown P. (2003) How climate changes affects all our lives. *The Guardian*. Wednesday August 27th 2003, pp. 10.

Walker R.R. and Perera M. D. A. E. S. (1990) The BRESIM technique for measuring air infiltration in large buildings. Building Research Establishment, August 1990.

Walker R.R. and White M.K. (1995) The passive gas tracer method for monitoring ventilation rates in buildings. Building Research Establishment, 1995.

Warren P.R. and Webb B.C. (1980) Ventilation measurements in housing. Proceedings of the CIBS Symposium "Natural ventilation by design", December 1980, pp 22-34. London, CIBS.

White paper, *Our Energy Future – Creating a Low Carbon Economy*. Crown Copyright 2003.

11.0 Relevant literature

Alkhaddar R.M., Dewsbury J. and Orłowski R. (1990) The design and testing of a calibration chamber used in the development of an AC pressurisation apparatus. Air Infiltration Review. March 1990, vol. 11, no. 2, pp. 7-9.

Anis W.A.Y. (2001) "The Impact of Airtightness On System Design". ASHRAE Journal, 43, pp 31 – 35.

ASHRAE Handbook 2001: Fundamentals. Chapter 16 Airflow around buildings.

ASHRAE Handbook 2001: Fundamentals. Chapter 33 HVAC Computational Fluid Dynamics

ASTM E 283-91 (Reapproved 1999) Standard Test Method for Determining Rate of Air Leakage Through Exterior Windows, Curtain Walls, and Doors Under Specified Pressure Differences Across the Specimen. American Society for Testing and Materials.

ASTM E 1827-96. Standard Test Methods for Determining Airtightness of Buildings Using an Orifice Blower Door. American Society for Testing and Materials.

Baldwin R., Barlett P.B., Leach S.J., Attenborough M.P. and Doggart J.V. (1993) BREEAM/Existing Offices 4/93 An environmental assessment for existing office buildings. BRE, 1993.

Baldwin R., Yates A., Howard N. and Rao S. (1998) BREEAM 98 for offices. BRE, 1998.

Bemrose C.R. and Smith I.E. (1992) Thermal stratification in intermittently heated heavyweight buildings (Churches). *Building Services Engineering Research and Technology*. 1992, vol.13, no.3, pp 119-131.

Bolin B., Doos B.R., Jager J. and Warrick R. A. (1986) *The greenhouse effect, climate change and ecosystems*. Chichester, John Wiley and Sons, 1986.

Bordass B. (2000) Envelope airtightness. *The Architects Journal*, vol. 14, no. 211, pp. 48-51.

BS 5925:1991. *Ventilation principles and designing for natural ventilation*. British Standards Institution.

BS EN ISO 6946:1997. *Building components and building elements – Thermal resistance and thermal transmittance – Calculation method*.

BS 8207:1985. *Energy efficiency in buildings*. British Standards Institution.

BS EN 13187:1999. *Thermal performance of buildings – Qualitative detection of thermal irregularities in building envelopes – Infrared method*. British Standards Institution.

BS EN 12114:2000 Thermal performance of buildings – Air permeability of building components and building elements – Laboratory test method.

BS EN ISO 13788:2002. Hygrothermal performance of building components and building elements – Internal surface temperature to avoid critical surface humidity and interstitial condensation – Calculation methods.

BCO (British Council for Offices) Guide 2000. Best practice in the specification for offices. October 2000.

Buchanan C.R. and Sherman M.H. (1998) Simulation of Infiltration Heat Recovery – Ventilation technologies in urban areas. 19th AVIC Conference, Oslo, September 1998.

Chiu Y.H. and Shao L. (2001) An Investigation into the Effect of Solar Double Skin Façade with Buoyancy-Driven Natural Ventilation. CIBSE National Conference.

CIBSE Building Energy Code (1981) Part 2 – Calculation of energy demands and targets for the design of new buildings and services – Section (a) Heated and Naturally Ventilated Buildings. The Chartered Institution of Building Services Engineers, 1981.

CIBSE Technical Memoranda TM22: (1999) Energy Assessment and Reporting Methodology: Office Assessment Method (1999) The Chartered Institution of Building Services Engineers, February 1999.

CIBSE Technical Memoranda TM22 Annex: (1999) Energy Assessment and Reporting Methodology: Banks and Agencies Assessment Method. Hotels Assessment Method.

Mixed-use Buildings Assessment Method (1999) The Chartered Institution of Building Services Engineers, February 1999.

CIBSE Guide B2 Ventilation and air conditioning (2001) The Chartered Institution of Building Services Engineers, August 2001.

CIBSE Guide to ownership, operation and maintenance of building services (2000) The Chartered Institution of Building Services Engineers, March 2000.

CIBSE Concise Handbook (2002) The Chartered Institution of Building Services Engineers, November 2001.

CIBSE Guide A (1999) Environmental design. The Chartered Institution of Building Services Engineers, October 1999.

CIBSE (2002) Technical Memoranda TM29:2002 HVAC strategies for well-insulated airtight buildings. The Chartered Institution of Building Services Engineers, January 2002.

CIBSE (2003) Improved life cycle performance of mechanical ventilation systems. The Chartered Institution of Building Services Engineers. London, February 2003.

Closs S., Chilengwe N. and Sharples S. (2003) Pressure testing a very large building: theory and practice. Proc. 24th AIVC Int. Conference 'Ventilation, Humidity Control and Energy', 271 – 276, Washington DC, 12-14th Oct. 2003.

Cohen R. (2003) Tightly knit. Building Services Journal. CIBSE. June 2003, vol. 25, no. 6, pp. 42-43, 45-46.

Cook M.J., Fiala D., Mardaljevic J. and Lomas K.J. (2001) Use of Computer Simulation in the Design of a Low Energy Learning Resource Centre. CIBSE National Conference

Crisp V.H.C., Doggart J. and Attenborough M. (1991) BREEAM 2/91 An environmental assessment for new superstores and supermarkets. BRE, 1991.

Crozier B. (2000) Enhancing the performance of oversized plant. Application Guide AG 1/2000. BSRIA, June 2000.

Cullen N.J. (2001) Climate change – designing buildings with a future. CIBSE national conference.

Daly B.B. (1978) Woods Practical Guide to Fan Engineering. Woods Of Colchester Limited.

David J. (1997) Breaking the energy barrier. M and E Design, October 1997, pp 28 – 30.

DEFRA/DTLR (2001) Limiting thermal bridging and air leakage: Robust construction details for dwellings and similar buildings.

Desjarlais A.O., Childs K.W. and Christian J.E. (1998) Thermal Performance of the Exterior Envelopes of Buildings VII. Conference Proceedings, Clearwater Beach, Florida, pp. 6-10.

Donaldson C. and Armstrong J. (2000) Toolkit for building Operation Audits. Application Guide AG 13/2000. BSRIA, December 2000.

DTI (2000) Energy Projections for the UK. Energy Paper 68. Energy Use and Energy Related Emissions of Carbon Dioxide in the UK, 2000 – 2020. UK Department of Trade and Industry, 2000.

ECON 18. Energy Efficiency in Industrial Buildings and Sites.

ECON 19. Energy use in offices.

ECON 36. Energy Efficiency in Hotels – A guide for Owners and Managers.

Elsayed M.A., Grant J.F. and Mortimer N.D. Energy Use in the United Kingdom Non-Domestic Building Stock: 2002 Catalogue of Results. Final Report for the Global Atmosphere Division of the Department for the Environment, Food and Rural Affairs, January 2002.

Emmerich S.J. and Persily A.K. Energy Impacts of Infiltration and Ventilation in U.S. Office Buildings Using Multizone Airflow Simulation. Proceedings of IAQ and Energy 98 Conference. New Orleans, LA 22-27 Oct. 1998. IAQ and Energy 98, pages 191-203.

Energy conservation: a study of energy consumption in buildings and possible means of saving energy in housing. BRE Working Party Report, June 1975.

Fletcher J. (1998) Building Control and Indoor Environmental Quality – a best practice guide. Technical Note TN 9/98. BSRIA, March 1998.

Fletcher J. (1999) HVAC Troubleshooting – a guide to solving indoor environmental and energy consumption problems. Application Guide AG 13/99. BSRIA, September 1999.

Fletcher J. (2000) Achieving Minimum Outdoor Air – Commissioning and Test Procedures. Application Guide AG 17/2000. BSRIA, December 2000.

Freeman J., Gale R. and Lilly J.P. (1983) Ventilation measurements in large buildings. Air infiltration reduction in existing buildings, 4th AIVC Conference, September 26-28th 1983, Elm, Switzerland, 5.1-5.14.

Furbringer J.M. and Foradini F. (1994) Bayesian Method for Estimating Airtightness Coefficients from Pressurisation Measurements. Building and Environment, Vol 29, No. 2, pp. 151-157.

Good Practice Report 30. A performance Specification for the Energy Efficient Office of the Future.

Good Practice Guide 61. Energy efficiency in advance factory units.

Good Practice Case Study 62. Energy efficiency in offices.

Good Practice Guide 71. Selecting air conditioning systems.

Good Practice Case Study 148. Energy management, J Sainsbury plc.

Good Practice Guide 190. Energy efficiency action pack – for retail premises.

Good Practice Case Study 201. Energy efficient refurbishment of retail buildings.

Good Practice Case Study 242. Energy efficiency in hotels – good energy management in a medium-sized hotel.

Good Practice Case Study 296. The Munich Park Hilton Hotel, Germany. Energy costs controlled as part of an Environmental Management Programme.

Good Practice Guide. The designers guide to energy-efficient buildings for industry.

Good Practice Guide 304. The purchaser's guide to energy-efficient buildings for industry.

Hanby V.I. and Angelov P.P. Application of univariate search methods to the determination of HVAC plant capacity. *Building Services Engineering Research and Technology*, vol. 21, no. 3, pp 161-166.

Hart J.M. (1991) A practical guide to infra-red thermography for building surveys.

BRE, 1991.

Haughey D. P. (1990) Retail warehouses: the potential for increasing energy efficiency.

IP8/90. BRE, July 1990.

HUGHES D. (1989) Energy efficient factories: design and performance. IP 13/89.

BRE, June 1989.

IHVE Guide (1970). The institute of Heating and Ventilation Engineers London, 1971.

Irving S. and Uys E. (1997) Natural ventilation in non-domestic buildings. CIBSE

Applications Manual AM10: 1997. The Chartered Institution of Building Services Engineers, March 1997.

Kato S., Murakami S., Shoya S and Hanyu F. (1995) "CFD analysis of flow and temperature fields in atrium with ceiling height of 130m". ASHRAE Trans. Vol. 101, Part 2, Paper number, SD-95-14-5, pp. 1144 - 1157.

Kingspan (2002) Approved Construction Details for Part L2 (England and Wales) and Part J (Scotland). Kingspan insulated roof and wall systems, 2002.

Knight K. D., Boyle B.J. and Phillips B.G. (2001) Performance of Exterior Envelopes of Whole Buildings VIII: Integration of Building Envelopes, Conference Proceedings, Clearwater Beach, Florida, December 2-7 2001, ASHRAE.

Lam J.C. and Chan A.L.S. (2001) CFD analysis and energy simulation of a gymnasium. *Building and Environment*, vol. 36, no. 3, pp 351-358.

Levermore G.J. and Doylend N.O (2002) North American and European Hourly Based Weather Data and Methods for HVAC Building Energy Analyses and Design by Simulation. *ASHRAE Trans*, vol. 108, part 2, paper number HI-02-16-1, pp 1053-1062.

Limb M.J. (1995) The AIVC's New Survey of Current Research into Air Infiltration, Ventilation and Indoor Air Quality. *Air Infiltration Review*, Vol. 16, No. 2, March 1995 pp. 12-14.

Lindsay C.R.T., Bartlett P.B., Baggett A., Attenborough M.P. and Doggart J.V. (1993) BREEAM/New Industrial Units 5/93 An environmental assessment for new industrial, warehousing and non-food retail units. BRE, 1993.

Love J.A. and Passmore R.S. (1987) Airtightness testing methods for row housing. (*ASHRAE Trans*) 1987, Part 1, Vol 93, 1359 –1370.

Lowe R.J. (2000) Ventilation strategy, energy use and CO₂ emissions in dwellings – a theoretical approach. *Building Services Research and Technology*, vol. 21, no.3, pp 179-185.

Lundin L. (1983) Air leakage in industrial buildings – preliminary results. Air infiltration reduction in existing buildings, 4th AIVC Conference, September 26-28th 1983, 6.1-6.8.

Lyberg M. and Honarbakhsh A. (1989) Determination of air leakiness of building envelopes using pressurisation at low values. Swedish Council for Building Research.

MCRMA (2002) Guidance for the design of metal roofing and cladding to comply with approved document L2:2001. The Metal Cladding and Roof Manufacturers Association Limited, January 2002.

Moss S.A. (1994) Energy consumption in public and commercial buildings. BRE Information Paper, September 1994.

Oseland N.A. and Humphreys M.A. (1994) Trends in thermal comfort research. BRE, 1994.

Parsloe C. (2001) Commissioning Air Systems – Application procedures for buildings. Application Guide AG 3/89.3. BSRIA, November 2001.

Pearson C. (2002) Thermal Imaging of Building Fabric – A best practice guide for continuous insulation. Technical Note TN 9/2002. BSRIA, April 2002.

Pennycook K. (2001) The Effective BMS – A guide to improving system performance. Application Guide AG 10/2001. BSRIA, August 2001.

Pennycook K. and Hamilton G. (1998) Specifying Building management Systems. Technical Note TN 6/98. BSRIA, February 1998.

Perera M.D.A.E.S., Henderson J. and Webb B.C. (1997) Simple air leakage predictor for office buildings – assessing envelope airtightness during design or before refurbishment. Proceedings, CIBSE National Conference, London, October 1997, vol. 2, pp. 21-26.

Perera M.D.A.E.S., Marshall S.G. and Solomon E.W. (1993) Controlled background ventilation for large commercial premises. Building Services Engineering Research and Technology. 1993, vol. 14, no. 3, pp 81-86.

Perera M.D.A.E.S., Stephen R.K. and Tull R.G. (1989) “Use of BREFAN to measure the airtightness of non-domestic buildings”. BRE, April 1989.

Perera M.D.A.E.S. and Webb B. (1997) Minimising air leakage in commercial premises. Building Services Journal, CIBSE. February 1997, vol. 19, no. 2, pp 45-46.

Persily A.K. (1998) Airtightness of Commercial and Institutional Buildings: Blowing Holes in the Myth of Tight Buildings. Thermal performance of the exterior envelopes of buildings VII. Conference proceedings, Clearwater Beach, Florida, 6-10 December 1998, pp 829-837.

Persily A.K. (1999) Myths about building envelopes. ASHRAE Journal., March 1999, vol. 41, no.3, pp. 39-47.

Potter I.N. (1997) A Specification Document for Neutralisation of Tesco Stores. Report 13230 Revision 2.1. BSRIA, July 1997.

Potter I.N. (1999) Envelope Integrity Demonstration Study. Technical Note TN 19/99.

BSRIA, July 1999.

Potter I.N. (2002) Envelope Integrity Testing of a Tesco Superstore at Doncaster.

Proposal 17113A No.1. BSRIA, March 2002.

Pout C.H., Moss S.A. and Davidson P.J. (1998) Non-domestic Building Energy Fact

File. Building Research Establishment for Global Atmosphere Division of the

Department of the Environment, Transport and the Regions, January 1998.

Prior J.J. (1993) BREEAM/New Offices 1/93 An environmental assessment for new

office designs. BRE, 1993.

Prior J.J. and Bartlett P.B. (1995) Homes for a greener world. BRE, 1995.

Proskiw G. (1995) The performance of energy-efficient residential building envelope

systems. (Thermal performance of the exterior envelopes of buildings VI. Conference

proceedings). Florida, ASHRAE, December 1995.

Race G.L. (2002) Design Checks for HVAC – A quality control framework for

building services engineers. Application Guide AG 1/2002. BSRIA, April 2002.

Rawlings R.H.D. (1999) Ground Source Heat Pumps – A Technology Review.

Technical Note TN 18/99. BSRIA, July 1999.

Rose P. (2003) Modelling Leakage in Buildings. Flovent News. Issue 4, February 2003.

Rousseau J. (1992). (Thermal Performance of the Exterior Envelopes of Buildings V. Proceedings of ASHRAE/DOE/BTECC/CIBSE Conference) Clearwater Beach, Florida, 7-10 December 1992, pp. 646-651.

Saulles T. (1999) An Illustrated Guide to Building Services – Comfort Systems 27/99. BSRIA, March 2000.

Saulles T. (2001) The Illustrated Guide to Electrical Building Services. Application Guide AG 14/2001. BSRIA, October 2001.

Scrase J.I. (2000) White-collar CO₂ – Energy consumption in the service sector. The Association for the Conservation of Energy, August 2000.

Seaman A. (June 2001) Condition based maintenance – An evaluation guide for building services. Application Guide BSRIA, June 2001.

Shaw C.Y., Reurdon J.T. and Cheung M.S. (1993) Changes in air leakage levels of six Canadian office buildings. ASHRAE Journal, February 1993, vol. 35, no.2, pp. 34-36.

Shaw C.Y., Magee R.J. and Rousseau J. (1991) Overall and component airtightness values of a five storey apartment building. ASHRAE, vol. 97, part 2, paper number 3528, pp. 347-353.

Simons M.W., Brouns C.E. and Waters J.R. Flovent C.F.D. as an aid to the measurement of air movement characteristics within buildings. FLOVENT library; 2001

Ward T. (1998) Metal cladding: assessing thermal performance. BRE IP 5/98.

Ward T. (2001) Assessing the affects of thermal bridging at junctions and around openings. BRE, August 2001.

Waters J.R. and Simons M.W. (2002) "Modelling ventilation by means of combined mixing and displacement flow". *Building Services Engineering Research and Technology*, **22** (2) pp. 19-29.

Webb B.C. and Barton R. (2002) Airtightness in commercial and public buildings. Building Research Establishment..

Yau R.H. and Whittle G.E. (1991) "Air flow analysis for large spaces in an airport terminal building: computational fluid dynamics and reduced-scale physical model tests". (*Seminar, Computational fluid dynamics – tool or toy?*) London, 26 November 1991, pp. 47-55.

Yoshino H. (1986) Airtightness and ventilation strategy in Japanese residences. *Energy in Buildings*. December 1986, vol. 9, no. 4, pp. 321-331.

Yuill G.K. (1991) The development of a method of determining air change rates in detached dwellings for assessing indoor air quality. ASHRAE, vol. 97, part 2, paper no. IN-91-12-2, pp. 896-903.

Appendix A.1 Formulae used in this study

A.1 *Altas main equations*

Calculation of Air Density

$$\text{GasConst} = 287$$

$$\text{DensityTemp} = 0.5 * (\text{TempStart} + \text{TempEnd})$$

$$\text{MeanBaromPress} = 0.5 * (\text{BaromStart} + \text{BaromEnd})$$

$$\text{Density} = ((\text{MeanBaromPress}) * 0.4 * 249.174) / (\text{GasConst} * (\text{DensityTemp} + 273))$$

Correction for air density

Pressurisation:

$$Q_c = Q_t * (0.5 (\text{InternalTempStart} + \text{InternalTempEnd}) + 273) / (0.5 (\text{ExternalTempStart} + \text{ExternalTempEnd}) + 273)$$

Depressurisation:

$$Q_c = Q_t * (0.5 (\text{ExternalTempStart} + \text{ExternalTempEnd}) + 273) / (0.5 (\text{InternalTempStart} + \text{InternalTempEnd}) + 273)$$

Calculation of factors m and b

$$d\text{SumXY} = \sum(\text{In } \Delta P_{\text{env}} * \text{In } Q_c)$$

$$d\text{SumXX} = \sum(\text{In } \Delta P_{\text{env}} * \text{In } \Delta P_{\text{env}})$$

$$d\text{SumYY} = \sum(\text{In } Q_c * \text{In } Q_c)$$

$$d\text{SumX} = \sum(\text{In } \Delta P_{\text{env}})$$

$$d\text{SumY} = \sum(\text{In } Q_c)$$

$$m = (d\text{SumX} * d\text{SumY} - \text{Numpnts} * d\text{SumXY}) / (d\text{SumX} * d\text{SumX} - d\text{SumXX} * \text{Numpnts})$$

$$b = (d\text{SumX} * d\text{SumXY} - d\text{SumXX} * d\text{SumY}) / (d\text{SumX} * d\text{SumX} - d\text{SumXX} * \text{Numpnts})$$

Calculation of Correlation Coefficient

$$\sigma^2 = (\text{Numpnts} * \text{dSumXX} - \text{dSumX} * \text{dSumX}) * (\text{Numpnts} * \text{dSumYY} - \text{dSumY} * \text{dSumY})$$

$$S_{xy} = \text{Numpnts} * \text{dSumXY} - \text{dSumX} * \text{dSumY}$$

$$\text{Correlation Coefficient} = S_{xy} / \sqrt{(\sigma^2)}$$

Correction to Standard Temperature and Barometric Pressure

This is achieved by correcting the factor "C" for density, where $C = \exp^b$.

$$C = C * (\text{Density} / 1.2)^{(1 - m)}$$

Calculation of Air Leakage Index

$$Q_{ALI} = C * (\Delta P_{ALI})^m$$

$$\text{AirLeakageIndex} = 3600 * Q_{ALI} / (ALI)_{\text{EnvArea}}$$

Calculation of Air Leakage Permeability Index

$$Q_{API} = C * (\Delta P_{API})^m$$

$$\text{AirPermIndex} = 3600 * Q_{API} / (API)_{\text{EnvArea}}$$

Calculation of Indicative Infiltration Rate

$$Q_{IIR} = C * (\Delta P)^m$$

$$\text{IndicInfilRate} = 3600 * (1/60) * Q_{IIR} / (IIR)_{\text{surfaceArea}}$$

Key:

Q: measured airflow rate of fan

Qt: total measured airflow rate of fans

Qc: corrected total measured airflow rate

ΔP_{env} : measured envelope pressure difference

In: natural logarithm

Numpnts: number of pairs (Q_t , ΔP_{env})

ALI: air leakage index

API: air permeability index

IRR: indicative infiltration rate

ELA: effective leakage area

Appendix A.2

A.2 Pressure testing a very large building: theory and practice

Paper published in the *Proceedings of the 24th AIVC international conference 'Ventilation, Humidity Control and Energy'*, 271 – 276, Washington DC, 12 – 14 October 2003.

PRESSURE TESTING A VERY LARGE BUILDING: THEORY AND PRACTICE

S. Closs¹, N. Chilengwe² and S. Sharples²

¹ HRS Services Ltd, The Maltings, 81 Burton Road, Sheffield, S3 8BX, UK

² Sheffield Hallam University, Sheffield, UK

ABSTRACT

The airtightness of a building envelope impacts upon the magnitude of uncontrolled air leakage and associated ventilation energy losses. A building's airtightness can be assessed using a steady state fan pressurisation technique. This paper describes a study on the largest building in the UK ever to have had its airtightness tested. Power law regression analysis revealed a good correlation between flow rate into the building and observed pressure differentials. Building internal - external pressure differentials were measured during the testing and compared with predicted values from a CFD model. The CFD analysis showed that using resistance areas derived from Effective Leakage Area calculations gave reasonable agreement between the predicted and measured differential pressures. However, further work on boundary conditions is required to improve the agreement.

KEYWORDS

airtightness, fans, loss coefficient, pressure distribution, CFD

INTRODUCTION

The gradual improvement in thermal insulation levels in buildings over the last thirty years has increased the relative proportion of energy losses associated with air infiltration. Consequently, it becomes more important to be able to design, test and seal buildings to have less leaky external envelopes. A recent study by Orme (2001) estimated, for 13 industrial countries, that unnecessary ventilation accounted for over 60% of the energy wastage, mainly through the loss of conditioned air. In cool climates exfiltrating air carries with it water vapour and lost energy. Water vapour condenses and causes wetting, bacterial growth and deterioration of the building envelope (Anis, 2001). Building envelopes with relatively airtight constructions help create more controllable internal environments, and the infiltration of pollutants and uncontrolled exfiltration of air can be minimised. Consequently, mechanical ventilation plant can be specified with confidence at a level that is both effective and efficient. However, despite these benefits, interest in air leakiness has, to date, been limited in the UK. The publication of the Approved Document L2 in the new UK Building Regulations (2002) introduced the requirement for building envelopes to attain a reasonable standard of airtightness for buildings with floor areas exceeding 1000 m². 'Reasonable' is defined as a leakage of no more than 10 m³/hr/ per m² of building envelope surface at a pressure differential of 50 Pascal. It is estimated that approximately 3000 new, large buildings per year in the UK would need testing. Very large buildings (floor areas exceeding 5000 m² floor area) have represented a particular problem for pressure testing using conventional steady state (DC) techniques. Unsteady techniques (AC and pulse techniques) have been suggested by Carey and Etheridge (2001) as alternatives to the conventional steady state technique. However, uncertainties introduced by the inertia of the flow through imperfections in the building envelope add increased complexity and uncertainty to the calculations and results. Therefore, the DC technique is preferable *if* an acceptable steady state differential pressure can be achieved across the building envelope. The main focus of this paper is to report on a pressurisation test carried out on a very large building (floor area of 57,440 m²). CFD simulations were carried out to model the pressure differentials obtained within the building. Measured data and CFD predictions are compared in this paper.

METHODOLOGY

The study of building envelope airtightness performance involves establishing a pressure difference Δp across the envelope. Measurements taken of the airflow rate Q in to a building produced by fans and the pressure difference Δp created across the envelope allow a relationship to be established between the two. In accordance with the current UK building regulations, adhering to CIBSE Technical Memorandum TM23 (2000), this Q - Δp relationship is defined in terms of the power law equation of the form:

$$Q = C (\Delta p)^n \quad (1)$$

where C and n are constants that are assumed to relate to the geometry of a single opening in the building envelope. During testing the building envelope is typically subjected to differential pressures ranging from 20 to 70 Pascal. The actual testing work was carried out on a very large retail distribution warehouse (359 x 160 x 15.5m high). This is the largest building ever pressure tested in the UK, and possible Europe. Three variable speed fans were used to generate the pressure differential Δp across the building envelope; one large fan, 2000 mm in diameter and two medium sized fans, 1250 mm in diameter. The 2000mm fan was mounted on the back of a 7.5 tonne truck and the 90kW power required by the fan was provided by a diesel engine. The 1250mm fans were driven using the power take off from other trucks with a similar design to the 2000 mm fan rig. The largest fan was connected with a flexible duct to a wooden screen situated within one of the loading bay openings. Figure 1 shows the large fan and part of the building being tested. The two medium sized fans were positioned within other loading bay entrances and sealed in with temporary wooden frames. All three fans had previously been calibrated to give actual volumetric flow rates within $\pm 2\%$ accuracy. Temperature measurements were made before, during and after the test using digital thermometers. These were calibrated to an accuracy of $\pm 0.5^\circ\text{C}$. The three fans were positioned at intervals along one long side of the building envelope. For the purpose of the tests all external doors and windows were closed, with internal doors to the offices left open. Mechanical ventilation openings on the building roof were sealed with impermeable sheet and adhesive tape. Large openings containing open louvers, which were going to be sealed, constituting an area of around 40m^2 , had been noted on previous site visits and these were also sealed during testing. Three 1m^2 openings in the building envelope remained unsealed to fulfil the requirement of ventilation to gas boilers. Three groups of two personnel were required to operate the fans and record the observed pressure differentials. Other observers were positioned around the building and on the roof to ensure that vents remained sealed and doors remained closed. Communication was maintained by two-way radio contact. The pressure differential across the building envelope was measured using a 60m length of 5mm internal diameter plastic tube that was connected to a differential digital manometer located inside the building at a 45° angle to the fan at ground level. A 20m length of tube was connected to the same manometer and placed outside the building at a 45° angle to the fan at ground level.



Figure 1: 2000mm diameter fan positioned in the loading bay door

The pressure differential across the building envelope was raised to 81 Pascal and then lowered in ten stages to 23 Pascal. Measurements were also made of the internal pressure distributions at a regular 7 x 7 grid of points inside the building when the differential pressure across the envelope was set at 50 Pascal. The first grid point was 20 m from the fan wall and 45 m from the side wall. These measurements were taken using 5mm internal diameter plastic tube, up to 140m in length. The tubing was arranged in straight lengths and did not come into contact with sources of heat. Using tubes of this length resulted in a damping of the fluctuations in pressure. These values were used as the basis of a comparison with pressure differentials predicted from the CFD software FLOVENT. This is an established commercial package that is typically used for building services application on a much smaller scale.

RESULTS AND DISCUSSION

The initial measurements established the relationship between the airflow through the fans, Q, and the differential pressure, Δp, observed across the building envelope. Figure 2 shows a log-log analysis of the Q-Δp data points for the retail distribution warehouse. Fitting a power law curve to these results gave a correlation coefficient of 1.00. The effect of pressure distributions within the building was investigated and Table 1 illustrates the pressure differentials observed at 20m intervals, with the building envelope Δp set at 50 Pascal. One of the objectives of this study was to test if CFD could be used to predict pressure distributions in very large spaces. Simplified methods have been suggested as a means of modelling mixing and displacement flows to give an indication of air distribution (Waters and Simons,2002). However, prediction of localised pressure distributions on such a large scale would require an established CFD package, coupled with currently available desktop computing power and considerable solving times. Investigations have been carried out into the airflow patterns in large buildings using CFD (for example, Simons et al, 2001; Yau and Whittle, 1991 and Kato et al, 1995). However, air leakage through building fabric was not incorporated into these studies.

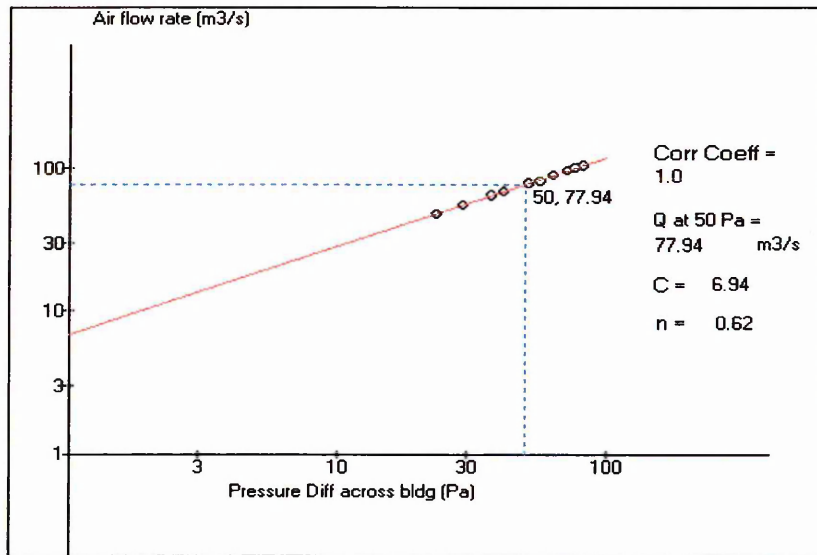


Figure 2: Q(m³/s) v. Δp(Pa) data points for the building pressurisation test with a power law regression fit

Table 1 Pressure differentials observed at monitor points within the building

Column	Distance from wall with mounted fans						
	20m	40m	60m	80m	100m	120m	140m
1	49 Pa	49 Pa	51 Pa	51 Pa	51 Pa	51 Pa	51 Pa
2	50 Pa	51 Pa	51 Pa	51 Pa	52 Pa	53 Pa	53 Pa
3	49 Pa	49 Pa	49 Pa	51 Pa	50 Pa	51 Pa	51 Pa
4	50 Pa	51 Pa	52 Pa	56 Pa	58 Pa	59 Pa	56 Pa
5	51 Pa	51 Pa	52 Pa	52 Pa	51 Pa	51 Pa	49 Pa
6	49 Pa	51 Pa	51 Pa	52 Pa	53 Pa	55 Pa	55 Pa
7	54 Pa	55 Pa	52 Pa	52 Pa	52 Pa	52 Pa	52 Pa

The simulation model was created in FLOVENT version 3.2 and comprised of a room measuring 359 x 160 x 15.5 m high. The three fans used in the test were represented as fixed flow fans and located to reflect the actual set up. Current limitations in FLOVENT meant that expected fabric leakage rates could not be applied to whole surfaces of the building. Instead, resistances to flow were applied to sections of the building fabric. Leakage paths in the building fabric initially had to be estimated in terms of size and location. A uniform width was assigned to the leakage paths represented as resistances, which were positioned along the perimeters of the building. An approximate size of the total leakage path was obtained from the effective leakage area, ELA, calculated from Eqn. 2 below.

$$(2) \quad ELA = Q(\rho/2\Delta p)^{0.5}$$

where ρ is the density of air. ELA was calculated to be 8.19m². A resistance width of 0.1m was applied evenly over the length of the building, resulting in a total leakage path area of 213.72m². To adjust this to the required effective leakage area a free area ratio of approximately 0.038 was applied to the resistances. The ELA was then used to estimate the loss coefficient k , given in Eqn. 3 below, representing the resistance (leakage path).

$$(3) \quad \Delta p = 0.5(k\rho v^2)$$

Uniform lighting of 15W/m² was also included at a high level in the warehouse. Following the actual test, known values for internal and external temperature were added to the model. A uniform grid totalling 230,000 cells was used. Convergence was achieved within 3000 iterations and changes to the false time step were not required. Once the model parameters were assigned as above and the simulation solved, a first approximation to the solution was obtained. Initial results showed lower pressure differentials than experienced for the actual test. Altering the free area ratio to the resistances representing the leakage paths then refined these. Further adjustment of the free area ratio eventually resulted in a figure that lead to a pressure distribution similar to that obtained from the actual test. A free area ratio of 0.0561 was the final figure applied to the resistances, giving an actual total leakage area of 11.2 m² (similar to the calculated value ELA of 8.19m², taking into account assumptions made and time limitations. The pressure difference distribution within the building at a height of 1.0 m above floor level obtained from CFD is shown in Figure 3. Table 2 shows a comparison of the measured pressure differentials at a height of 1 metre and those values predicted from the CFD analysis. Differences are generally less than $\pm 10\%$, which is encouraging given the size of the building and the complexity of the modelling. However, differential pressures observed near the wall adjacent to the fans were generally higher than predicted from the CFD model, particularly with readings taken in line with the 2000mm fan. This may possibly be due to discrepancies between the positioning of the resistances in the model and the actual leakage paths present within the building.

Table 2 Comparison of measured and predicted pressure differentials

Distance from wall with mounted fans		Pressure differential (Pa) at Column number						
		1	2	3	4	5	6	7
20m	Measured	49	50	49	50	51	49	54
	Predicted	51.6	52.1	51.6	51.7	51.7	51.9	51.6
	% difference	-5.3%	-4.2%	-5.3%	-3.4%	-1.4%	-5.9%	4.4%
40m	Measured	49	51	49	51	51	51	55
	Predicted	51.6	51.8	51.6	51.6	51.7	51.9	51.7
	% difference	-5.3%	-1.6%	-5.3%	-1.2%	-1.4%	-1.8%	6.0%
60m	Measured	51	51	49	52	52	51	52
	Predicted	51.6	51.8	51.7	51.7	51.8	51.9	51.7
	% difference	-1.2%	-1.6%	-5.5%	0.6%	0.4%	-1.8%	0.6%
80m	Measured	51	51	51	56	52	52	52
	Predicted	51.7	51.8	51.7	51.8	51.8	51.8	51.7
	% difference	-1.4%	-1.6%	-1.4%	7.5%	0.4%	0.4%	0.6%
100m	Measured	51	52	50	58	51	53	52
	Predicted	51.7	51.9	51.8	51.8	51.8	51.8	51.7
	% difference	-1.4%	0.2%	-3.6%	10.7%	-1.6%	2.3%	0.6%
120m	Measured	51	53	51	59	51	55	52
	Predicted	51.8	51.9	51.8	51.9	51.8	51.8	51.7
	% difference	-1.6%	2.1%	-1.6%	12.0%	-1.6%	5.8%	0.6%
140m	Measured	51	53	51	56	49	55	52
	Predicted	51.8	51.9	51.9	51.9	51.8	51.8	51.7
	% difference	-1.6%	2.1%	-1.8%	7.3%	-5.7%	5.8%	0.6%

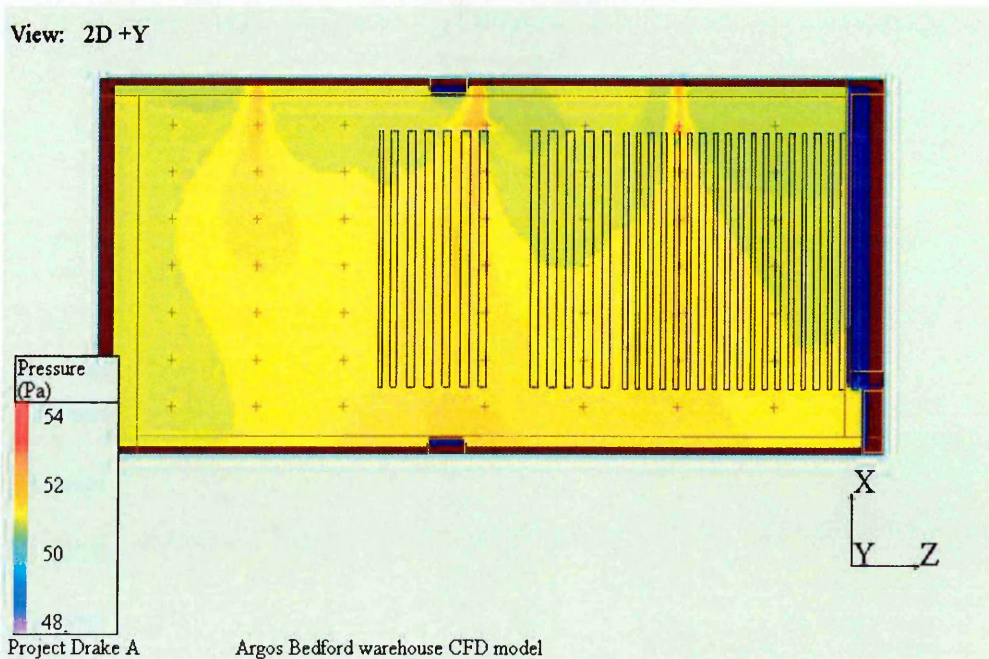


Figure 3: Predicted differential pressure distribution within the building at 1.0 m above ground level

CONCLUSION

This study has investigated some practical aspects of pressure testing a very large building and the possibility of using CFD modelling as a tool to predict the pressure distribution within the building. A relatively simple method was used to incorporate the impact of leakage paths into the CFD model, and this was quite successful in predicting pressure differentials. However, more work is needed to refine the application of CFD to building pressurisation testing. Software developers will need to produce better methods of representing the leakage of building fabric, and such developments are being made in the industry (Rose, 2003). Findings from this study will hopefully lead to more accurate methods of applying fabric leakage to models and so provide more precise ways of determining pressure distributions within buildings.

The authors would like to thank the UK Government's Teaching Company Scheme (Programme No. 3790) for their financial support of this work and Gazeley Properties for allowing access to the retail distribution warehouse.

REFERENCES

- Anis W A Y. (2001) The impact of airtightness on system design. *ASHRAE Journal*, **43**, 31–35.
- Building Regulations, *Approved Document Part L2* (2002).
- Carey P S and Etheridge D W. (2001) Leakage measurements using unsteady techniques with particular reference to large buildings. *Building Services Engineering Research & Technology*, **22**, 69-82.
- CIBSE Technical Memorandum TM23 (2000). *Testing buildings for air leakage*, CIBSE, London
- Kato S, Murakami S, Shoya S and Hanyu F. (1995) CFD analysis of flow and temperature fields in atrium with ceiling height of 130m. *ASHRAE Transactions*, **101**, Part 2: Paper number SD-95-14-5, 1144-1157.
- Orme M. (2001). Estimates of the energy impact of ventilation and associated financial expenditures. *Energy and Buildings*, **33**, 199-205.
- Rose P. (2003) *Modelling leakage in buildings*. FLOVENT News, Issue 4 February.
- Simons M W, Brouns C E and Waters J R. (2001) *Flovent C.F.D. as an aid to the measurement of air movement characteristics within buildings*. FLOVENT library.
- Waters J R and Simons M W. (2002) Modelling ventilation by means of combined mixing and displacement flow. *Building Services Engineering Research and Technology*, **23**, 19-29.
- Yau R H and Whittle G E. (1991) Airflow analysis for large spaces in an airport terminal building: computational fluid dynamics and reduced-scale physical model tests. Proceedings of the workshop *Computational fluid dynamics – tool or toy?*; Institution of Mechanical Engineers, London, 26 November 1991: 47-55.

Appendix A.3

A.3 *Sample of Building C Dynamic Thermal Modelling output data*

Project Drake - Infiltration = 0.25ac/hr - Peak Heating Loads

Hilson Moran Partnership Ltd
Hilson Moran Partnership Ltd
156 Tooley Street
London
County/State
SE1 2TZ
England
+44 (0) 20 7940 8888

Project Name: Project Drake
Engineer's Name: Keith Harding
Number of bsos: 1
Day Range: January 31 - January 31
Boiler Design Margin (%): 0

Natural Ventilation is not included.
Ventilation is not included.
Lighting Sensible gain is not included.
Occupancy Sensible gain is not included.
Occupancy Latent gain is not included.
Equipment Sensible gain not is included.
Equipment Latent gain is not included.
Outside Air Temperature is fixed at -4.00C.
Wind Speed is fixed at 3.00m/s.
Solar Radiation is not included.
NB: The Heating Calculation does not allow for fresh air

Peak Total Sensible Load (kW)	Total Infiltration Loss (kW)	Total Fabric Loss (kW)	Peak Sensible Load (W) per Square Metre	Day of Peak Load	Hour of Peak Load
2425.838	1443.708	982.131	10	31	1

Project Name: Project Drake
 BSO Name: Drake025.bso
 BDF Name: Drake025.bdf.03
 WFL Name: HMP_CLGHTG_28.wfl
 Zone Range: 1 to 60

Zone Number	Zone Name	Peak Sensible Load (kW)	Infil. Loss (kW)	Fabric Loss (kW)	Sensible Load (W) per square metre	Day of Peak Load	Hour of Peak Load	Air temperature (c)	Resultant Temperature (c)
1	WHouse East Perim	36.741	25.153	11.589	12	31	1	16.0	15.5
2	WHouse South Perim	18.310	12.310	6.000	12	31	1	16.0	15.4
3	WHouse West Perim	38.815	26.581	12.234	12	31	1	16.0	15.4
4	WHouse Interior	450.308	381.184	69.124	10	31	1	16.0	15.6
5	Battery North P	14.701	9.298	5.403	14	31	1	18.0	17.2
6	Battery East P	2.924	1.725	1.199	15	31	1	18.0	17.2
7	Battery I.	0.725	0.005	0.720	6	31	1	18.0	17.3
8	1st North Perim	6.661	4.561	2.100	12	31	1	16.0	15.5
9	1st East Perim	40.639	27.571	13.068	12	31	1	16.0	15.5
10	1st South Perim	18.442	12.310	6.133	12	31	1	16.0	15.4
11	1st West Perim	39.234	26.581	12.653	12	31	1	16.0	15.4
12	1st Interior	474.913	385.255	89.659	10	31	1	16.0	15.5
13	Hi Lvl North Perim	32.889	10.912	21.976	22	31	2	16.0	15.4
14	Hi Lvl East Perim	75.038	25.305	49.733	21	31	3	16.0	15.4
15	Hi Lvl South Perim	32.694	10.912	21.782	22	31	7	16.0	15.3

Project Name: Project Drake
 BSO Name: Drake025.bso
 BDF Name: Drake025.bdf.03
 WFL Name: HMP_CLGHTG_28.wfl
 Zone Range: 1 to 60

Zone Number	Zone Name	Peak Sensible Load (kW)	Infil. Loss (kW)	Fabric Loss (kW)	Sensible Load (W) per square metre	Day of Peak Load	Hour of Peak Load	Air temperature (c)	Resultant Temperature (c)
16	Hi Lvl West Perim	75.085	25.305	49.779	21	31	6	16.0	15.4
17	Hi Lvl Interior	974.220	346.074	628.146	20	31	5	16.0	15.3
18	Roof Level	0.000	87.044	-87.044	0	31	1	15.7	14.7
19	Office Stairs Perim	0.584	0.349	0.235	8	31	1	18.0	17.6
20	Office Perim West	0.947	0.242	0.705	22	31	1	21.0	19.9
21	Office Perim N	10.453	2.097	8.356	29	31	1	21.0	19.5
22	Office Stairs P	0.662	0.193	0.469	17	31	1	18.0	17.2
23	Office Internal	2.991	0.019	2.962	4	31	1	21.0	20.4
24	Office WC	0.624	0.524	0.100	6	31	1	18.0	17.8
25	Energy Centre P	2.391	1.389	1.002	10	31	1	21.0	20.4
26	Office Stairs P	1.282	0.621	0.661	19	31	1	18.0	17.3
27	Office West P	2.115	0.430	1.685	50	31	1	21.0	19.4
28	Office North P	14.753	3.728	11.025	40	31	1	21.0	19.4
29	Office Stairs P	0.853	0.344	0.509	22	31	1	18.0	17.3
30	Office WC	1.040	0.931	0.109	10	31	1	18.0	17.8

Project Name: Project Drake
 BSO Name: Drake025.bso
 BDF Name: Drake025.bdf.03
 WFL Name: HMP_CLIGHTG_28.wfl
 Zone Range: 1 to 60

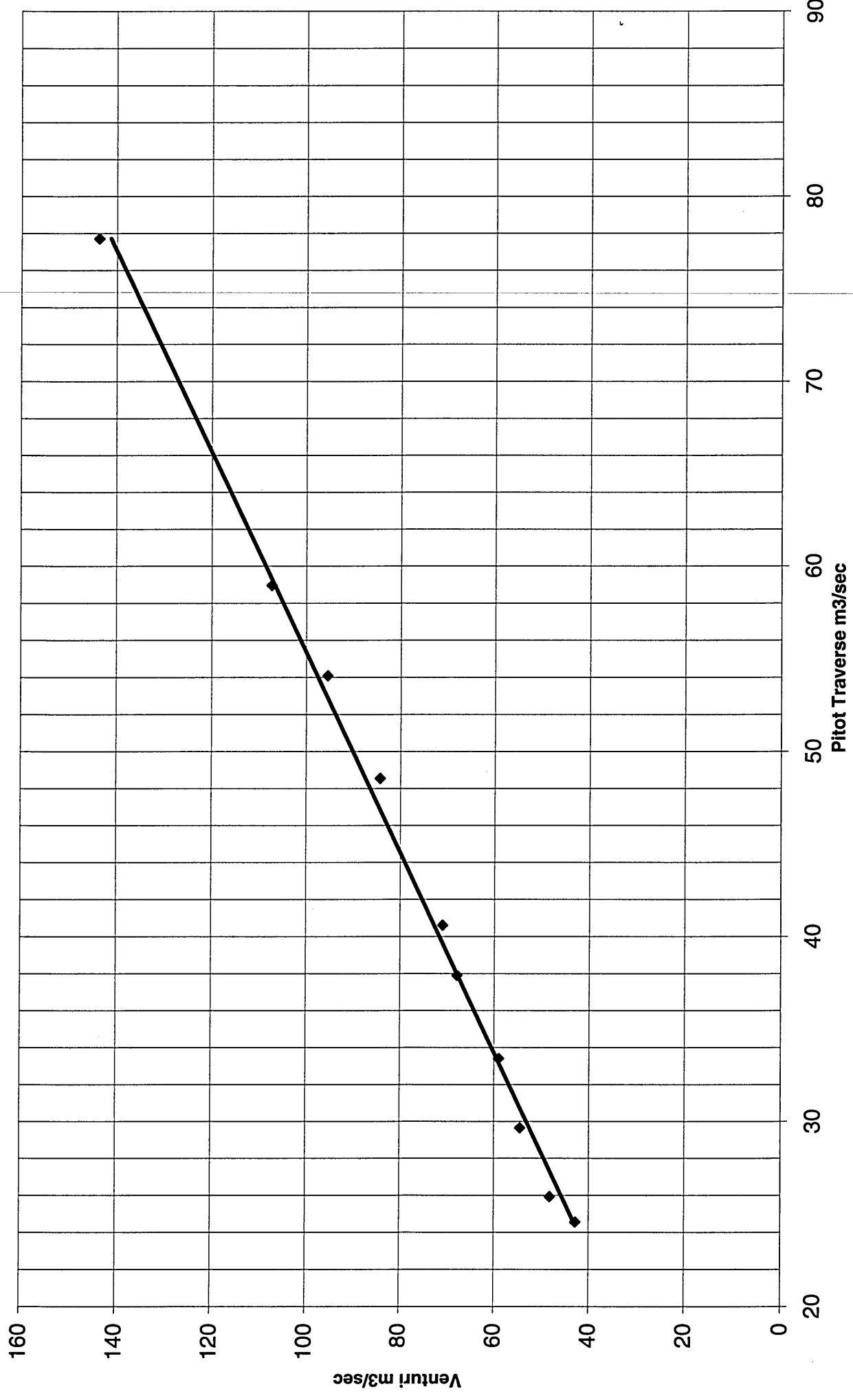
Zone Number	Zone Name	Peak Sensible Load (kW)	Infil. Loss (kW)	Fabric Loss (kW)	Sensible Load (W) per square metre	Day of Peak Load	Hour of Peak Load	Air temperature (c)	Resultant Temperature (c)
31	Office Interior	4.473	0.034	4.439	5	31	1	21.0	20.3
32	Energy Centre P	3.782	2.470	1.312	16	31	1	21.0	20.3
33	Despatch Office P SW	1.003	0.081	0.922	71	31	1	21.0	18.6
34	Despatch Office P SW	2.728	0.638	2.090	25	31	1	21.0	19.5
35	Despatch Rest P NW	2.822	0.452	2.370	36	31	1	21.0	19.0
36	Despatch WC CDoor P	0.517	0.304	0.213	9	31	1	18.0	17.7
37	Despatch Stair I	0.096	0.001	0.095	2	31	1	18.0	17.8
38	Despatch FAID I	0.211	0.001	0.210	4	31	1	21.0	20.5
39	Despatch Training P	3.771	0.879	2.893	44	31	1	21.0	19.4
40	Despatch Office P	3.025	0.987	2.038	31	31	1	21.0	19.7
41	Despatch Manager P	1.596	0.217	1.379	75	31	2	21.0	18.9
42	Despatch WC CDoor P	0.797	0.541	0.257	13	31	1	18.0	17.7
43	Despatch Stairs I	0.109	0.002	0.107	2	31	1	18.0	17.8
44	Despatch Rest Room I	0.296	0.002	0.294	5	31	1	21.0	20.5
45	GoodsIn Stairs I	0.095	0.001	0.094	2	31	1	18.0	17.8

Project Name: Project Drake
 BSO Name: Drake025.bso
 BDF Name: Drake025.bdf.03
 WFL Name: HMP_CLIGHTG_28.wfl
 Zone Range: 1 to 60

Zone Number	Zone Name	Peak Sensible Load (kW)	Infil. Loss (kW)	Fabric Loss (kW)	Sensible Load (W) per square metre	Day of Peak Load	Hour of Peak Load	Air temperature (c)	Resultant Temperature (c)
46	GoodsIn Insp I	0.119	0.001	0.118	4	31	1	21.0	20.5
47	GoodsIn WC CDoor	0.381	0.374	0.007	10	31	1	18.0	18.0
48	GoodsIn CDoor P	0.303	0.201	0.102	8	31	1	18.0	17.8
49	Goods In Office P S	2.806	0.466	2.339	35	31	1	21.0	19.3
50	GoodsIn Office P E	2.894	0.450	2.444	37	31	1	21.0	19.1
51	GoodsIn Rest P N	1.184	0.185	0.999	37	31	1	21.0	19.3
52	Goods In WC I	0.030	0.000	0.030	1	31	1	18.0	17.8
53	Goods In WC P	0.118	0.053	0.066	11	31	1	18.0	17.6
54	GoodsIn Stairs I	0.096	0.002	0.094	2	31	3	18.0	17.8
55	GoodsIn Restroom I	0.358	0.003	0.356	5	31	3	21.0	20.5
56	GoodsIn CDoor P	0.400	0.295	0.105	12	31	1	18.0	17.8
57	GoodsIn Manager P	1.573	0.376	1.197	43	31	1	21.0	19.5
58	GoodsIn Office P	7.402	1.991	5.411	38	31	1	21.0	19.1
59	Hi Lvl over Despatch	5.996	1.870	4.126	23	31	12	16.0	15.2
60	Hi Lvl over G.In	6.052	1.879	4.173	23	31	3	16.0	15.2

$y = 1.847x - 2.2542$
 $R^2 = 0.996$

Graph of Mega Fan 2000mm Venturi against Actual Measured flow



High Rise Spreadsheet

Reading No.	Vertical Traverse	Sq root	Reading No.	Horizontal Traverse	Sq root	Reading No.	Horizontal Traverse (Pa)	Sq root	
1		57 7.549834	1		41 6.403124	1		56 7.483315	
2		31 5.567764	2		54 7.348469	2		43 6.557439	
3		27 5.196152	3		37 6.082763	3		30 5.477226	
4		19 4.358899	4		22 4.690416	4		21 4.582576	
5		24 4.898979	5		26 5.09902	5		39 6.244998	
6		32 5.656854	6		34 5.830952	6		40 6.324555	
7		46 6.78233	7		46 6.78233	7		51 7.141428	
8		52 7.211103	8		30 5.477226	8		52 7.211103	
Average of square roots		5.715831	Average of square roots		6.033868	Average of square roots			6.37783

Average Reading (Pa) 36.51192
Venturi Reading (Pa) 110

Atmospheric Pressure (Pa) 100300
 Average Air Temp (Deg C) 21.4
 Density of air (kg/m³) 1.19

Open Area of Venturi (m²) 3.142
 Area of Discharge Duct (m²) 3.142

Pitot Volume
 Alpha = 0.997
 Mass Flow = Alpha x Area x (2 density x Pa)^{0.5} 29.16583 kg/sec
 Volume = Mass Flow/Density = 24.56932 m³/sec

Venturi Velocity = (2 x Pa/density)^{0.5} = 13.61353 m/sec
 Venturi Volume = Velocity x Area = 42.77371 m³/sec

High Rise Spreadsheet

Reading No.	Vertical Traverse (Pa)	Sq root	Reading No.	Horizontal Traverse Sq root	Reading No.	Horizontal Traverse (Pa)	Sq root		
1		47	6.855655	1	45	6.708204	65	8.062258	
2		52	7.211103	2	67	8.185353	60	7.745967	
3		25	5	3	47	6.855655	35	5.91608	
4		18	4.242641	4	27	5.196152	21	4.582576	
5		22	4.690416	5	20	4.472136	44	6.63325	
6		37	6.082763	6	35	5.91608	46	6.78233	
7		60	7.745967	7	44	6.63325	62	7.874008	
8		49	7	8	40	6.324555	60	7.745967	
Average of square roots		5.975506		Average of square roots		6.280976		Average of square roots	

Average Reading (Pa)
Venturi Reading (Pa)

Atmospheric Pressure (Pa)
 Average Air Temp (Deg C)
 Density of air (kg/m³)

Open Area of Venturi (m²)
 Area of Discharge Duct (m²)

Pitot Volume
 Alpha =
 Mass Flow = Alpha x Area x (2 density x Pa)^{0.5}
 Volume = Mass Flow/Density =

Venturi Velocity = (2 x Pa/density)^{0.5} =
 Venturi Volume = Velocity x Area =

High Rise Spreadsheet

Reading No.	Vertical Traverse (Pa)	Sq root	Reading No.	Horizontal Traverse Sq root	Reading No.	Horizontal Traverse (Pa)	Sq root	
1	74	8.602325	1	48	1	100	10	
2	71	8.42615	2	44	2	66	8.124038	
3	39	6.244998	3	46	3	51	7.141428	
4	28	5.291503	4	20	4	61	7.81025	
5	34	5.830952	5	29	5	51	7.141428	
6	57	7.549834	6	54	6	57	7.549834	
7	83	9.110434	7	55	7	82	9.055385	
8	70	8.3666	8	35	8	77	8.774964	
Average of square roots		7.293742	Average of square roots		Average of square roots			8.199666

Average Reading (Pa)
Venturi Reading (Pa)

Atmospheric Pressure (Pa)
 Average Air Temp (Deg C)
 Density of air (kg/m3)

Open Area of Venturi (m2)
 Area of Discharge Duct (m2)

Pitot Volume
 Alpha =

Mass Flow = Alpha x Area x (2 density x Pa)^{0.5}
 Volume = Mass Flow/Density =

Venturi Velocity = (2 x Pa/density)^{0.5} =
 Venturi Volume = Velocity x Area =

High Rise Spreadsheet

Reading No.	Vertical Traverse (Pa)	Sq root	Reading No.	Horizontal Traverse Sq root	Reading No.	Horizontal Traverse (Pa)	Sq root
1	95	9.746794	1	83	1	110	10.48809
2	65	8.062258	2	98	2	88	9.380832
3	52	7.211103	3	78	3	55	7.416198
4	32	5.656854	4	51	4	41	6.403124
5	35	5.91608	5	41	5	69	8.306624
6	60	7.745967	6	54	6	67	8.185353
7	96	9.797959	7	89	7	80	8.944272
8	84	9.165151	8	56	8	100	10
Average of square roots		7.733859	Average of square roots		Average of square roots		8.640561

Average Reading (Pa)
Venturi Reading (Pa)

Atmospheric Pressure (Pa)
 Average Air Temp (Deg C)
 Density of air (kg/m3)

Open Area of Venturi (m2)
 Area of Discharge Duct (m2)

Pitot Volume
 Alpha =

Mass Flow = Alpha x Area x (2 density x Pa)^{0.5}
 Volume = Mass Flow/Density =

Venturi Velocity = (2 x Pa/density)^{0.5} =
 Venturi Volume = Velocity x Area =

High Rise Spreadsheet

Reading No.	Vertical Traverse (Pa)	Sq root	Reading No.	Horizontal Traverse	Sq root	Reading No.	Horizontal Traverse (Pa)	Sq root
1	108	10.3923	1	133	11.53256	1	143	11.95826
2	96	9.797959	2	135	11.61895	2	95	9.746794
3	53	7.28011	3	108	10.3923	3	90	9.486833
4	32	5.656854	4	70	8.3666	4	59	7.681146
5	46	6.78233	5	40	6.324555	5	82	9.055385
6	70	8.3666	6	76	8.717798	6	90	9.486833
7	107	10.34408	7	92	9.591663	7	127	11.26943
8	102	10.0995	8	69	8.306624	8	138	11.74734
Average of square roots		8.589968	Average of square roots		9.356382	Average of square roots		10.054

Average Reading (Pa) 87.11331
Venturi Reading (Pa) 278

Atmospheric Pressure (Pa) 100400
 Average Air Temp (Deg C) 20.7
 Density of air (kg/m3) 1.19

Open Area of Venturi (m2) 3.142
 Area of Discharge Duct (m2) 3.142

Pitot Volume
 Alpha = 0.997

Mass Flow = $\text{Alpha} \times \text{Area} \times (2 \text{ density} \times \text{Pa})^{0.5}$ 45.12659 kg/sec
 Volume = Mass Flow/Density = 37.88651 m3/sec

Venturi Velocity = $(2 \times \text{Pa}/\text{density})^{0.5}$ = 21.60546 m/sec
 Venturi Volume = Velocity x Area = 67.88435 m3/sec

High Rise Spreadsheet

Reading No.	Vertical Traverse (Pa)	Sq root	Reading No.	Horizontal Traverse (Pa)	Sq root
1	113	10.63015	1	125	11.18034
2	112	10.58301	2	148	12.16553
3	61	7.81025	3	121	11
4	39	6.244998	4	65	8.062258
5	55	7.416198	5	70	8.3666
6	92	9.591663	6	83	9.110434
7	145	12.04159	7	115	10.72381
8	118	10.86278	8	74	8.602325
Average of square roots		9.397579	Average of square roots		9.901411

Average Reading (Pa) **99.951**
Venturi Reading (Pa) **303.5**

Atmospheric Pressure (Pa) **100400**
 Average Air Temp (Deg C) **21**
 Density of air (kg/m3) **1.19**

Open Area of Venturi (m2) **3.142**
 Area of Discharge Duct (m2) **3.142**

Pitot Volume
 Alpha = **0.997**
 Mass Flow = Alpha x Area x (2 density x Pa)^{0.5} **48.31279 kg/sec**
 Volume = Mass Flow/Density = **40.60296 m3/sec**

Venturi Velocity = (2 x Pa/density)^{0.5} = **22.58614 m/sec**
 Venturi Volume = Velocity x Area = **70.96567 m3/sec**

Average of square roots **9.397579**
 Average of square roots **9.901411**
 Average of square roots **10.69366**

High Rise Spreadsheet

Reading No.	Vertical Traverse (Pa)	Sq root	Reading No.	Horizontal Traverse (Pa)	Sq root	Reading No.	Horizontal Traverse (Pa)	Sq root
1	190	13.78405	1	157	12.52996	1	176	13.2665
2	149	12.20656	2	224	14.96663	2	169	13
3	92	9.591663	3	152	12.32883	3	99	9.949874
4	59	7.681146	4	126	11.22497	4	77	8.774964
5	73	8.544004	5	111	10.53565	5	152	12.32883
6	134	11.57584	6	129	11.35782	6	131	11.44552
7	206	14.3527	7	186	13.63818	7	211	14.52584
8	174	13.19091	8	121	11	8	222	14.89966
Average of square roots		11.36586	Average of square roots		12.19776	Average of square roots		12.2739

Average Reading (Pa) 142.703
Venturi Reading (Pa) 428

Atmospheric Pressure (Pa) 100400
 Average Air Temp (Deg C) 21.3
 Density of air (kg/m3) 1.19

Open Area of Venturi (m2) 3.142
 Area of Discharge Duct (m2) 3.142

Pitot Volume
 Alpha = 0.997

Mass Flow = Alpha x Area x (2 density x Pa)^{0.5} 57.69839 kg/sec
 Volume = Mass Flow/Density = 48.54027 m3/sec

Venturi Velocity = (2 x Pa/density)^{0.5} = 26.83528 m/sec
 Venturi Volume = Velocity x Area = 84.31644 m3/sec

High Rise Spreadsheet

Reading No.	Vertical Traverse (Pa)	Sq root	Reading No.	Horizontal Traverse Sq root	Reading No.	Horizontal Traverse (Pa)	Sq root
1	289	17	1	190	1	295	17.17556
2	177	13.30413	2	266	2	200	14.14214
3	121	11	3	142	3	160	12.64911
4	77	8.774964	4	102	4	107	10.34408
5	89	9.433981	5	121	5	193	13.89244
6	199	14.10674	6	163	6	182	13.49074
7	246	15.68439	7	202	7	237	15.3948
8	215	14.66288	8	160	8	259	16.09348
Average of square roots		12.99589	Average of square roots		Average of square roots		14.14779

Average Reading (Pa) 177.6531
Venturi Reading (Pa) 550

Atmospheric Pressure (Pa) 100500
Average Air Temp (Deg C) 20.8
Density of air (kg/m3) 1.19

Open Area of Venturi (m2) 3.142
Area of Discharge Duct (m2) 3.142

Pitot Volume
Alpha = 0.997
Mass Flow = Alpha x Area x (2 density x Pa)^{0.5} 64.46425 kg/sec
Volume = Mass Flow/Density = 54.08621 m3/sec

Venturi Velocity = (2 x Pa/density)^{0.5} = 30.37947 m/sec
Venturi Volume = Velocity x Area = 95.45229 m3/sec

High Rise Spreadsheet

Reading No.	Vertical Traverse (Pa)	Sq root	Reading No.	Horizontal Traverse (Pa)	Sq root	Reading No.	Horizontal Traverse (Pa)	Sq root	
1	275	16.58312	1	225	15	1	439	20.95233	
2	254	15.93738	2	229	15.13275	2	306	17.49286	
3	119	10.90871	3	158	12.56981	3	158	12.56981	
4	101	10.04988	4	114	10.67708	4	93	9.643651	
5	111	10.53565	5	141	11.87434	5	222	14.89966	
6	172	13.11488	6	197	14.03567	6	240	15.49193	
7	340	18.43909	7	278	16.67333	7	321	17.91647	
8	284	16.8523	8	196	14	8	310	17.60682	
Average of square roots		14.05263	Average of square roots		13.74537	Average of square roots			15.82169

Average Reading (Pa) 211.4086
Venturi Reading (Pa) 696

Atmospheric Pressure (Pa) 100500
 Average Air Temp (Deg C) 20.5
 Density of air (kg/m³) 1.19

Open Area of Venturi (m²) 3.142
 Area of Discharge Duct (m²) 3.142

Pitot Volume
 Alpha = 0.997
 Mass Flow = Alpha x Area x (2 density x Pa)^{0.5}

Volume = 70.35835 kg/sec
 Mass Flow/Density = 58.97115 m³/sec

Venturi Velocity = (2 x Pa/density)^{0.5} = 34.15715 m/sec
 Venturi Volume = Velocity x Area = 107.3218 m³/sec

High Rise Spreadsheet

Reading No.	Vertical Traverse (Pa)	Sq root	Reading No.	Horizontal Traverse (Pa)	Sq root	Reading No.	Horizontal Traverse (Pa)	Sq root
1	527	22.95648	1	400	20	1	738	27.16616
2	538	23.19483	2	451	21.23676	2	449	21.18962
3	261	16.15549	3	251	15.84298	3	270	16.43168
4	133	11.53256	4	196	14	4	165	12.84523
5	179	13.37909	5	333	18.24829	5	365	19.10497
6	325	18.02776	6	363	19.05256	6	401	20.02498
7	468	21.63331	7	556	23.57965	7	550	23.45208
8	435	20.85665	8	323	17.9722	8	499	22.33831
Average of square roots		18.46702	Average of square roots		18.74155	Average of square roots		20.31913

Average Reading (Pa)
Venturi Reading (Pa)

Atmospheric Pressure (Pa)
 Average Air Temp (Deg C)
 Density of air (kg/m³)

Open Area of Venturi (m²)
 Area of Discharge Duct (m²)

Pitot Volume
 Alpha =
 Mass Flow = Alpha x Area x (2 density x Pa)^{0.5}

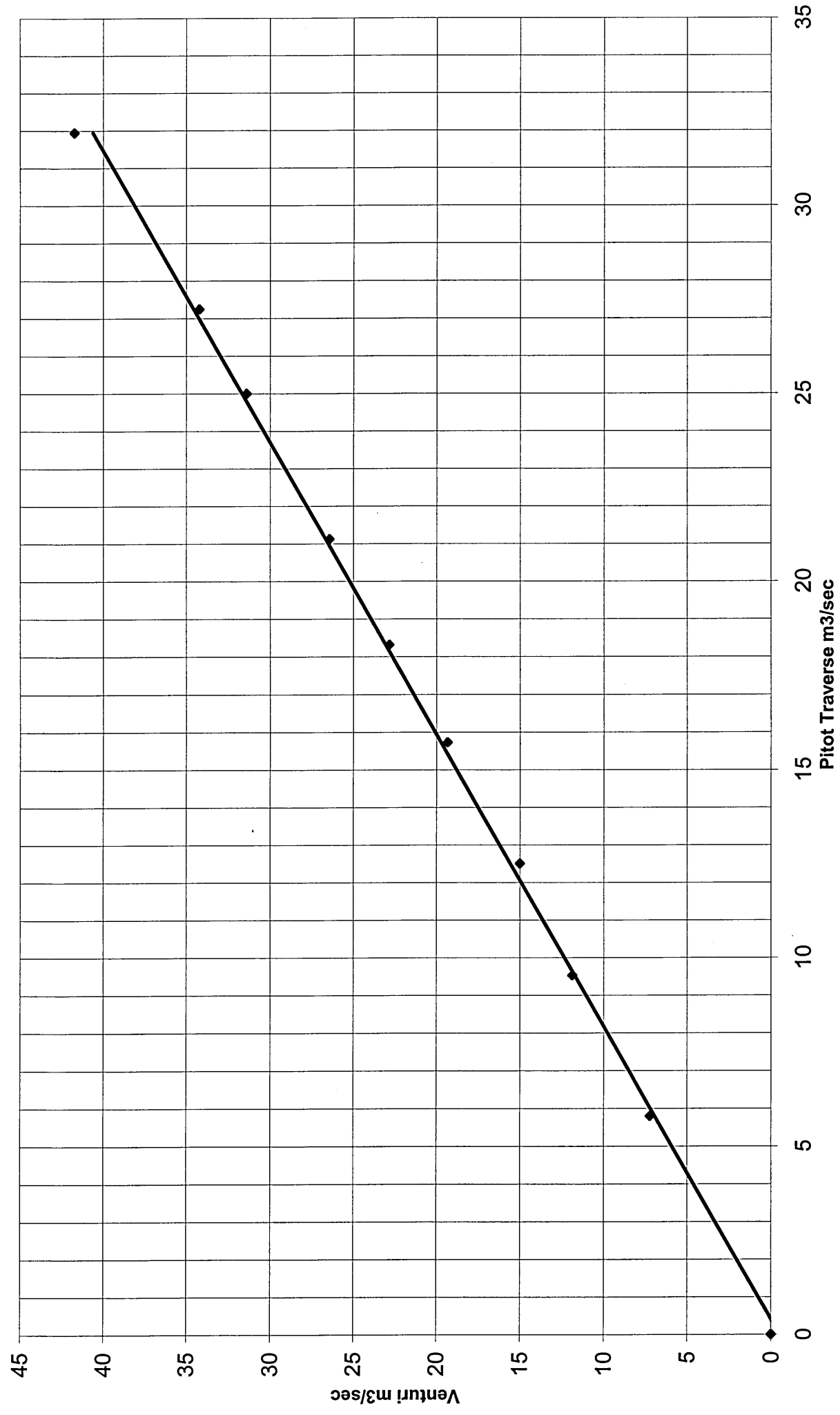
Volume = Mass Flow/Density =

Venturi Velocity = (2 x Pa/density)^{0.5} =
 Venturi Volume = Velocity x Area =

TSR.D = X688SM = 11
K88.D = 891

ST. LOUIS, MISSOURI, 1911

Graph of MIDI Fan Venturi 2 against Actual Measured flow
 $y = 1.2883x - 0.5287$
 $R^2 = 0.9984$



High Rise Spreadsheet

Reading No.	Vertical Traverse	Sq root	Reading No. Horizontal Traverse	Sq root	Reading No. Horizontal Traverse (Pa)	Sq root
1		10 3.162278	1	11 3.316625	20	4.472136
2		14 3.741657	2	11 3.316625	22	4.690416
3		12 3.464102	3	12 3.464102	18	4.242641
4		12 3.464102	4	10 3.162278	17	4.123106
5		11 3.316625	5	11 3.316625	17	4.123106
6		10 3.162278	6	12 3.464102	22	4.690416
7		7 2.645751	7	13 3.605551	18	4.242641
8		9 3	8	13 3.605551	24	4.898979
Average of square roots		3.279542	Average of square roots		4.43543	

Average Reading (Pa)
Venturi Reading (Pa)

13.67264
 21

Atmospheric Pressure (Pa)
 Average Air Temp (Deg C)
 Density of air (kg/m3)

101600
 17.9
 1.22

Open Area of Venturi (m2)
 Area of Discharge Duct (m2)

1.227
 1.227

Pitot Volume
 Alpha =
 Mass Flow = Alpha x Area x (2 density x Pa)^{0.5}
 Volume = Mass Flow/Density =

0.997
 7.056915 kg/sec
 5.798916 m3/sec

Venturi Velocity = (2 x Pa/density)^{0.5} =
 Venturi Volume = Velocity x Area =

5.874766 m/sec
 7.208338 m3/sec

High Rise Spreadsheet

Reading No.	Vertical Traverse (Pa)	Sq root	Reading No.	Horizontal Traverse Sq root	Reading No.	Horizontal Traverse (Pa)	Sq root
1	39	6.244998	1	48	1	35	5.91608
2	46	6.78233	2	43	2	33	5.744563
3	40	6.324555	3	37	3	38	6.164414
4	36	6	4	34	4	34	5.830952
5	34	5.830952	5	33	5	35	5.91608
6	34	5.830952	6	36	6	35	5.91608
7	35	5.91608	7	34	7	40	6.324555
8	31	5.567764	8	32	8	34	5.830952
Average of square roots		6.132838	Average of square roots		Average of square roots		5.955459

Average Reading (Pa) 36.91601
Venturi Reading (Pa) 57

Atmospheric Pressure (Pa) 101600
 Average Air Temp (Deg C) 18
 Density of air (kg/m3) 1.22

Open Area of Venturi (m2) 1.227
 Area of Discharge Duct (m2) 1.227

Pitot Volume
 Alpha = 0.997
 Mass Flow = $\text{Alpha} \times \text{Area} \times (2 \text{ density} \times \text{Pa})^{0.5}$ 11.59369 kg/sec
 Volume = Mass Flow/Density = 9.530215 m3/sec

Venturi Velocity = $(2 \times \text{Pa}/\text{density})^{0.5}$ = 9.680394 m/sec
 Venturi Volume = Velocity x Area = 11.87784 m3/sec

High Rise Spreadsheet

Reading No.	Vertical Traverse (Pa)	Sq root	Reading No.	Horizontal Traverse	Sq root	Reading No.	Horizontal Traverse (Pa)	Sq root	
1	60	7.745967	1	78	8.831761	1	60	7.745967	
2	65	8.062258	2	80	8.944272	2	67	8.185353	
3	60	7.745967	3	65	8.062258	3	65	8.062258	
4	55	7.416198	4	60	7.745967	4	63	7.937254	
5	50	7.071068	5	58	7.615773	5	68	8.246211	
6	55	7.416198	6	61	7.81025	6	72	8.485281	
7	70	8.3666	7	69	8.306624	7	57	7.549834	
8	50	7.071068	8	65	8.062258	8	66	8.124038	
Average of square roots		7.689179	Average of square roots		8.188129	Average of square roots			8.042025

Average Reading (Pa) 63.5705
Venturi Reading (Pa) 91

Atmospheric Pressure (Pa) 101600
 Average Air Temp (Deg C) 17.9
 Density of air (kg/m³) 1.22

Open Area of Venturi (m²) 1.227
 Area of Discharge Duct (m²) 1.227

Pitot Volume
 Alpha = 0.997
 Mass Flow = $\text{Alpha} \times \text{Area} \times (2 \text{ density} \times \text{Pa})^{0.5}$ 15.21656 kg/sec
 Volume = Mass Flow/Density = 12.50399 m³/sec

Venturi Velocity = $(2 \times \text{Pa}/\text{density})^{0.5} =$ 12.2293 m/sec
 Venturi Volume = Velocity x Area = 15.00535 m³/sec

High Rise Spreadsheet

Reading No.	Vertical Traverse (Pa)	Sq root	Reading No.	Horizontal Traverse	Sq root	Reading No.	Horizontal Traverse (Pa)	Sq root
1	90	9.486833	1	100	10	1	105	10.24695
2	117	10.81665	2	115	10.72381	2	85	9.219544
3	110	10.48809	3	115	10.72381	3	95	9.746794
4	90	9.486833	4	110	10.48809	4	90	9.486833
5	90	9.486833	5	90	9.486833	5	100	10
6	95	9.746794	6	95	9.746794	6	105	10.24695
7	105	10.24695	7	110	10.48809	7	110	10.48809
8	98	9.899495	8	97	9.848858	8	98	9.899495
Average of square roots		9.965569	Average of square roots		10.23677	Average of square roots		9.916832

Average Reading (Pa) 100.7961
Venturi Reading (Pa) 151

Atmospheric Pressure (Pa) 101600
 Average Air Temp (Deg C) 17.9
 Density of air (kg/m³) 1.22

Open Area of Venturi (m²) 1.227
 Area of Discharge Duct (m²) 1.227

Pitot Volume
 Alpha = 0.996
 Mass Flow = Alpha x Area x (2 density x Pa)^{0.5} 19.14145 kg/sec
 Volume = Mass Flow/Density = 15.7292 m³/sec

Venturi Velocity = (2 x Pa/density)^{0.5} = 15.75322 m/sec
 Venturi Volume = Velocity x Area = 19.3292 m³/sec

High Rise Spreadsheet

Reading No.	Vertical Traverse (Pa)	Sq root	Reading No.	Horizontal Traverse	Sq root	Reading No.	Horizontal Traverse (Pa)	Sq root	
1	115	10.72381	1	150	12.24745	1	145	12.04159	
2	155	12.4499	2	125	11.18034	2	160	12.64911	
3	130	11.40175	3	135	11.61895	3	150	12.24745	
4	115	10.72381	4	130	11.40175	4	160	12.64911	
5	110	10.48809	5	110	10.48809	5	165	12.84523	
6	115	10.72381	6	120	10.95445	6	160	12.64911	
7	122	11.04536	7	150	12.24745	7	175	13.22876	
8	122	11.04536	8	130	11.40175	8	150	12.24745	
Average of square roots		11.07524	Average of square roots		11.44253	Average of square roots			12.56973

Average Reading (Pa)
Venturi Reading (Pa)

Atmospheric Pressure (Pa)
 Average Air Temp (Deg C)
 Density of air (kg/m3)

Open Area of Venturi (m2)
 Area of Discharge Duct (m2)

Pitot Volume
 Alpha =
 Mass Flow = Alpha x Area x (2 density x Pa)^{0.5}
 Volume = Mass Flow/Density =

Venturi Velocity = (2 x Pa/density)^{0.5} =
 Venturi Volume = Velocity x Area =

High Rise Spreadsheet

Reading No.	Vertical Traverse (Pa)	Sq root	Reading No.	Horizontal Traverse Sq root	Reading No.	Horizontal Traverse (Pa)	Sq root
1	260	16.12452	1	205	14.31782	170	13.0384
2	215	14.66288	2	210	14.49138	170	13.0384
3	200	14.14214	3	180	13.41641	180	13.41641
4	180	13.41641	4	160	12.64911	175	13.22876
5	155	12.4499	5	150	12.24745	180	13.41641
6	160	12.64911	6	165	12.84523	170	13.0384
7	175	13.22876	7	175	13.22876	190	13.78405
8	200	14.14214	8	185	13.60147	180	13.41641
Average of square roots		13.85198	Average of square roots		13.3497	Average of square roots	

Average Reading (Pa)
Venturi Reading (Pa)

Atmospheric Pressure (Pa)
 Average Air Temp (Deg C)
 Density of air (kg/m³)

Open Area of Venturi (m²)
 Area of Discharge Duct (m²)

Pitot Volume
 Alpha =
 Mass Flow = Alpha x Area x (2 density x Pa)^{0.5}
 Volume = Mass Flow/Density =

Venturi Velocity = (2 x Pa/density)^{0.5} =
 Venturi Volume = Velocity x Area =

High Rise Spreadsheet

Reading No.	Vertical Traverse (Pa)	Sq root	Reading No.	Horizontal Traverse	Sq root	Reading No.	Horizontal Traverse (Pa)	Sq root	
1	275	16.58312	1	260	16.12452	1	250	15.81139	
2	310	17.60682	2	305	17.46425	2	255	15.96872	
3	275	16.58312	3	270	16.43168	3	240	15.49193	
4	255	15.96872	4	235	15.32971	4	245	15.65248	
5	235	15.32971	5	210	14.49138	5	245	15.65248	
6	235	15.32971	6	215	14.66288	6	275	16.58312	
7	250	15.81139	7	255	15.96872	7	270	16.43168	
8	250	15.81139	8	280	16.7332	8	245	15.65248	
Average of square roots		16.128	Average of square roots		15.90079	Average of square roots			15.90553

Average Reading (Pa) 255.2999
Venturi Reading (Pa) 399

Atmospheric Pressure (Pa) 101600
Average Air Temp (Deg C) 17.8
Density of air (kg/m3) 1.22

Open Area of Venturi (m2) 1.227
Area of Discharge Duct (m2) 1.227

Pitot Volume
Alpha = 0.995
Mass Flow = Alpha x Area x (2 density x Pa)^{0.5} 30.43804 kg/sec
Volume = Mass Flow/Density = 25.00341 m3/sec

Venturi Velocity = (2 x Pa/density)^{0.5} = 25.60311 m/sec
Venturi Volume = Velocity x Area = 31.41502 m3/sec

High Rise Spreadsheet

Reading No.	Vertical Traverse (Pa)	Sq root	Reading No.	Horizontal Traverse	Sq root	Reading No.	Horizontal Traverse (Pa)	Sq root	
1	340	18.43909	1	370	19.23538	1	265	16.27882	
2	350	18.70829	2	375	19.36492	2	310	17.60682	
3	340	18.43909	3	310	17.60682	3	305	17.46425	
4	295	17.17556	4	290	17.02939	4	275	16.58312	
5	275	16.58312	5	265	16.27882	5	285	16.88194	
6	275	16.58312	6	255	15.96872	6	305	17.46425	
7	315	17.74824	7	310	17.60682	7	325	18.02776	
8	295	17.17556	8	280	16.7332	8	300	17.32051	
Average of square roots		17.60651	Average of square roots		17.47801	Average of square roots			17.20343

Average Reading (Pa) 303.7811
Venturi Reading (Pa) 474

Atmospheric Pressure (Pa) 101600
Average Air Temp (Deg C) 17.8
Density of air (kg/m3) 1.22

Open Area of Venturi (m2) 1.227
Area of Discharge Duct (m2) 1.227

Pitot Volume
Alpha = 0.994
Mass Flow = Alpha x Area x (2 density x Pa)^0.5 33.1692 kg/sec
Volume = Mass Flow/Density = 27.24693 m3/sec

Venturi Velocity = (2 x Pa/density)^0.5 = 27.90586 m/sec
Venturi Volume = Velocity x Area = 34.24049 m3/sec

High Rise Spreadsheet

Reading No.	Vertical Traverse (Pa)	Sq root	Reading No.	Horizontal Traverse	Sq root	Reading No.	Horizontal Traverse (Pa)	Sq root	
1	480	21.9089	1	500	22.36068	1	375	19.36492	
2	490	22.13594	2	500	22.36068	2	390	19.74842	
3	470	21.67948	3	420	20.4939	3	375	19.36492	
4	420	20.4939	4	420	20.4939	4	380	19.49359	
5	390	19.74842	5	370	19.23538	5	410	20.24846	
6	400	20	6	400	20	6	450	21.2132	
7	430	20.73644	7	420	20.4939	7	370	19.23538	
8	390	19.74842	8	410	20.24846	8	395	19.87461	
Average of square roots		20.80644	Average of square roots		20.71086	Average of square roots			19.81794

Average Reading (Pa) 418.0013
Venturi Reading (Pa) 705

Atmospheric Pressure (Pa) 101600
Average Air Temp (Deg C) 17.6
Density of air (kg/m3) 1.22

Open Area of Venturi (m2) 1.227
Area of Discharge Duct (m2) 1.227

Pitot Volume 0.994
Alpha =
Mass Flow = Alpha x Area x (2 density x Pa)^{0.5} 38.92179 kg/sec
Volume = Mass Flow/Density = 31.95043 m3/sec

Venturi Velocity = (2 x Pa/density)^{0.5} = 34.02134 m/sec
Venturi Volume = Velocity x Area = 41.74419 m3/sec